7-1-2011

Blends of UV-cross-linkable model compound and polyimide; Effect of UV exposure on viscosity and mechanical properties

Indraneel Zope

BLENDS OF UV-CROSS-LINKABLE MODEL COMPOUND AND POLYIMIDE; EFFECT OF UV EXPOSURE ON VISCOSITY AND MECHANICAL PROPERTIES

A Graduate Thesis Presented

By

Indraneel Suhas Zope

July 2011

A thesis submitted in partial fulfillment of the requirements for the degree of

Master of Science

Department of Materials Science and Engineering

Rochester Institute of Technology

Rochester, NY.

BLENDS OF UV-CROSS-LINKABLE MODEL COMPOUND AND POLYIMIDE;

EFFECT OF UV EXPOSURE ON VISCOSITY AND MECHANICAL PROPERTIES

A Graduate Thesis Presented

By

Indraneel S. Zope

_____ _____

Indraneel Suhas Zope Date

BLENDS OF UV-CROSS-LINKABLE MODEL COMPOUND AND POLYIMIDE;

EFFECT OF UV EXPOSURE ON VISCOSITY AND MECHANICAL PROPERTIES

A Graduate Thesis Presented

By

Indraneel Suhas Zope

Approved as to style and content by:

Marvin Illingsworth, Ph.D.
Professor of Chemistry, Thesis Advisor

Gerald Takacs, Ph.D.
Professor of Chemistry, Committee Member

Spencer Kim, Ph.D
Professor of Packaging Science, Committee Member

KSV Santhanam, PhD.
Director, Center of Materials Science & Engineering

ACKNOWLEDGEMENTS

Research is no one man's job. It's a cumulative effort of many, may it be providing valuable leads when you face a dead-end or motivating you while not having a slightest clue about the research work. Help, support and time of many has gone into this work, for which I humbly thank all.

I would especially like to thank my advisor Dr. M. Illingsworth for giving me an opportunity to work in his group and for his support, guidance and encouragement throughout my research work towards M.S. program at R.I.T. I also sincerely thank my research committee, Dr. G. Takacs and Dr. S. Kim for their time and guidance.

I am truly grateful to Dr. G. Takacs for providing UV lamp and Dr. S. Kim for granting me the access to Tensile Tester. I would also like to thank Dr. R. Hailstone, Dr. S. Gupta and (Late) Dr. A. Langner for their assistance towards my research work. I thank Mr. S. Blondell for providing Spectro-photometer. My sincere gratitude to Mr. T. Allston for his time and assistance.

A special thanks to my lab mates, Stacy Kowsz, Alex Haruk, Greg Horrocks for their help and support. I am also really thankful to Zach Loughery and Ciara Poolman for helping me out with tensile tests. Thanks to Jack Alvarenga, Fei Lu, Ameya Khot, Mike Logan, Rudy Valladares, Chengkai Cheng, Dave Gallipeau, Nitin Kalra and Suhasini Gattu for making my M.S. journey fun and memorable.

I would like to extend my gratitude to Dr. K.S.V. Santhanam for giving me an opportunity to join RIT family. Also, I would like to thank Brenda Mastrangelo and stockroom staff.

Very special thanks to my family and friends goes without saying.

Dedicated to my loving Mom and Dad.

TABLE OF CONTENTS

LIST OF FIGURES

LIST OF TABLES

ABBREVIATIONS

UV	Ultra-Violet Light
NLO	Non Linear Optical
NLO-phore	Non Linear Optical Chromophore
MADA	Mellitic Acid Dianhydride
6FDA	4,4'-(Hexafluoroisopropylidene)diphthalic anhydride
Bis-AP-AF	2,2 Bis(3-amino-4-hydroxyphenyl)hexafluoropropane
PI	Polyimide
MC	Model Compound
PSPI	Photo Sensitive Polyimide
ASTM	American Society for Testing and Materials
DMA	Dynamic Mechanical Analyzer
^{1}H NMR	1-Proton Nuclear Magnetic Resonance Spectroscopy
FT-IR	Fourier Transform-Infrared Spectroscopy
LC-MS	Liquid Chromatography-Mass Spectroscopy
UV-Vis	Ultra-Violet Spectroscopy
DSC	Differential Scanning Calorimeter
TGA	Thermo-gravimetric Analysis
TLC	Thin Layer Chromatography
CaH_2	Calcium Hydride
$N_2(l)$	Liquid Nitrogen
P_2O_5	Phosphorous Pentoxide
d^1-$CDCl_3$	Deuterated Chloroform
d^6-DMSO	Deuterated Dimethyl Sulfoxide
KOH	Potassium Hydroxide
KBr	Potassium Bromide
$KHCO_3$	Potassium Bicarbonate
K_2CO_3	Potassium Carbonate
NMP	N-Methylpyrrolidone
DMAc	Dimethylacetamide
DMF	Dimethylformamide
THF	Tetrahydrofuran
2ME	2-methoxyethanol
F	Load
E	Young's Modulus (Tensile Modulus)
E'	Storage Modulus
E"	Loss Modulus
TBS	Tensile Breaking Strength
e	Elongation
M	Molecular Weight
M_c	Critical Molecular Weight
t_c	Critical UV Exposure Time
RT	Room Temperature
RBF	Round Bottom Flask
σ	Standard Deviation

ABSTRACT

BLENDS OF UV-CROSS-LINKABLE MODEL COMPOUND AND POLYIMIDE; EFFECT OF UV EXPOSURE ON VISCOSITY AND MECHANICAL PROPERTIES

Indraneel Suhas Zope

The ultimate goal of this project is to synthesize a novel UV-cross-linkable non-linear optical (NLO) pendant polyimide. The following work is dedicated to the synthesis and exposure optimization of the UV cross-linkable component. Knowing that highly stable NLO properties can be achieved through cross-linked polymer matrices, where polymer chain immobilization leads to unidirectional orientation of NLO-phores in poled polymer resulting in maximized operational lifetime and the complete cross-linking cannot be achieved even after a long irradiation time for a photo-cross-linkable polymer, a chalcone-based UV curable Model Compound was synthesized and exposed to UV light. Optimization was carried out with respect to four factors: (1) UV light wavelength, (2) Solvent for exposure, (3) Solution concentration and (4) Optimum exposure time. For (1)-(3), UV light of 300nm, lower concentrations of solutions and tetrahydrofuran as a solvent were established using LC Mass Spectroscopy, UV-Vis Spectroscopy, FTIR and NMR characterization techniques. For (4), we determined the optimum curing time for maximum polymer chain immobilization, as reflected by Model Compound solution viscosity and mechanical properties of Model Compound-Polyimide blends (1:7 by weight). Tensile and Dynamic Mechanical Analysis (DMA) analysis of blend films agreed with viscosity results that exposure beyond 45 minutes yielded little additional cross-linking in our UV exposure apparatus.

Keywords: NLO-, Polyimide, UV, Cross-linking, Blend, Film, Tensile, Dynamic Mechanical Analysis, Viscosity.

CHAPTER 1:

INTRODUCTION

1. INTRODUCTION

Extensive research is being carried out to develop non-linear optical (NLO) materials, which will bring on "Generation Next" of telecommunication technology. Developing NLO-based devices like Electro-Optic switches and modulators will not only provide greatly enhanced speed but also improved quality of data transfer[1]. Apart from electro-optic modulation, second order NLO-based polymers are also best known for frequency doubling, frequency tuning, ultra-short electric pulse generation and terahertz (THz) wave generation and detection[2].

In order to extract highest quality output throughout the life cycle of these polymeric NLO devices, it is very important to sustain a non-centro-symmetric orientation of NLO groups inside the polymer matrix. However, relaxation of these highly polar NLO-phores is routinely observed due to their high anti-parallel dipole-dipole aggregation resulting in loss of poling efficiency[3] and thus, bulk electro-optic activity. Dedicated research carried out by many research groups has reported an enhanced relaxation stability of oriented NLO-phores through two main techniques:

1. Cross-linking the NLO polymer matrix during or after poling of NLO-phores.[3b, 4, 5]
2. Embedding NLO-phores onto high glass transition temperature polymers.[6]

Polymer chain immobilization thus achieved in NLO-based polymer matrix leads to stable unidirectional orientation of NLO-phores resulting in maximized operational lifetime.

Study of this cross-linking phenomenon with respect to its Mechanical, Visco-elastic and Viscometric Properties for a photosensitive cross-linker constitutes the core of this research work.

1.1 Cross-linking of polymers

Cross-linking is one of the most important processes in the polymer industry.[7] Cross-linking can be defined as the introduction of bridges between different polymeric chains via covalent bonding to form a three dimensional network structure.[8] Ideally, the cross-linked mass essentially has only one molecule, instead of numerous discrete molecules. In actual practice it is not feasible to cross-link the complete

mass, so the term cross-linking is quantified and always given in terms of "degree of cross-linking". This expression refers to the extent of cross-linking and is the controlling process parameter. The molecular weight of such polymers is infinite, in the sense that it is too high to be measured by standard techniques. A high degree of cross-linking makes polymer insoluble in all solvents. All tri- and multifunctional monomers yields network structures, but lack separate chemistry to control degree of cross-linking.

Cross-linking is essentially done to reduce the mobility of polymeric chains. Under external force the chains slip over each other, whereas in case of cross-linked polymer, the inter-chain covalent bonds resist the slip and hold the chains intact, thus reducing the chain mobility. This leads to large improvement in polymer properties, like enhanced dimensional stability under load and elevated temperatures, higher long-term thermal stability[9], improved stress crack resistance, higher creep resistance, better chemical resistance, improved toughness and better general thermo-mechanical stability.[10] Vulcanization of rubber is the most common example of the cross-linking process.[11] Specialized applications include wrinkle and crease resistant cellulose fabrics[12], control of gas permeability of polymer, primarily due to reduction in diffusion coefficient after cross-linking[13], etc.

There are various methods employed for cross-linking polymers[12] via covalent bonds. Some of the most common are tabulated in Table 1.1.

Table 1.1 – Cross-linking Methodologies[12]

Cross-linking Methodologies	**Typical Examples**
Reactions of functional groups	Phenolic resins
Vulcanization using peroxides, elemental sulfur, or metal oxides	Cross-linked Polyethylene (XLPE) using di-cumyl peroxide
Free radical reactions caused by ionizing radiations	Polyacrlamide
Ionic cross-linking	Chlorosulfonated polyethylene
Photochemical cross-linking involving UV or visible light	Polyimide (PI)

1.2 Polyimides and Photo-Sensitive Polyimides

Since commercialization of Kapton® (a DuPont polyimide, or "PI"), a large variety of polyimides with different properties has been synthesized. Polyimides are known for their outstanding properties, such as high modulus, high mechanical strength, very good electrical properties, good chemical resistance, high thermal stability, low dielectric constant and low thermal expansion. The most prominent applications of polyimides are in the micro-electronics industry, and include miniaturization, large scale-integration and high speed signal processing in semiconductor-based components to name few.[14] Also PI coatings are used in a variety of interconnect and packaging applications, including stress buffers on integrated circuits and interlayer dielectrics in high density interconnects on multi-chip modules.[15]

The following are typical, widely implemented PI cross-linking techniques:

1. Thermal imidization.[16, 17]
2. Chemical imidization.[18, 19]
3. Irradiation of ions.[20]
4. Addition of metal salts.[21]
5. UV exposure.[4b, 22, 23]

Apart from significant improvement in the long-term NLO-phore orientation stability[4b], photo-cross-linking can be carried out at various temperatures and its complete independence from electrical poling makes photosensitive polyimides (PSPI) more promising and user-friendly. Thus, considering the potential importance of UV curing of PSPI in the manufacturing process, we have concentrated our study on photo-cross-linking only (#5 above). Photo cross-linking can be brought about in two main ways[12]:

- Incorporation of photo-sensitizers

  High energy light such as UV rays excite the sensitizer which abstracts a hydrogen atom from the polymer chain thus generating a free radical site which eventually takes part in the cross-linking reaction. Benzophenones are the most common examples of photo-sensitizers.

- Incorporation of UV responsive groups in/on the polymer backbone

  A wide variety of functional groups has been used for light induced cross-linking.

- Cinnamate (PhCH=CHCOOR).[24, 25]
- Stilbene (PhCH=CHPh).[12]
- Dimethoxy dimethylsilane.[26]
- o-Nitrobenzyl ester.[27]
- Chalcone (PhCH=CHCOPh).[28, 29]

Upon UV exposure, these UV-responsive groups undergo a photo-cyclo-addition reaction forming cyclo-butane rings at cross-link sites. Although many photo-sensitive cross-linkable groups have been implemented, chalcones possess a slight edge over others due to their better spectral match, i.e., providing higher photo-sensitivity without any need of photo-sensitizers.[30]

CHAPTER 2:

RESEARCH AIM

2. RESEARCH AIM

The ultimate goal is to synthesize a novel, pendent NLO, UV cross-linkable novel polyimide, see Fig. 2.1, which will not only be efficient over the long run but also easily fabricated making it commercially viable. Synthesis of a key component, mellitic acid dianhydride (MADA), the structure of which is shown in Fig. 2.2, has been successfully developed .[31] MADA is particularly significant because it provides two cross-linker attachment sites on a rigid six-membered ring, which should dramatically increase the thermal stability of the NLO-based polymer system. Concurrent to this project, known high efficiency NLO-phores are being prepared.

The following thesis work is dedicated to the synthesis and optimization of the cross-linking component of the desired polymer and will be divided into two main stages.

Stage 1- Synthesis of model compound with UV cross-linkable groups; attach two chalcone moieties to terephthalic acid through spacer groups (see Fig. 2.3), and optimization of the system for next stage.

Stage 2- Mechanical and Viscometric Study; evaluate optimum UV exposure time using polymer properties.

The structure of model compound strongly resembles the UV cross-linkable MADA-containing component of ultimate co-polyimide structure, whose synthesis will constitute a future stage of the project. The photo-reactive component, chalcone, and a spacer group of various lengths constitute the cross-linkable pendent group of the model compound.

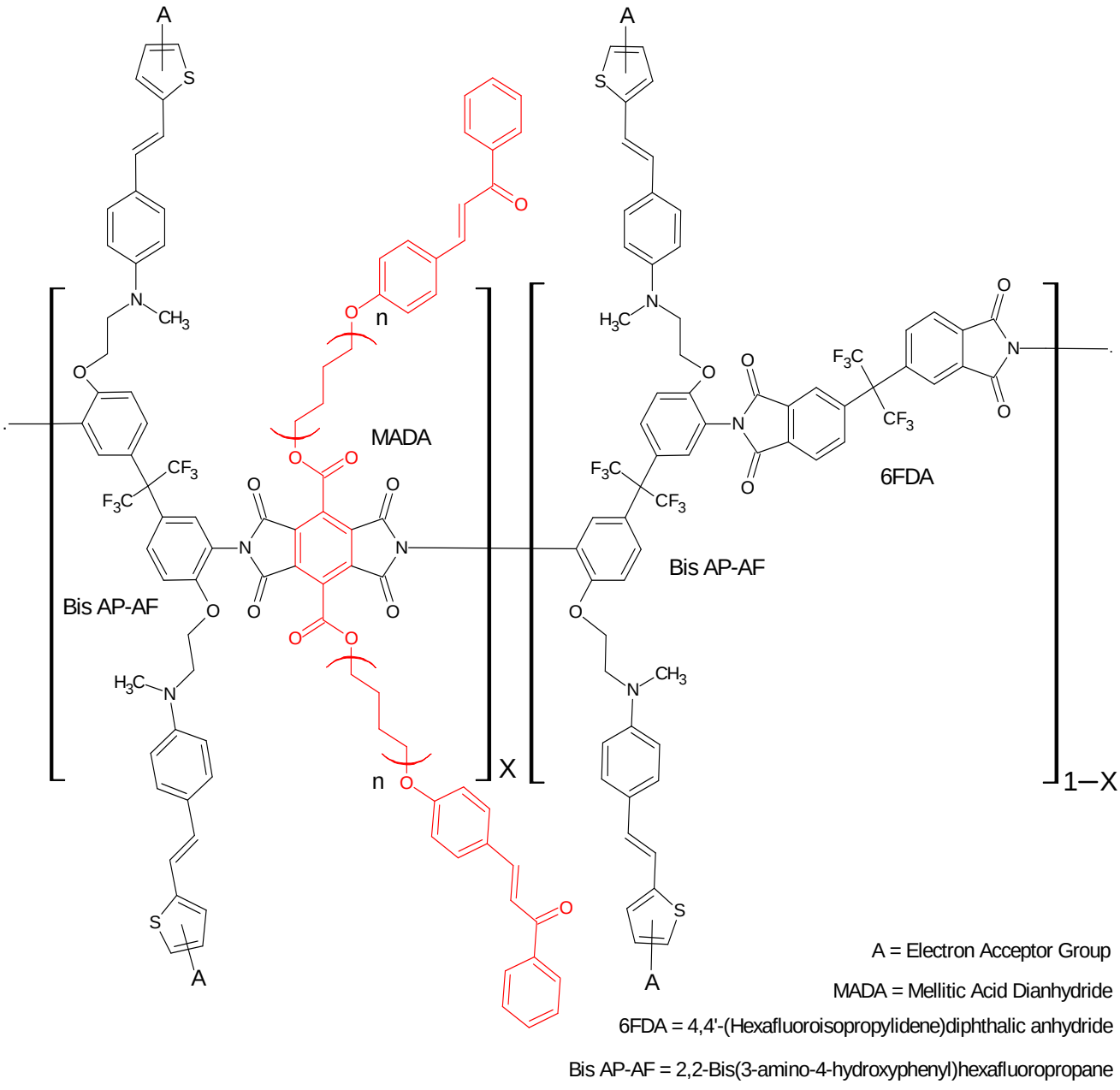

Figure 2.1 – Structure of a Novel, UV-Cross-linkable, MADA-containing, Non-Linear Optical (NLO) Pendent Polyimide. "A" represents various electron acceptor groups.

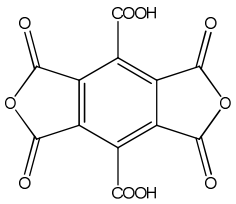

Figure 2.2 – Mellitic Acid Di-anhydride (MADA) Structure.

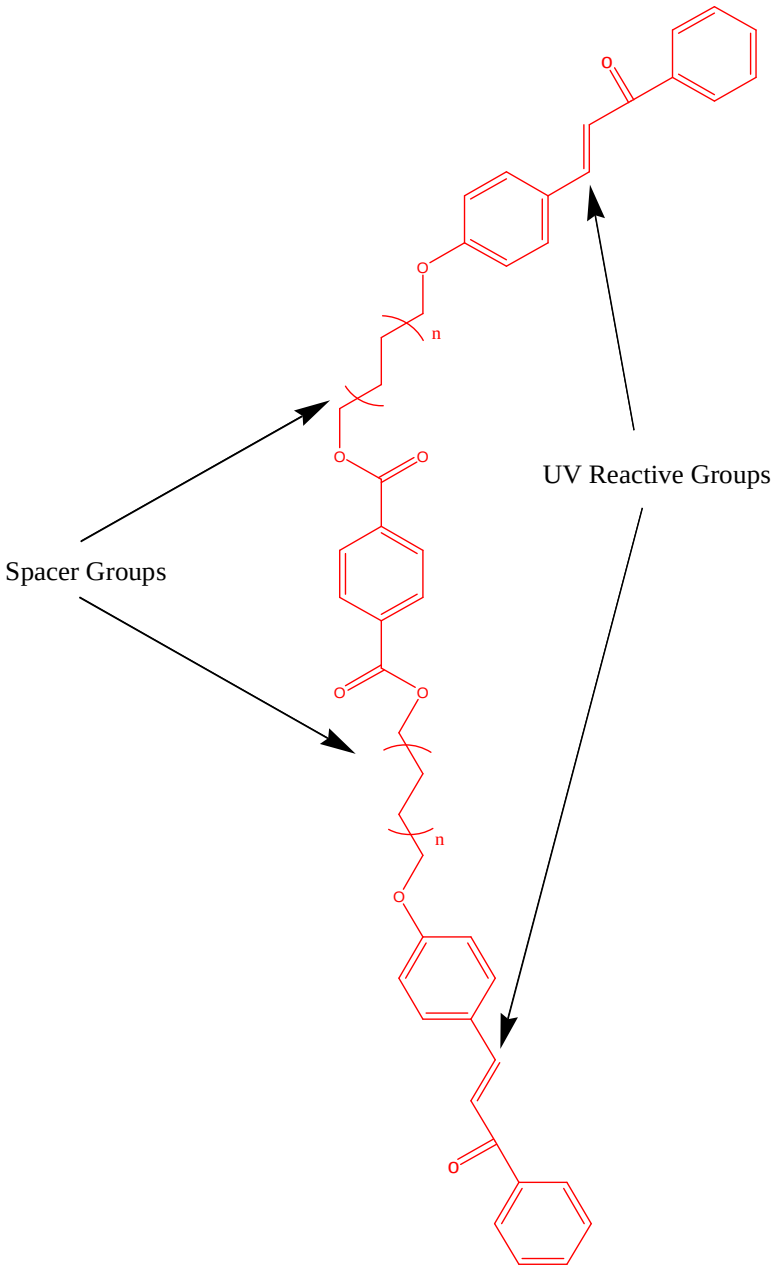

Figure 2.3 – General Structure of the Model Compound (n=0, 1, 2).

Ahmed Rehab et.al.[32] showed that for a photo-cross-linkable polymer, complete cross-linking cannot be achieved even after a long irradiation time. With reference to this, we propose to determine the optimum curing time for maximum polymer chain immobilization, as reflected by particular mechanical properties. Thus, the conditions that lead to the least possible chain mobility can be identified.

Fig. 2.4 schematically represents the poling (i.e., alignment) and cross-linking processes for NLO-based polymers.

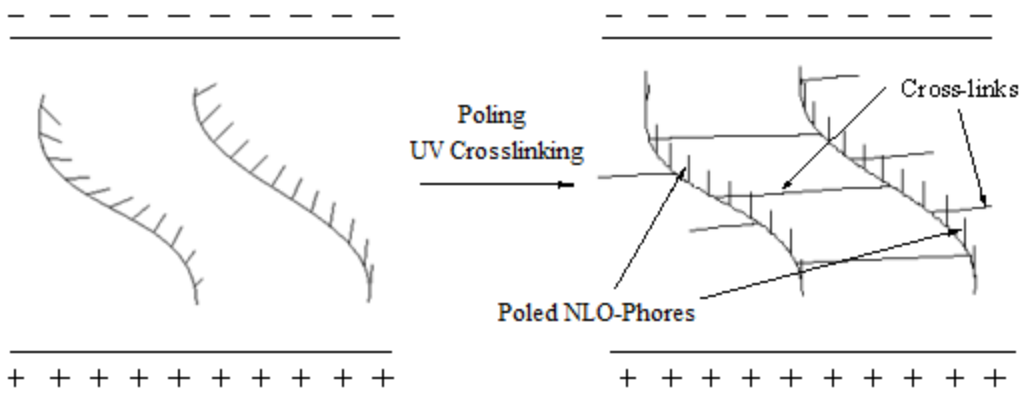

Figure 2.4 – Schematic Representation of NLO-phore Alignment ("Poling") Preserved by Cross-linking.

CHAPTER 3:

EXPERIMENTS

3 EXPERIMENTAL

3.1 Materials

Table 3.1 – Materials Used for Experimental Work

Chemicals	**Manufacturers**
4-Hydroxychalcone	Alfa Aesar
4,4'-(Hexafluoroisopropylidene)diphthalic anhydride (6FDA)	Alfa Aesar
18-Crown-6	Alfa Aesar
2,2-Bis(3-amino-4-hydroxyphenyl)hexafluoropropane (Bis AP-AF)	TCI America
Terephthalic acid	Sigma Aldrich
N,N-Dimethylacetamide	Sigma Aldrich
1,4-Dibromobutane	Sigma Aldrich
Potassium Carbonate	J.T. Baker Inc.
Potassium Hydroxide	J.T. Baker Inc.
2-Methoxyethanol (2ME)	J.T. Baker Inc.
Hexanes	J.T. Baker Inc.
N-Methyl-2-pyrrolidinone (NMP)	Alfa Aesar
Acetonitrile	EMD Chemicals
Dimethylformamide (DMF)	Acros Organics
Tetrahydrofuran (THF)	Acros Organics
Chloroform	Mallinckrodt Chemicals
Ethyl Ether	Mallinckrodt Chemicals

NMP and THF were dried by heating at reflux with calcium hydride (CaH_2) under Nitrogen (N_2) atmosphere for at least 6 hours and distilled prior to use.

Deuterated solvents like Chloroform-d^1 and Dimethyl sulfoxide-d^6 used for Proton Nuclear Magnetic Resonance Spectroscopy were obtained from Wilmad Lab Glass and Cambridge Isotope Laboratories, Inc. respectively. Silica chromatography sheets used for thin layer chromatography (TLC) were obtained from Fisher Scientific.

Glassware used was cleaned using Alconox detergent and were oven dried at ≈110 ^{0}C for at least 6 hours prior to use. The reactions were performed under Nitrogen or Argon atmosphere with minimum tank pressure of 500 psi.

3.2 Purification of Reactants

Terephthalic acid was purified by double sublimation under vacuum at 295-305 ^{0}C using a liquid nitrogen [$N_2(l)$] trap. It was stored in a desiccator with phosphorus pentoxide (P_2O_5) to prevent any absorption of moisture. The cold finger of the sublimation apparatus was filled with ice-water.

Following the same procedure Bis-AP-AF and 6FDA were purified by double sublimation under vacuum at temperatures 230-240 ^{0}C and 235-245 ^{0}C respectively.

3.3 Synthesis of Terephthalic Acid-based Compound with UV Cross-linkable Group.

3.3.1 Synthesis of UV-Crosslinkable Compound: Literature Review

Sang Kyu Lee et.al.[33] has demonstrated one of the techniques used to synthesize the desired terephthalic acid-based model compound with two UV cross-linkable groups. Terephthalic acid was treated with potassium hydroxide in 1:2 ratio to obtain the potassium salt[34], which was then treated with dibromoalkane to form an intermediate compound. Potassium salt of 4-hydroxychalcone was lastly reacted with the intermediate compound to obtain desired model compound. Refer to Fig. 3.1.

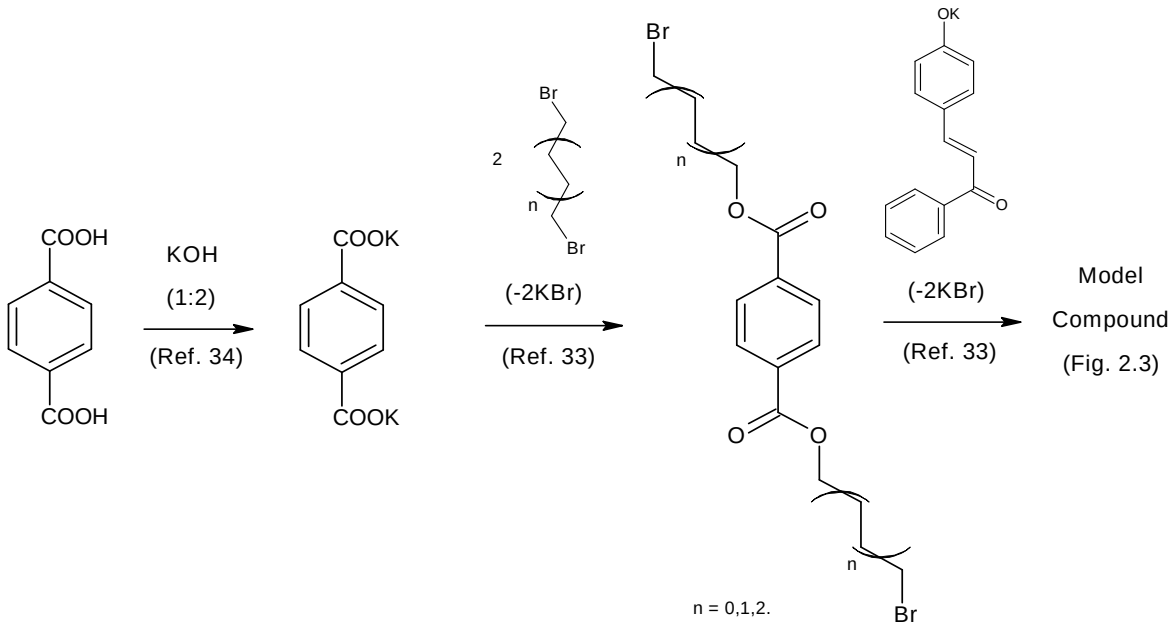

Figure 3.1 – Complete Reaction Scheme Demonstrated be Sang Kyu Lee et.al.

Wei Guo et. al.[35] demonstrated a variation to the above reaction using a different base, solvent and temperature. The reaction performed also gave the bromo-alkane substituted terephthalic acid, which on further treatment with 4-hydroxychalcone yield the model compound.[33, 36, 37] Refer Fig. 3.2.

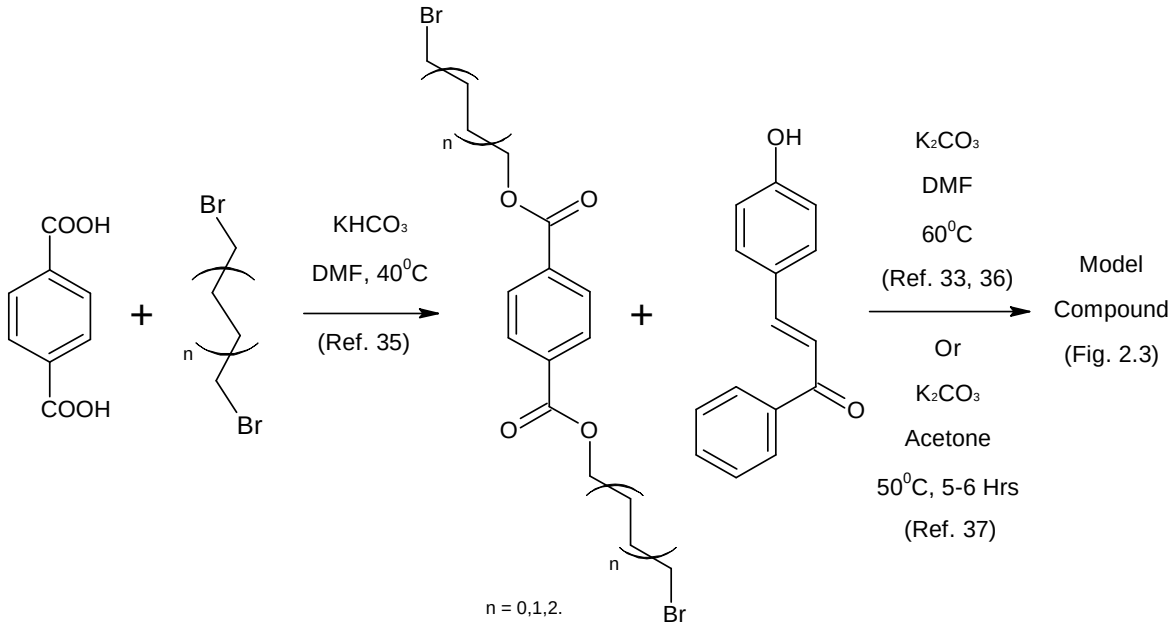

Figure 3.2 – Complete Reaction Scheme Demonstrated by Wei Guo et.al.

Alternately instead of halogenated alkane, diols were used to synthesize model compounds. Seung Woo Lee et. al.[34] carried out the reaction between Terephthalic acid and excess diol under specified reaction conditions to obtain hydroxyl alkane substituted Terephthalic acid. The Mitsunobu Reaction[38, 39] was used to convert this substituted acid into model compound using commercially available 4-hydroxychalcone. Refer to Fig. 3.3

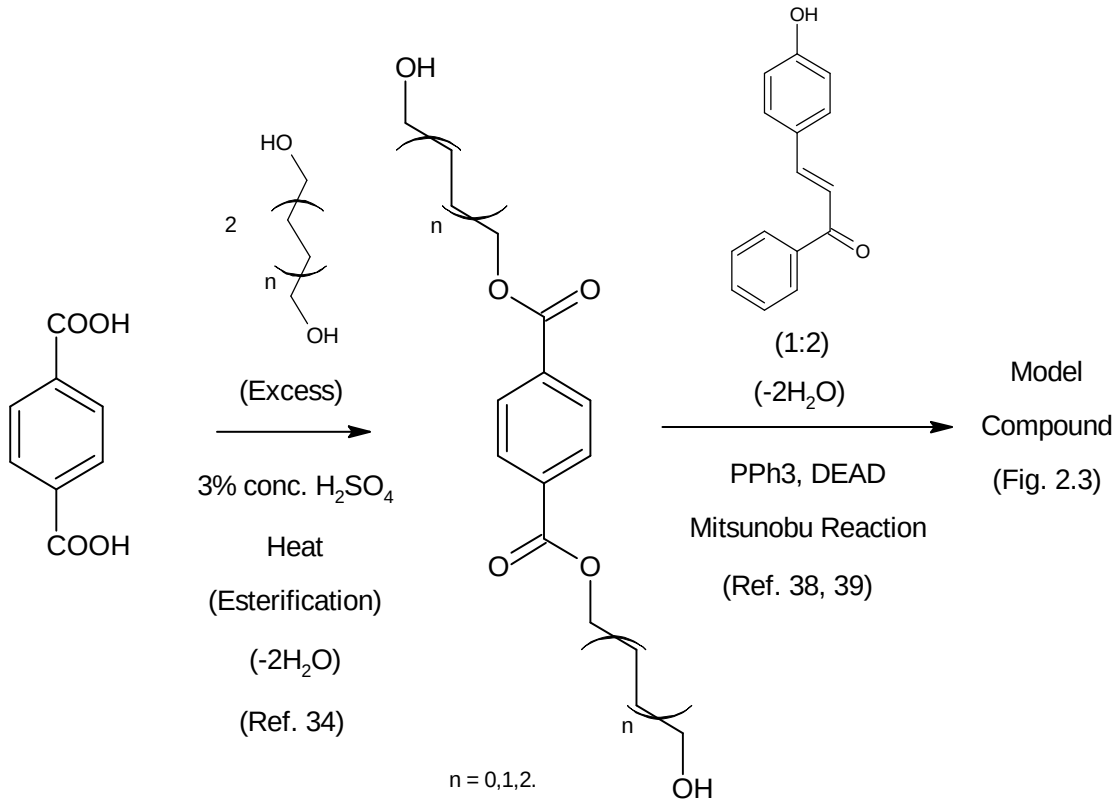

Figure 3.3 – Complete Reaction Scheme Demonstrated by Seung Woo Lee et.al.

3.3.2 Synthesis of UV-Crosslinkable Compound

The synthesis of 4-hydroxychalcone-based terephthalic acid model compound was carried out in two steps, as depicted below,

Step 1: Synthesis of UV-crosslinker

4-Hydroxychalcone was dissolved in dimethylformamide (DMF) solvent. Upon complete dissolution, potassium carbonate was added to the reaction mixture forming insoluble potassium salt of 4-hydroxychalcone. During this deprotonation reaction, the color change of solution was observed, yellow to orange to red. 1,4-Dibromobutane was then added to mixture and initial TLC was performed using 1:1 ethyl acetate:hexanes as eluent. The left spot of 4-hydroxychalcone solution was compared to the right spot comprising the reactant mixture. Reaction was carried out for 24 hours and was monitored by periodic TLC's to check the disappearance of 4-hydroxychalcone from reactant mixture. TLC of product yielded light yellow colored spot and $R_f = 0.83$. Refer to Fig. 3.4.

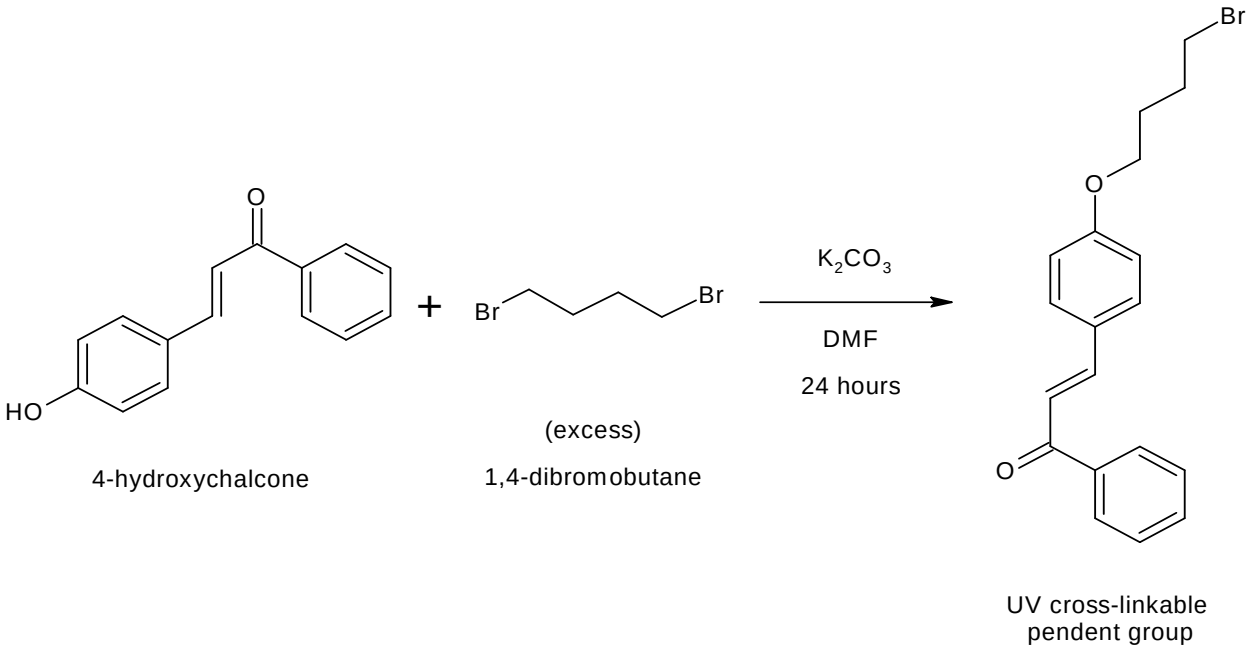

Figure 3.4 – Synthesis of UV Cross-linkable Pendent Group

Upon completion of reaction, reaction solution appears yellow and opaque due to insolubility of salt. The salt was isolated using suction filtration process and Buchner funnel. Filtered salt was thoroughly washed by acetone to extract any traces of reaction solution. Rota-evaporation of filtrate was performed under vacuum at 45 ^{0}C to yield yellow solid mass which was then dissolved in chloroform.

Undissolved salt particles were filtered out, if any. Hexanes were added to the filtrate to precipitate out the solid yellow product upon refrigeration for 24 hrs. Using suction filtration, a bright yellow solid product was obtained with the UV cross-linkable group and was stored in dark to avoid light exposure.

Reaction Calculations:

Reactant quantities based on 10 g of 4-hydroxychalcone.

224.25 g of 4-hydroxychalcone = 1 mol

So, 10 g = (10/224.25) = 0.0446 mol

Next,

Molar ratio of (4-hydroxychalcone:Potassium Carbonate)= 1:1.6

138.21 g of Potassium Carbonate = 1 mol

So, amount of Potassium Carbonate required = 1.6*(0.0446*138.21)

= 9.86 g

Lastly,

Molar ratio of (4-hydroxychalcone:1,4-dibromobutane) = 1:4

Amount of 1,4-dibromobutane required = (4*0.0446) = 0.1784 mol

1 mol of 1,4-dibromobutane = 215.91 g

So, amount of 1,4-dibromobutane required = (0.1784*215.91)

= 38.51 g

As, density of 1,4-dibromobutane = 1.808 g/mL

amount of 1,4-dibromobutane required = (38.51/1.808) = 21.3 mL

Yield Calculation:

For every mole of product formed we have equal number of moles of HBr as by-product.

Amount of HBr = (number of moles of 4-hydroxychalcone*Mol. Wt. of HBr)

=3.61 g

Theoretical Yield = (g of reactants) – (g of by-product) = 44.9 g

Obtained Yield = 12.9842 g

Thus,

% Yield = (12.9842/44.9) * 100

= 28.9 %

Step 2: Attachment of UV Cross-linker to Terephthalic acid

The synthesis of UV Cross-linkable model compound consisted of dissolution of Potassium Hydroxide and Crown ether (also called, 18-Crown-6) in 150 mL NMP. Twice sublimed terephthalic acid was dissolved in 80 mL NMP. The clear solutions were combined in a 500 mL RBF, to which UV cross-linkable pendent group compound, pre-dissolved in 50 mL NMP, was added. The RBF was covered with aluminum foil to avoid any exposure to light. Initial TLC was performed using 1:2 ethyl acetate:hexanes as eluent. Reaction mixture was spotted and was compared with that of UV cross-linkable pendent group starting material. The reaction was carried out for 3-4 days with continuous stirring and reaction temperature of 30^0C. Refer to Fig. 3.5.

The reaction was continuously monitored using TLC. Complete disappearance of yellow colored spot for UV cross-linkable pendent group marked the completion of reaction. TLC of final product yielded colorless spot and R_f = 0.61. The reaction mixture was then blended with ice-water mixture for 15-30 minutes to precipitate out the off-white colored product. Suction filtration followed by acetone wash was performed to isolate the final product.

Reaction Calculations:

Reactant quantities based on <u>10 g of UV curable pendent group</u>.

359.26 g of UV curable pendent group = 1 mol

So, 10 g = (10/359.26) = 0.0278 mol

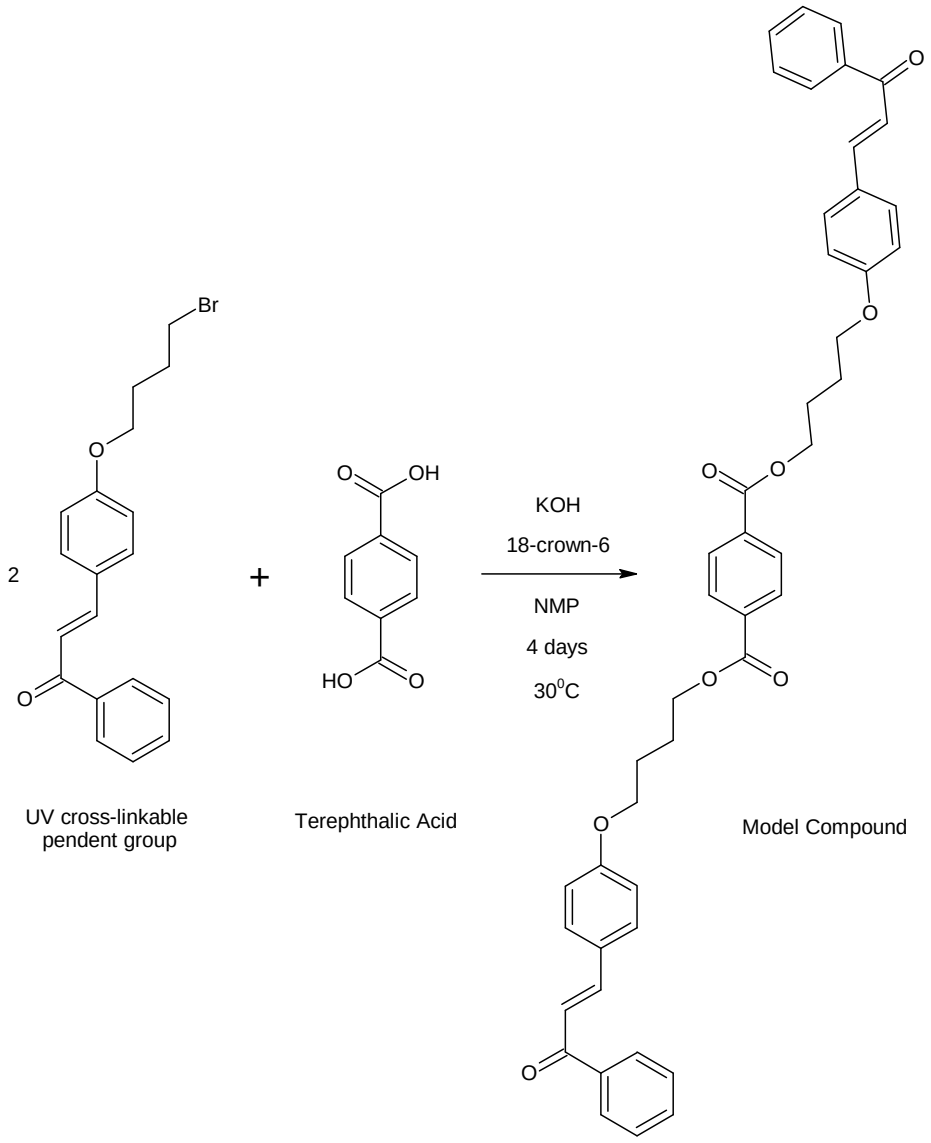

Figure 3.5 – Synthesis of Terephthalic Acid-based, UV Cross-linkable Model Compound

Next,

Molar ratio of (UV curable pendent group:Terephthalic acid)= 1:0.5

166.13 g of Terephthalic acid = 1 mol

So, <u>amount of Terephthalic acid required</u> = 0.5*(0.0278*166.13)

= 2.309 g

Further,

Molar ratio of (UV curable pendent group:Potassium hydroxide) = 1:1

56.11 g of Potassium hydroxide = 1 mol

So, amount of Potassium hydroxide required = (0.0278*56.11)

= 1.56 g

Lastly,

Molar ratio of (UV curable pendent group:18-Crown-6) = 1:1

264.12 g of 18-Crown-6 = 1 mol

So, amount of 18-Crown-6 required = (0.0278*264.12)

= 7.343 g

Yield Calculation:

For every mole of product formed we have two of moles of HBr as by-product.

Amount of HBr = 2*(number of moles of Terephthalic acid *Mol. Wt. of HBr)

= 2.249 g

Theoretical Yield = (g of reactants) – (g of by-product)

= 10.06 g

Obtained Yield = 8.41 g

Thus,

% Yield = (8.41/10.06) * 100

= 83.6 %

3.4 Synthesis of Poly[4,4'-(Hexafluoroisopropylidene)diphthalic anhydride / 2,2 Bis(3-amino-4-hydroxyphenyl)hexafluoropropane]imide, PI[6FDA/Bis-AP-AF]

Dissolution of accurately weighed 2x sublimed 6FDA was carried out in dried NMP for 1 hour in a 2-neck 500 mL RBF with magnetic stir bar. The solution was then cooled to 0-5 ^{0}C using ice-water mixture prior to addition of accurately weighed purified Bis AP-AF to the reaction mixture. The temperature of 0-5 ^{0}C was maintained for 6 hours during which the viscosity of reaction solution was

observed to rise due to formation of poly(amic acid). The poly(amic acid) solution was then allowed to warm to room temperature and was stirred for 5 days.

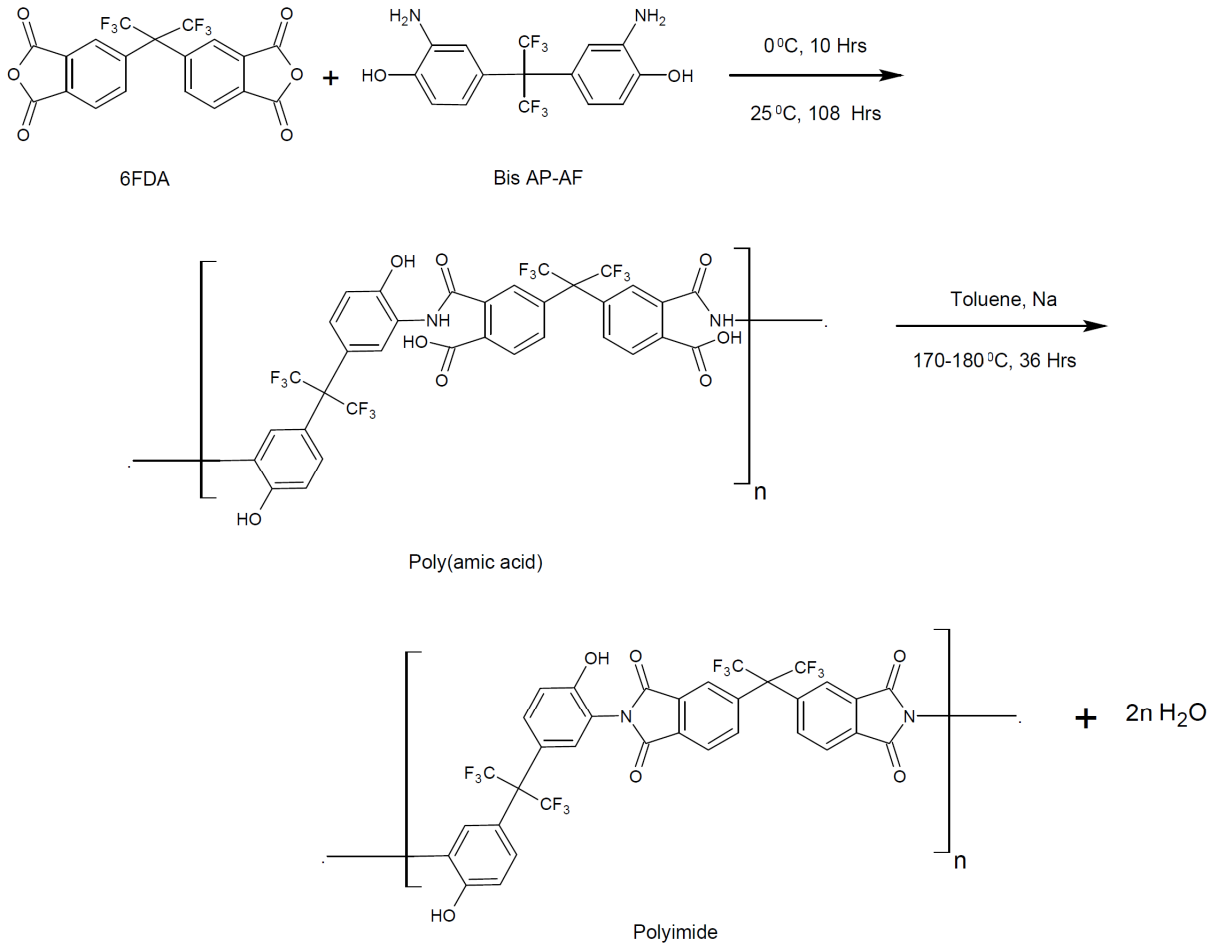

Figure 3.6 – Complete Synthesis of Polyimide from Bis-AP-AF and 6FDA

In order to carry out imidization of poly(amic acid) and to remove water formed as a by-product of imidization reaction, a sodium metal charged Dean Stark Trap apparatus was set up over the 2-neck RBF. 50 mL toluene was added to the reaction mixture to form an azeotropic mixture and expedite transfer of water to the Dean Stark trap. The imidization reaction was carried out 180-190 ^{0}C for 18-20 hours. Reddish-brown colored solution of polyimide in NMP was obtained upon completion of reaction.

No change in solution viscosity was observed. All the reactions were carried out under inert argon atmosphere. Complete reaction is shown in Fig. 3.6.

Polyimide product was isolated by precipitation. Polyimide solution was poured over ice-water mixture in an explosion-resistant blender. Sticky tan clumpy precipitate of polyimide on ice-water mixture was blended for 8-10 hours to obtain fine polyimide particulates floating on blended mixture. Degree and time of agitation govern the particle size. The precipitate was vacuum filtered using a crucible filter with coarse frit. The filtered product was rinsed with distilled water and was air-dried overnight, followed by vacuum drying at 100 ^{0}C for 24 hours to obtain a pale brown colored PI powdered product.

Reaction Calculations:

Reactant quantities based on 10 g of Bis AP-AF.

366.26 g of Bis AP-AF = 1 mol

So, 10 g = (10/366.26) = 0.0273 mol

Next,

Molar ratio of (Bis AP-AF:6FDA)= 1:1

444.24 g of 6FDA = 1 mol

So, amount of 6FDA required = 1*(0.0273*444.24)

= 12.128 g

Yield Calculation:

For every mole of product formed we have two moles of H_2O as by-product.

Amount of H_2O = 2*(number of moles of Bis AP-AF*Mol. Wt. of H_2O)

= 0.9828 g

Theoretical Yield = (g of reactants) – (g of by-product)

= 21.15 g

Obtained Yield = 20.914 g

Thus,

% Yield = (20.914/21.15) * 100

= 98.9 %

3.5 UV Exposure and Blend Film Fabrication

3.5.1 UV Light Exposure

3.5.1.1 Optimization – Solvent and UV Light Wavelength

Solvent nature affects the photosensitivity of the C=C bond of the chalcone unit.[32, 40] Taking this into consideration, five different solvents were used for UV exposure. 4-Hydroxychalcone, being the "cross-linkable" component of the Model Compound, was used for this study. The commercial availability and the well-documented cyclo-addition characteristics of 4-hydroxychalcone justifies its use.

One gram of 4-hydroxychalcone was dissolved in 10 mL of each solvent, NMP, DMAc, DMF, THF and 2ME. Each solution was poured over 4 glass slides. One pair was exposed to 300 nm light for 5 hours while other pair was exposed to 366 nm light for 40 minutes. Exposure to 300 nm UV light was carried out in Rayonet Reactor, Model RPR-100 while UVP portable UV lamp, Model UVGL-25 was used as a source for 366 nm UV light, see Fig. 3.7. Further details regarding the UV light exposure apparatus used are included in Appendix A.

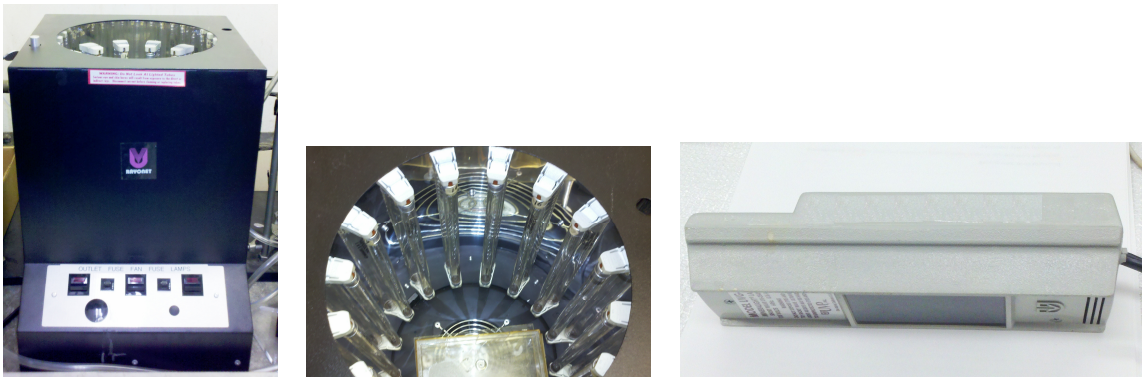

Figure 3.7 – UV lamps, Rayonet Reactor (left), Exposure Chamber in Rayonet Reactor (center) and UVP Portable UV Lamp (right).

Following exposure, the glass plates were placed in a dark ventilated hood for solvent evaporation. After 4-5 days, the solid residues were scrapped from the glass plates and were subsequently used for characterization purposes.

3.5.1.2 Optimization – Solution Concentration

Researchers[32, 40] have demonstrated the relationship between concentration and extent of cyclo-addition reaction for chalcone moieties. Along similar lines, study of effect of solution concentration on photosensitivity for our system was studied. Measured quantities of Model Compound were dissolved in dried NMP such that the final solution concentrations were 0.5 w%, 5 w%, 10 w%, 15 w% and 20 w%. Each of these solutions was exposed to 300 nm UV light using a 3.5 mL cylindrical fluorescence quartz cuvette, refer Fig. 3.8, for 5 hours. Following UV exposure, NMP was evaporated from each solution using vacuum (15 mm Hg) and temperature (45^0C) to obtain reacted Model Compound residue. After 10 days under these conditions, residues of dried exposed Model Compound were obtained which were further used for characterization purposes.

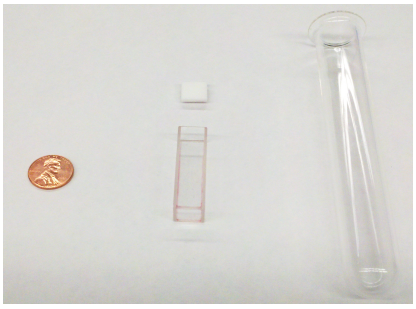

Figure 3.8 - Cylindrical Fluorescence Quartz Cuvette (left) and Quartz Tube (right), Size Comparison with American One Cent Coin.

3.5.1.3 Final Exposures of PI and Model Compound Blends.

PI[Bis-AP-AF/6FDA], the structure of which matches one component of the desired pendent NLO polymer (see Fig. 2.1), was used as a polymer matrix for film casting due to the inability of exposed

Model Compound alone to form a strong film. The Trail-Error technique was used to determine the exact composition of Model Compound-Polyimide solution. A calculated quantity of Model Compound was dissolved in 30 mL dried THF at room temperature for 1 hour using magnetic stirring in a 50 mL beaker covered with aluminum foil. Polyimide powder was added in steps to this solution to avoid any lump formation. Dissolution with stirring was continued for an additional 1 hour. The 30 mL blend solutions were made such that final compositions contained 30 w% PI and 5 w% Model Compound.

The solution was exposed to UV light using 35 mL Quartz tube, refer Fig. 3.8. To study the effect of UV exposure time on photo-cross-linking of Model Compound, solutions were exposed for pre-determined time intervals. Time intervals used were 15 min, 30 min, 45 min, 90 min, 180 min and 300 min. To achieve uniform UV exposure the quartz tube was suspended at the center of exposure chamber (Refer Fig. 3.7). To check for any heating of solution during exposure, the temperature of exposure chamber was monitored. A nominal 1 ^{0}C rise was observed.

After exposure, each solution was divided into two portions, 4 mL and 25 mL. Viscometric studies were carried out using the 4 mL portions. However, direct use of these solutions had a fatal drawback. Due to its low boiling point, THF, the solvent of these solutions, tended to evaporate too quickly at room temperature, causing a thin film to form on the internal surface of the capillary of the Ubbelohde viscometer. In order to avoid errors attributed to this process, secondary solutions were prepared by adding 8 mL dried NMP to each of the original 4 mL exposed solutions. The secondary solutions were thoroughly mixed and were then used for viscometric study. High boiling NMP, being readily miscible with THF and being a good solvent for both Model Compound and Polyimide, was the first choice.

The remaining 25 mL portions of exposed solutions were casted onto glass plates to obtain films for mechanical tests.

3.5.2 Blend Film Fabrication

Equal calculated quantities of PI[Bis-AP-AF/6FDA] powder were added to all exposed MC-PI mixtures. This ensured that the film formation upon casting could tolerate the forces experienced during handling, finishing and mechanical clamping. Since all six sample sets (exposure times = 15, 30, 45, 90, 180 and 300 min) have exact same final composition, 90 w% PI and 10 w% MC, comparative study of mechanical properties remains unaffected by addition of extra polyimide.

All six solutions of 90PI-10MC in THF were casted individually on thoroughly cleaned glass plate film mold. Multiple layers (6 layers) of Scotch tape formed the walls for the film mold. Because of the high volatility of THF solvent at RT, 24 hours of drying time was sufficient to obtain good blend films perfectly suitable for Mechanical Tests.

Film edges were smoothened using ultra-fine Emery paper to remove any defects leading to stress concentration areas during test loads. Film samples were filed into sizes prescribed by ASTM D882 (Tensile Test)[41] and ASTM D4065 (DMA).[42]

3.6 Primary Testing Methods

3.6.1 Tensile Testing – ASTM D882

Instrument : Instron 4301, Software – Blue Hill ver. 2

Testing Parameters : Strain rate = 25mm/min

Gauge length = 50.8 mm (2 in)

Initial strain rate = 0.5 mm/mm-min

Sample Conditioning : 23 ± 2^0C for 24 hours

Number of Samples : 4 – 5

Sample Dimensions : Length = 100 ± 2 mm

Avg. Width = 12 mm, $\sigma = 3.2119$

Avg. Thickness = 0.4743 mm, $\sigma = 0.06831$

3.6.2 Dynamic Mechanical Analyzer – ASTM D4065

Instrument : Seiko DMS200, Software – T Slice Analysis

Testing Parameters : Test Temperature = Room Temperature

Test Frequencies = 0.1 Hz, 1 Hz, 10 Hz, 20 Hz

Sample Conditioning : 23 ± 2^0C for 24 hours

Number of Samples : 2 (Each tested twice)

Sample Dimensions : Length = 50 ± 1 mm Test Length = 20 mm

Avg. Width = 8 mm

Avg. Thickness = 0.4743 mm, σ = 0.06831

3.6.3 Ubbelohde Viscometry

Viscometer Type : Ubbelohde Viscometer, Size 2B

Solution Composition : 4mL 30PI-5MC in THF + 8mL Pure Dried NMP

Calculations:

$$\text{Normalized Viscosity} = \frac{\text{Avg. time (in sec.) for Sample Solution}}{\text{Avg. time (in sec.) for Solvent (NMP+THF) Solution}}$$

3.7 Characterization Methods

3.7.1 1-D Proton Nuclear Magnetic Resonance Spectroscopy (1-D ^{1}H NMR)

Proton NMR was used for structural confirmation of products. 300 MHz Bruker NMR Spectrometer with Bruker's Icon NMR software was used to obtain spectra. Integrations and data analysis were done using XWin NMR software. Products to be analyzed were dissolved in deuterated solvents like deuterated chloroform (d^1-$CDCl_3$) or deuterated dimethylsulfoxide (d^6-DMSO). Use of vortex plate ensured complete dissolution.

3.7.2 2-D Proton Nuclear Magnetic Resonance Spectroscopy (2-D ^{1}H-^{1}H NMR)

A 2-D ^{1}H NMR spectrum was obtained for the UV cross-linker pendent group and Model Compound. Both compounds were dissolved in deuterated chloroform (d^{1}-$CDCl_3$) and deuterated dimethylsulfoxide (d^{6}-DMSO), and were vortexed into solution. The two-dimensional NMR spectrum were obtained at room temperature using a 300 MHz Bruker NMR Spectrometer using Bruker's Topspin NMR software. (See Appendix B)

3.7.3 Fourier Transform-Infrared Spectroscopy (FT-IR)

Structural confirmation was also obtained using FT-IR spectroscopy. A Shimadzu IR Prestige-21 was used for this purpose. Spectra were obtained in absorbance mode with range from 4000 to 400 cm^{-1} with a resolution of 4 cm^{-1}.

3.7.4 Liquid Chromatography-Mass Spectroscopy (LC-MS)

LC-MS was used to analyze the extent of cyclo-addition reaction for 4-hydroxychalcone exposed to two different UV light sources and in five different solvents. Applied Biosystems 3200 Q Trap LC/MS/MS was used for this purpose. Acetonitrile with a 1% acetic acid spike was used as the solvent for all the products.

3.7.5 Ultraviolet-Visible Spectroscopy (UV-Vis)

A Shimadzu High Resolution UV-2401 was used to obtain the UV spectra for UV exposed 4-hydroxychalcone, Model Compound, Polyimide and PI-MC blends. Acetonitrile was used as solvent.

3.7.6 Differential Scanning Calorimeter (DSC)

A TA Instruments DSC 2010 was used to study the glass transition temperature and melting point of Model Compound and Polyimide. DSC was carried out in inert atmosphere of nitrogen. Process

parameters used were: Sample Size - 3 to 5 mg in enclosed Aluminum pan, Heating Rate - 2 ^{0}C/min from RT to 150 ^{0}C and N_2 gas flow rate - 50 mL/min.

3.7.7 Thermogravimetric Analysis (TGA)

A TA Instruments TGA 2050 was used to study the thermal degradation behavior of Model Compound and Polyimide, to help understand their relative thermal stabilities. TGA was carried out at room atmosphere. Process parameters used were: Sample Size - 10 to 20 mg in Platinum TGA pan, Heating Rate - 10 ^{0}C/min from RT to 500 ^{0}C and air flow rate - 115 mL/min.

CHAPTER 4:
RESULTS

4 RESULTS

4.1 UV Cross-linker Characterization

4.1.1 1-D Proton Nuclear Magnetic Resonance Spectroscopy

^{1}H NMR was used for structural confirmation of the product. Consistency of all observed peaks with proposed structures, thus, confirmed the formation of UV cross-linkable tethered group and UV cross-linker following the successive reactions.

The ^{1}H NMR spectrum for UV cross-linkable tethered group is shown in Fig. 4.1. Aliphatic protons associated with alkane chain are observed at 2.00 ppm (m; 2H), 3.42 ppm (t; 2H) and 4.02 ppm (t; 2H). Peaks observed at 7.35 ppm (d; 2H) and 7.75 ppm (d; 2H) correspond to protons associated with photo-reactive unsaturation, prominent site for UV cross-linking. The aromatic protons of benzene ring are observed at 6.87 ppm (d; H), 7.45 ppm (d; H), 7.53 ppm (d; H) and 7.95 ppm (d; H).

^{1}H NMR ($CDCl_3$, ppm): 2.00 (m; 2H), 3.42 (t; 2H), 4.02 (t; 2H), 7.35 (d; H), 7.75 (d; H), 6.87 (d; H), 7.45 (d; H), 7.53 (d; H) and 7.95 (d; H).

^{1}H NMR spectrum for UV cross-linker is shown in Fig. 4.2. Prominent shift of all peaks from their original positions was observed in ^{1}H NMR spectra upon attachment of UV cross-linkable tethered group to Terephthalic acid molecule, thus, confirming the synthesis of UV cross-linker. Apart from this, presence of strong peak at 8.20 ppm (s; 4H) associated with aromatic protons in Terephthalic acid, further confirms the product formation.

^{1}H NMR ($CDCl_3$, ppm): 2.00 (m; 4H), 4.02 (t; 4H), 4.40 (t; 4H), 7.35 (d; 2H), 7.75 (d; 2H), 6.87 (d; 2H), 7.45 (d; 2H), 7.53 (d; 2H) and 7.95 (d; 2H) and 8.20 (s; 4H).

Corroboration of these assignments was accomplished using 2-D proton vs. proton NMR. The details of these experiments are included in Appendix B.

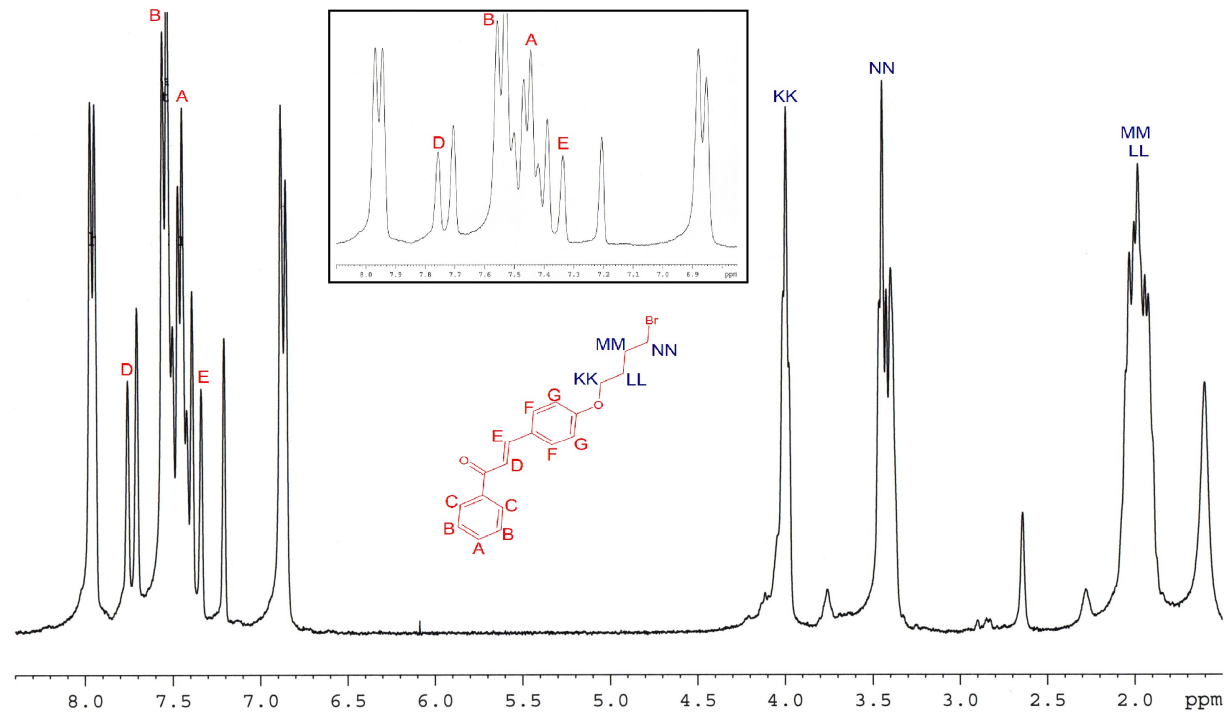

Figure 4.1 – ^{1}H NMR of Synthesized UV Cross-linkable Pendent Group

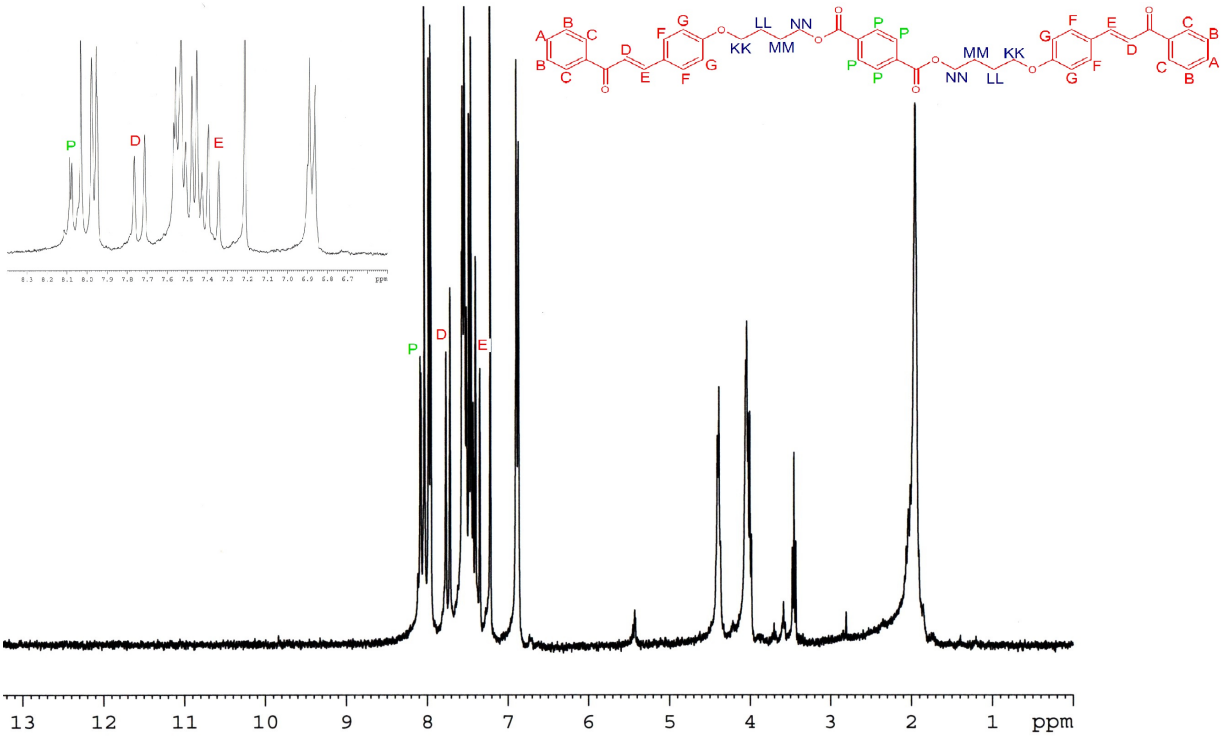

Figure 4.2 – ^{1}H NMR of Synthesized Terephthalic Acid-based, UV Cross-linkable Model Compound

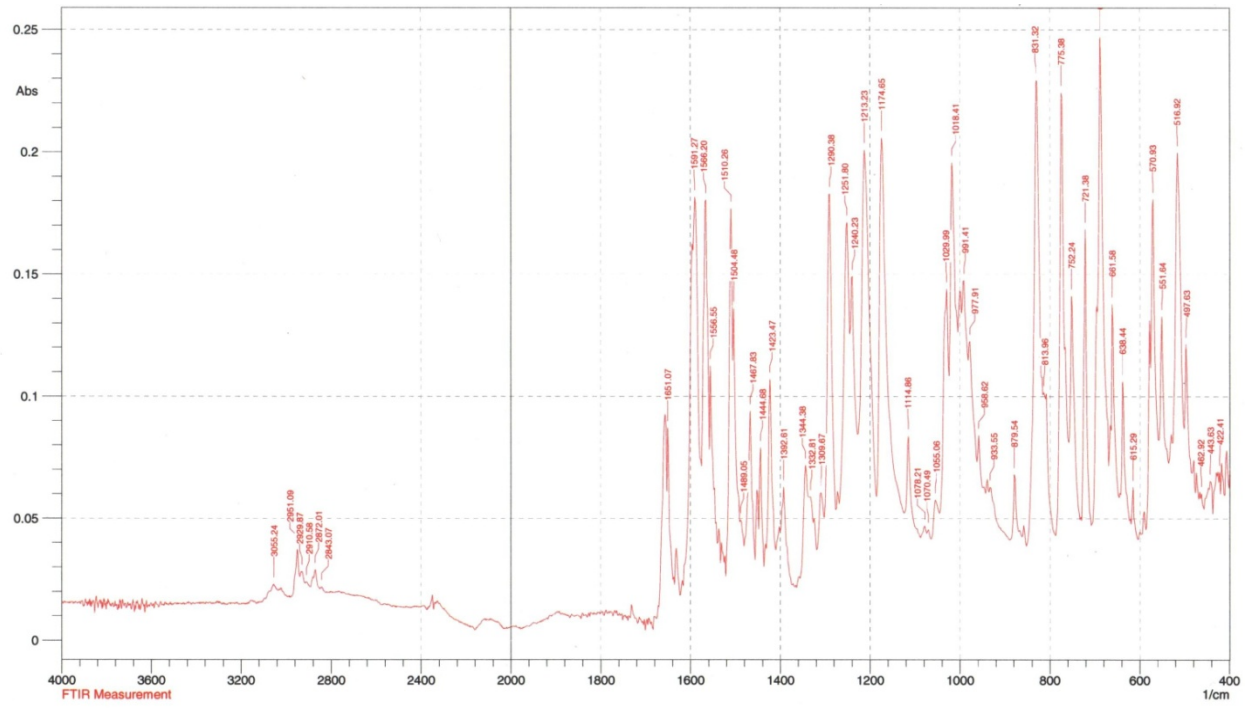

Figure 4.3 – FT-IR of UV Cross-linkable Pendent Group

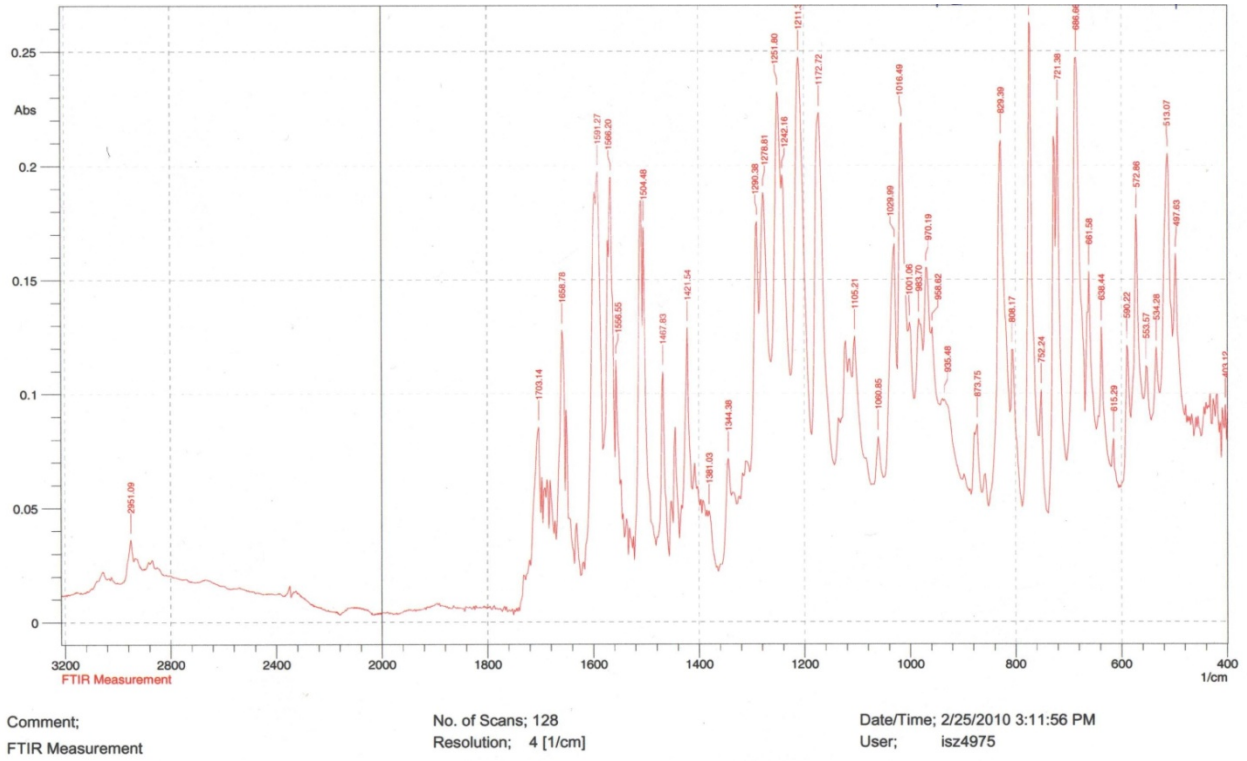

Figure 4.4 – FT-IR of Terephthalic Acid-based, UV Cross-linkable Model Compound

4.1.2 Fourier Transform-Infrared Spectroscopy

FT-IR provided structural confirmation for both intermediate as well as final product. Fig 4.3 depicts FT-IR spectrum for UV cross-linkable tether group, intermediate product. Peaks at 570 cm^{-1} associated with C-Br, along with peak at 1658 cm^{-1} for C=O, at 1591 cm^{-1} for conjugated C=C and 775 cm^{-1} for CH_2 bend (4 or more) alkane verify the presence for both reactants. Most importantly, peaks at 1290, 1018 cm^{-1} corresponding to C-O ether linkage confirms the successful reaction between 4-hydroxychalcone and 1,4-dibromobutane.

FT-IR spectrum for UV cross-linker is as shown in Fig 4.4. All peaks except for C-Br Peak are observed with new strong peak at 1703 cm^{-1} corresponding to ester linkage (-COO-) verify the reaction completion yielding UV cross-linker.

4.1.3 Differential Scanning Calorimeter

DSC thermogram, performed for unexposed Model Compound is as shown in Fig. 4.5. It was observed that unexposed model compound is heat sensitive. The low melting point observed at 69 ^0C imposed restrictions on test conditions. During cooling three distinct exothermic peaks associated with crystallization were observed consistent with the occurrence of polymerization of MC by thermo-cyclo-addition reaction, resulting polymer with very broad molecular weight distribution. As no crystallization peak below 69 ^0C was observed, complete exhaustion of MC monomer can be concluded.

4.1.4 Thermo-gravimetric Analysis

Thermo-gravimetric analysis was performed for unexposed and UV exposed model compound. It was observed that degradation on-set temperature of UV-cured sample is higher, consistent with the polymerization reaction of model compound upon UV exposure. TGA thermograms for exposed-unexposed Model Compound are shown in Figs. 4.6a - 4.6b.

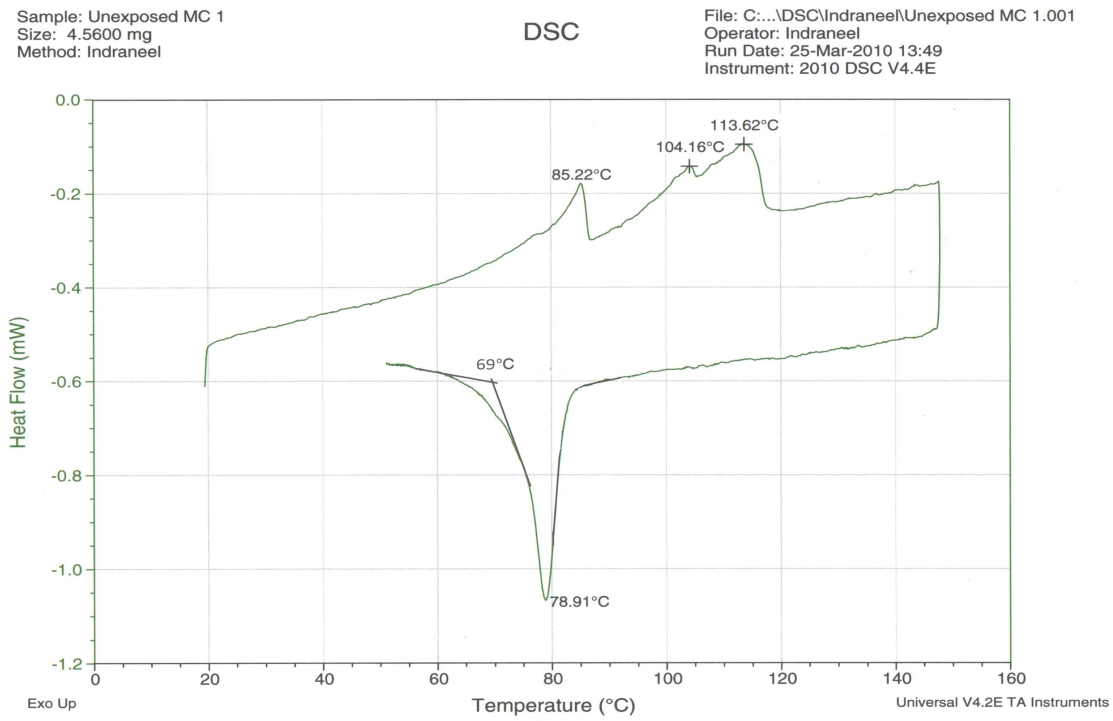

Figure 4.5 – DSC Thermogram of Unexposed Model Compound

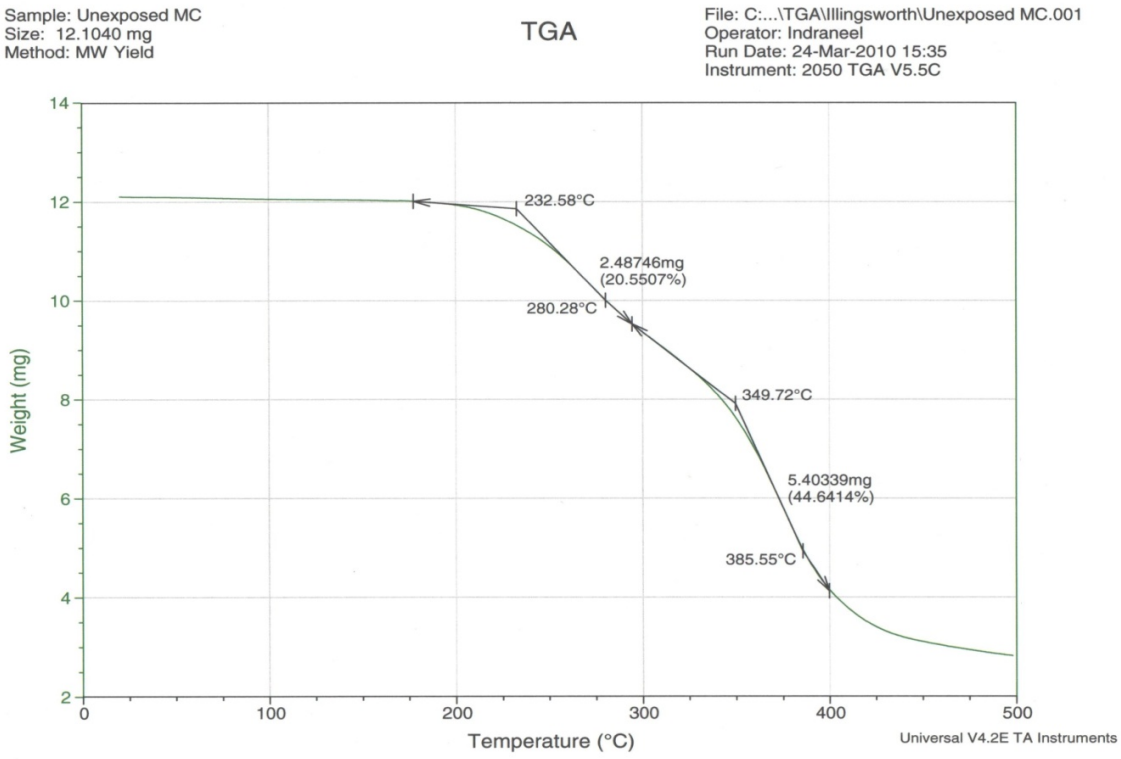

Figure 4.6a – TGA Thermogram of Unexposed Model Compound

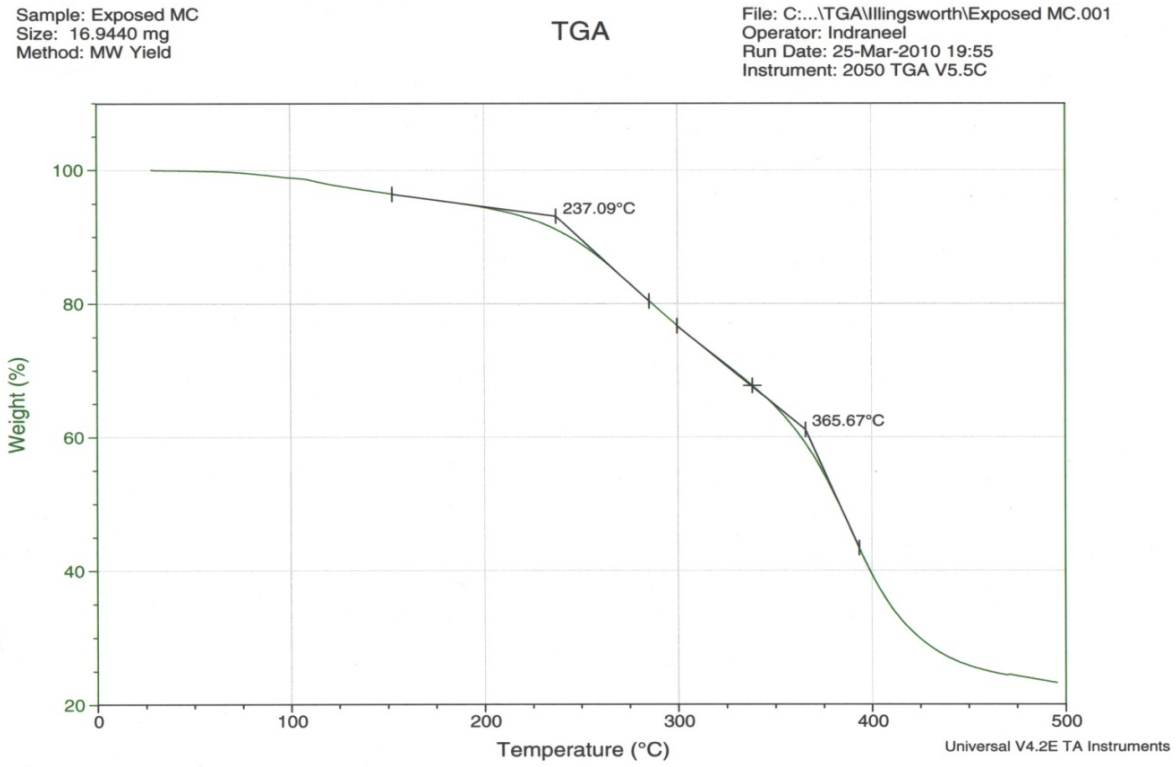

Figure 4.6b – TGA Thermogram of UV Exposed Model Compound

4.2 PI[6FDA/Bis-AP-AF] Characterization

4.2.1 1-D Proton Nuclear Magnetic Resonance Spectroscopy

Structural confirmation for Polyimide product was provided by ^{1}H NMR. All peaks observed are in accordance with the expected structure, thus, confirming the synthesis of PI[6FDA/Bis-AP-AF].[43, 44] ^{1}H NMR spectrum for Polyimide is shown in Fig. 4.7. Protons associated with hydroxyl group of two phenols in Bis AP-AF are indicated by peak at 10.34 ppm (s; 2H). Aromatic protons corresponding to the Bis AP-AF residue are observed at 6.99 ppm (s; 2H), 7.13 ppm (s; 2H) and 7.42 ppm (s; 2H). Peaks for aromatic protons present in 6FDA residue are observed at 7.64 ppm (s; 2H), 7.85 ppm (s; 2H) and 8.05 ppm (s; 2H).

^{1}H NMR ($CDCl_3$, ppm): 6.99 ppm (s; 2H), *7.13* ppm (s; 2H), 7.42 ppm (s; 2H), 7.64 ppm (s; 2H), 7.85 ppm (s; 2H), 8.05 ppm (s; 2H), 10.34 ppm (s; 2H).

4.2.2 Fourier Transform-Infrared Spectroscopy

Structural verification for polyimide was provided by FT-IR. The FT-IR spectrum for Polyimide is as shown in Fig. 4.8. Peaks at 1788, 1726, 1371 and 723 cm^{-1} verify the successful synthesis of polyimide.[43, 44] Broad peak at 3000 for O-H stretch, sharp peaks at 1105 for C-OH stretch and 642 for OH out-of-plane deformation demonstrate the presence of phenol groups. Peaks at 1254 and 1172 cm^{-1} correspond to aliphatic C-F stretch.

4.2.3 Differential Scanning Calorimeter

DSC thermogram, performed for polyimide is as shown in Fig. 4.9. Synthesized polyimide was observed to have very high glass transition temperature beyond the temperature range studied (23 ^{0}C - 350 ^{0}C), and no melting point.

4.2.4 Thermo-gravimetric Analysis

TGA thermogram, performed for polyimide is as shown in Fig. 4.10. Minor weight loss was observed around 100^{0}C, due to evaporation of residual water. First major weight loss was observed around 200^{0}C, most likely due to evolution of occluded NMP. Based on this, care was taken to remove as much NMP as possible from polyimide powder prior to its use. Thermal degradation starting around 370^{0}C, is in accordance with thermal stability displayed by most polyimides.

4.3 4-Hydroxychalcone Characterization – Optimization

4.3.1 Solvent and UV Light Wavelength

4.3.1.1 1-D Proton Nuclear Magnetic Resonance Spectroscopy

^{1}H NMR spectra were obtained for 4-hydroxychalcone exposed to two different UV light wavelengths; 300 nm and 366 nm, with five different solvent mediums; NMP, DMAc, DMF, THF and 2ME, as shown in Figs. 4.11-4.16. Susceptibility of formation of more than one configuration upon cross-linking for chalcone moieties is a well-documented fact throughout the literature.[29-30, 32, 45]

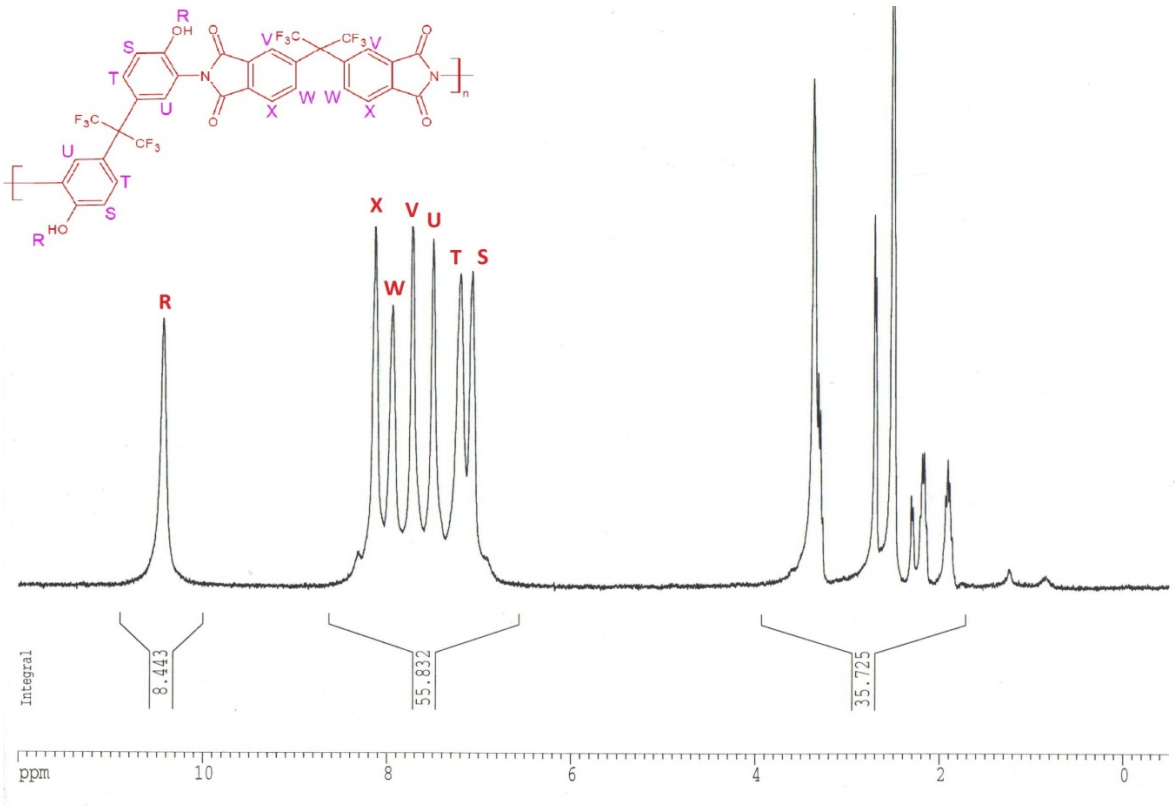

Figure 4.7 – ^{1}H NMR of Synthesized Polyimide

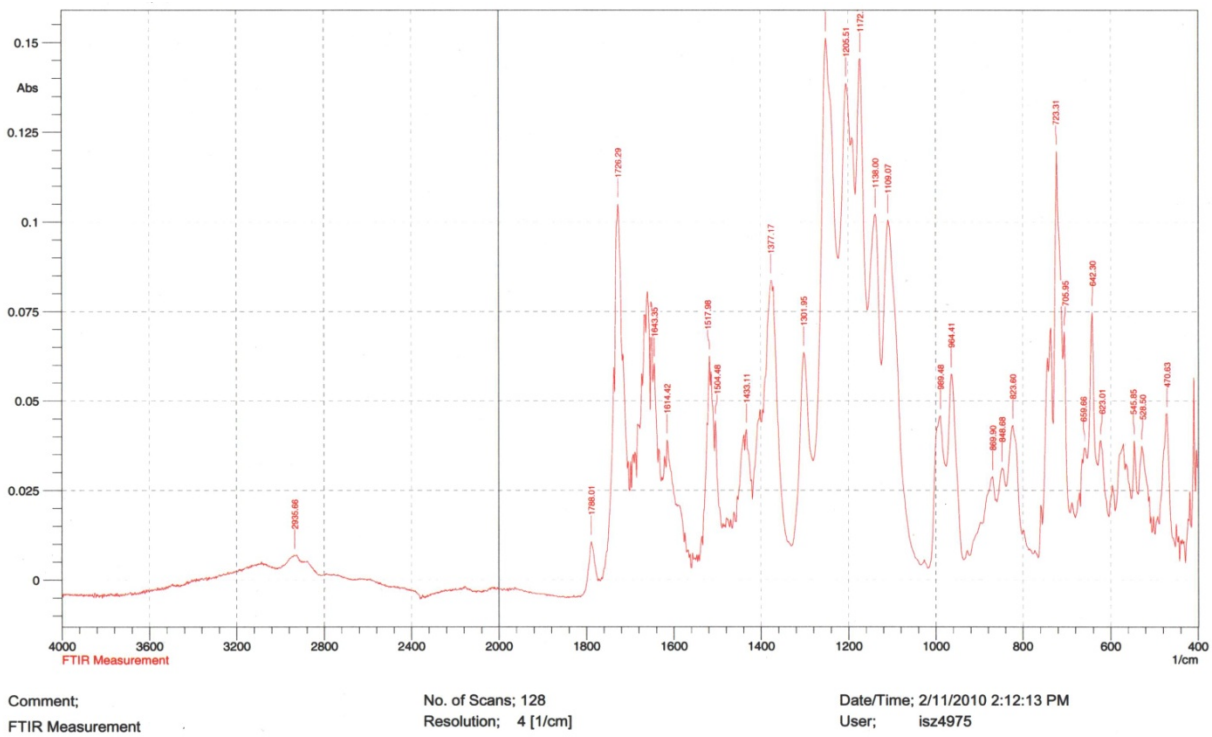

Figure 4.8 – FT-IR of Polyimide

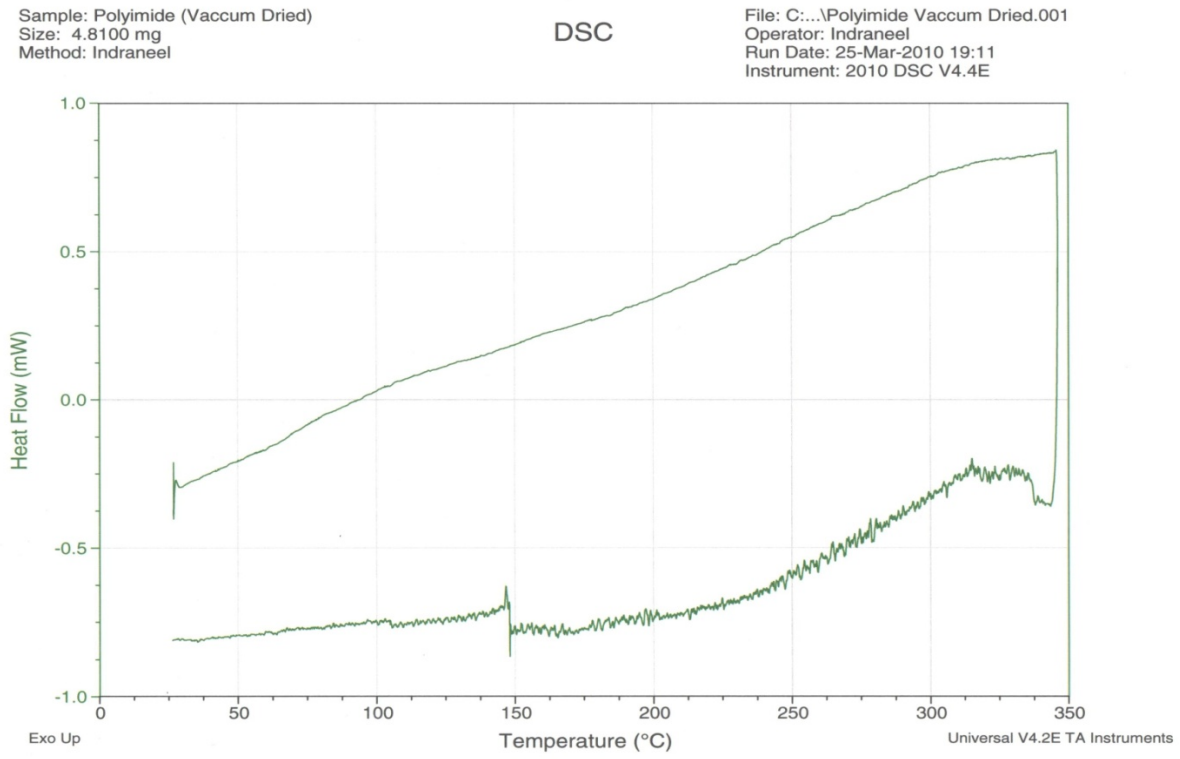

Figure 4.9 – DSC Thermogram of Polyimide

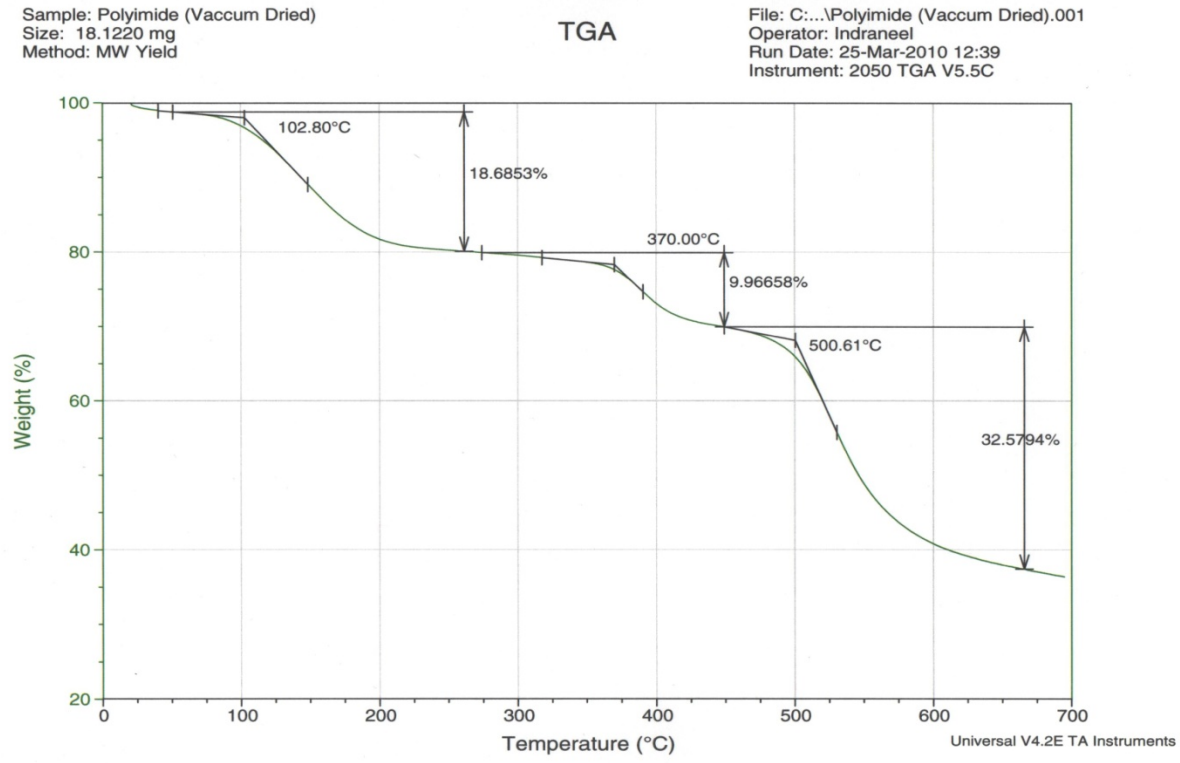

Figure 4.10 – TGA Thermogram of Polyimide

During cross-linking, 4-hydroxychalcone undergoes (2π+2π) cyclo-addition reaction resulting in mixture of cis- as well as trans- configurations around the formed cyclo-butane ring. Observation of peaks associated with both configurations consolidated the presence of mixture of both isomers upon UV exposure. Amongst all the solvent used as medium for UV exposure, NMP and DMF showed most prominent effect followed by THF. While amongst the two UV light wavelengths used, only 300 nm UV light exposed solutions have positive indication of formation of 4-membered ring structure.

Predicted ^{1}H NMR for unexposed 4-hydroxychalcone, exposed 4-hydroxychalone with both cis- and trans- configuration were obtained using web-based database-simulation software for NMR prediction.[46] Guidelines provided by these predicted NMR spectra not only confirmed the formation of 4-membered ring structure, but also presence of mixture of both configuration products in actual NMR. A detailed study would be required to completely understand and locate peaks associated with each configuration individually, which is currently beyond the scope of this project. Refer to Fig. 4.17.

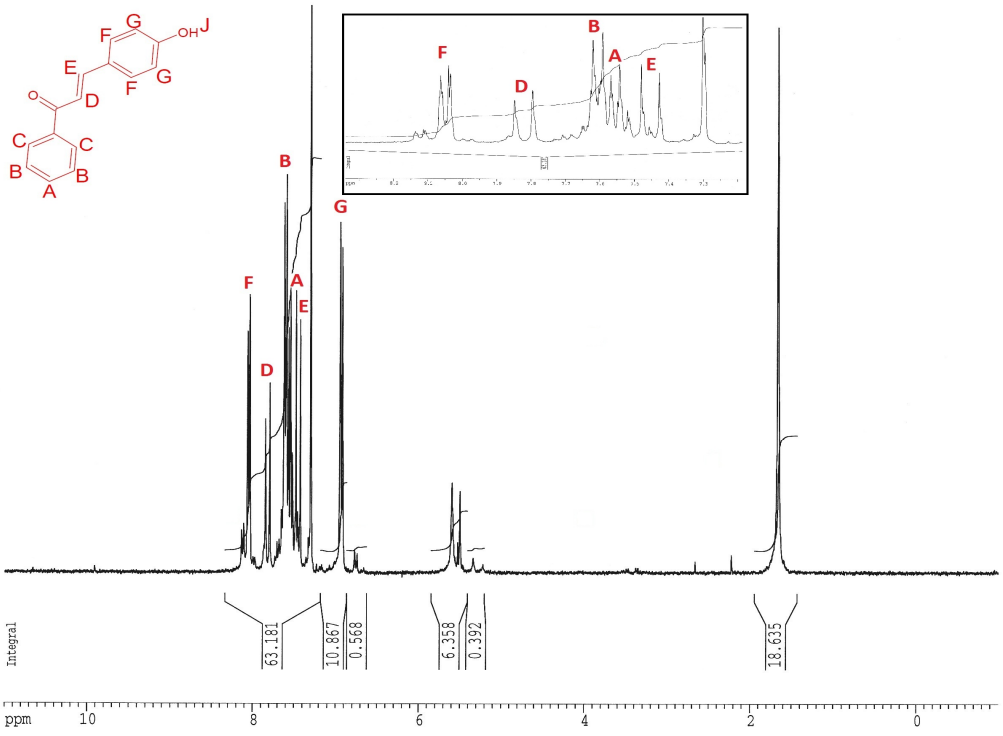

Figure 4.11 – ^{1}H NMR of Unexposed 4-Hydroxychalcone

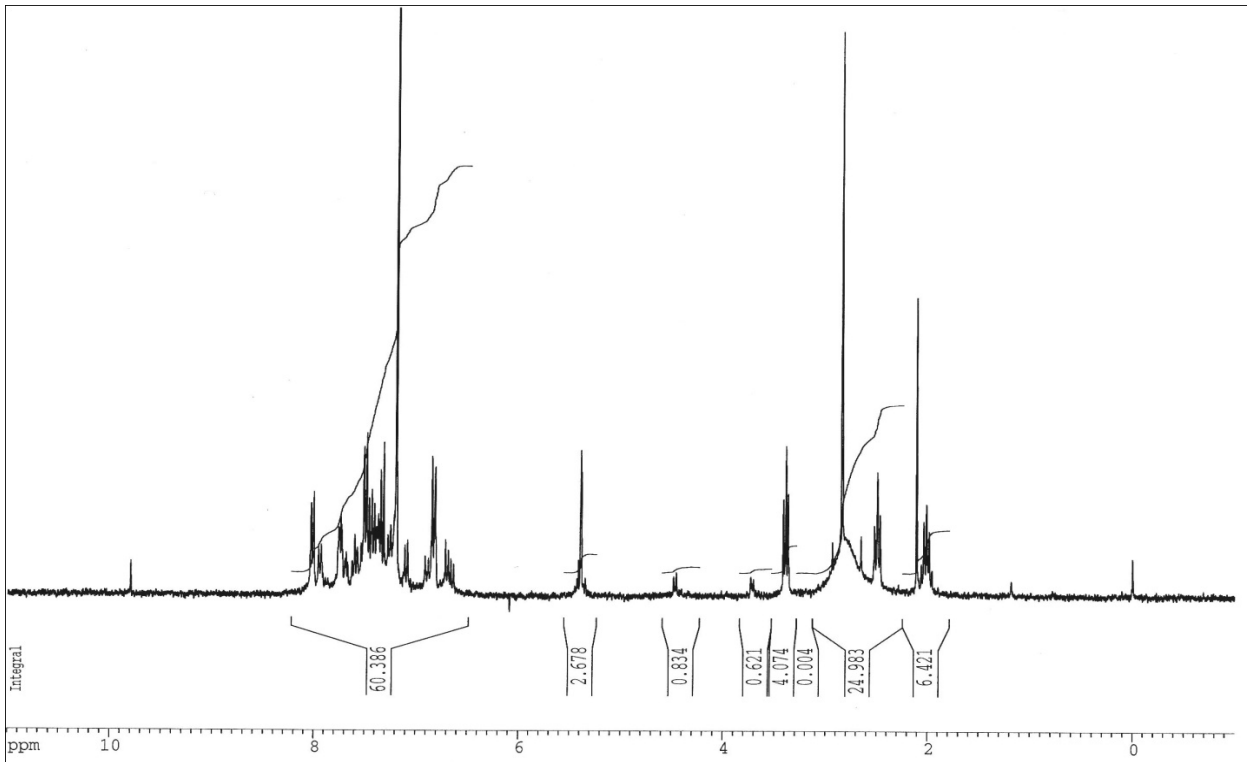

Figure 4.12 – ^{1}H NMR of 4-Hydroxychalcone Exposed to 300 nm UV Light in NMP Solvent

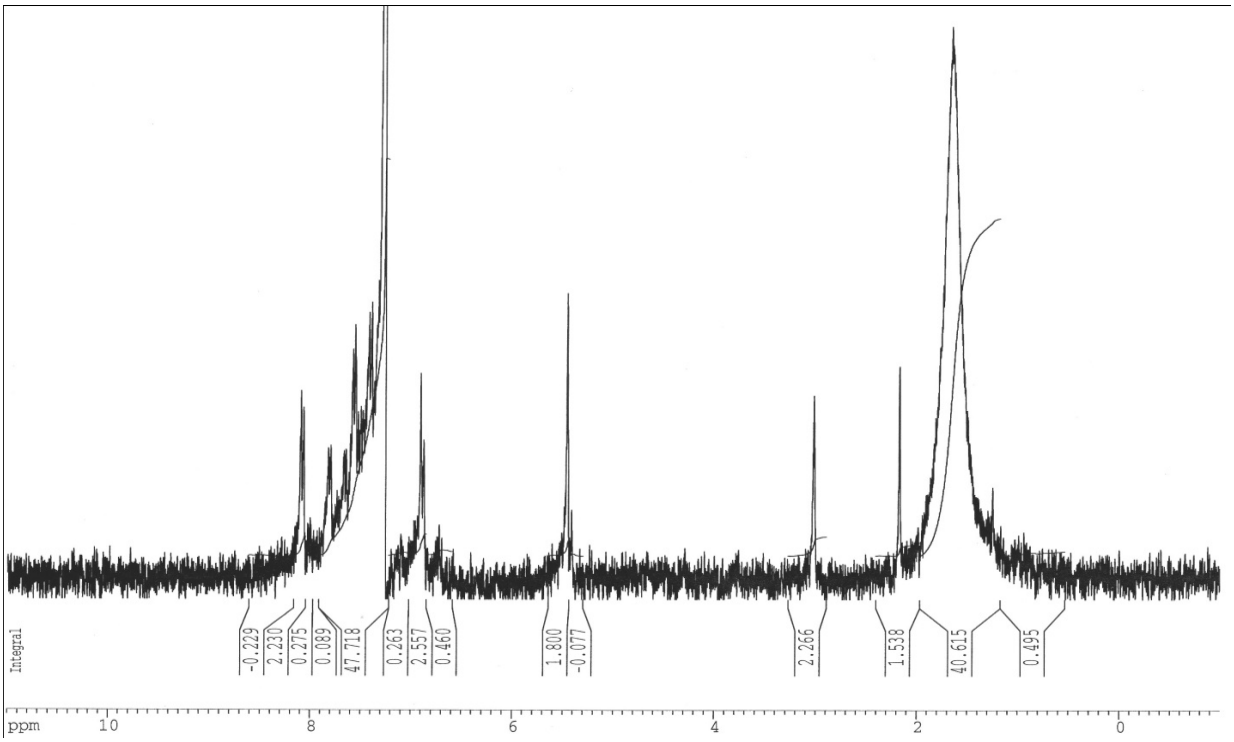

Figure 4.13a – ^{1}H NMR of 4-Hydroxychalcone Exposed to 300 nm UV Light in DMAc Solvent

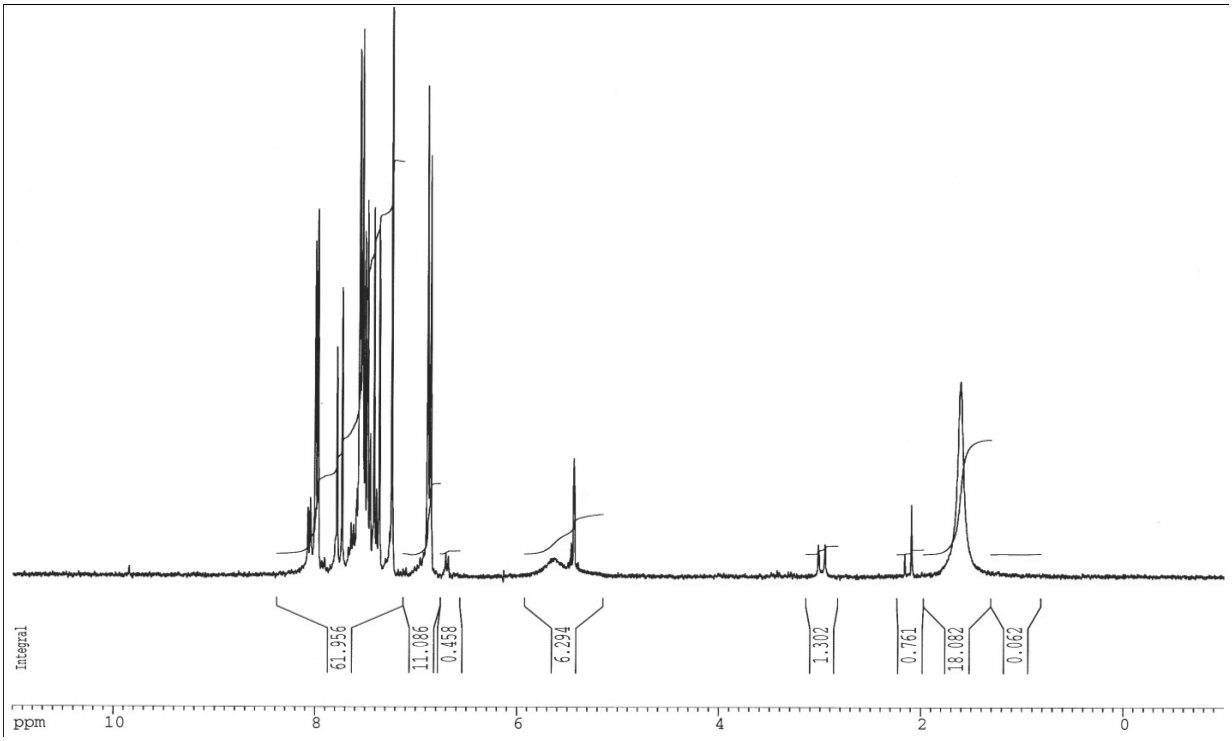

Figure 4.13b – ^{1}H NMR of 4-Hydroxychalcone Exposed to 366 nm UV Light in DMAc Solvent

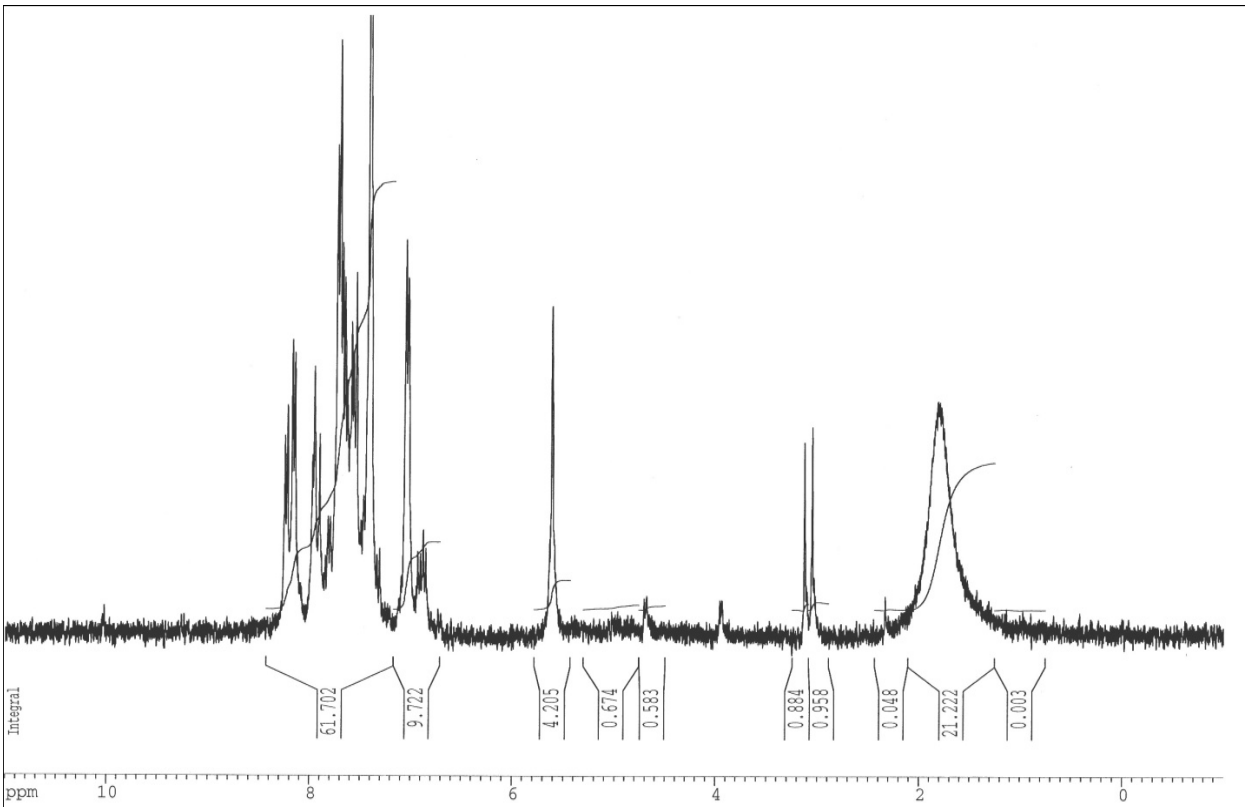

Figure 4.14a – ^{1}H NMR of 4-Hydroxychalcone Exposed to 300 nm UV Light in DMF Solvent

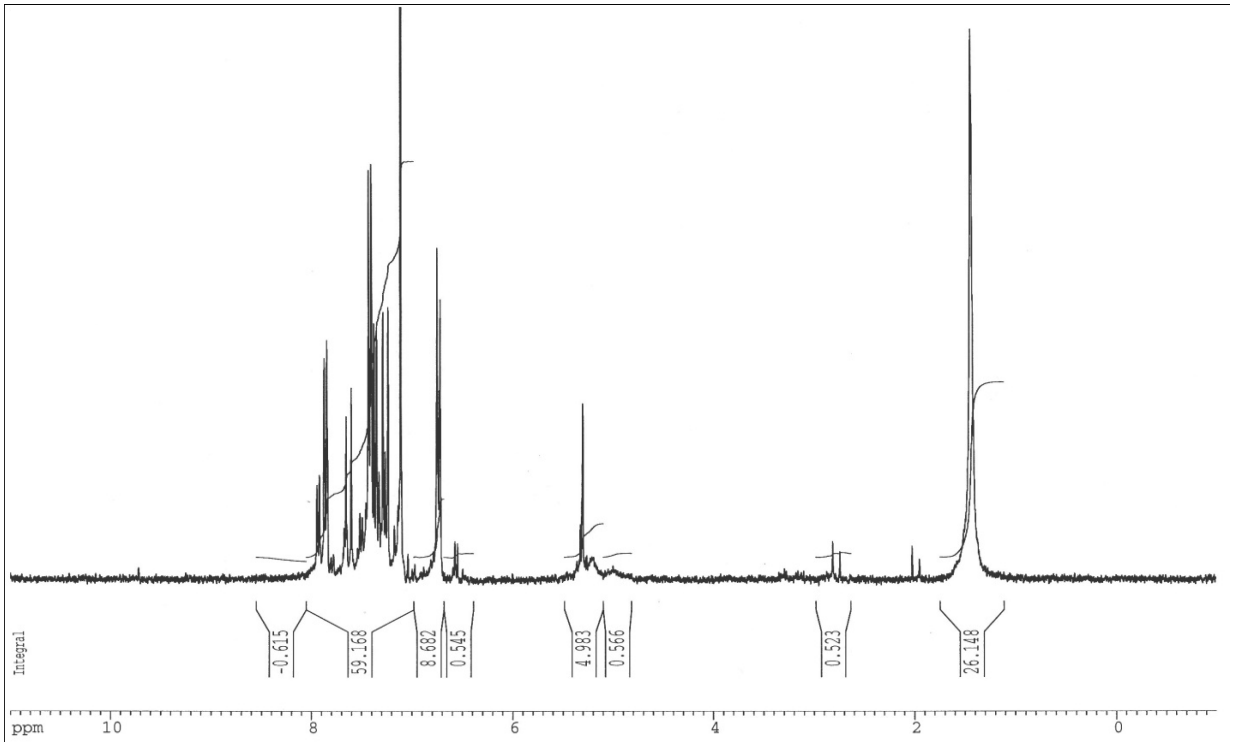

Figure 4.14b – ^{1}H NMR of 4-Hydroxychalcone Exposed to 366 nm UV Light in DMF Solvent

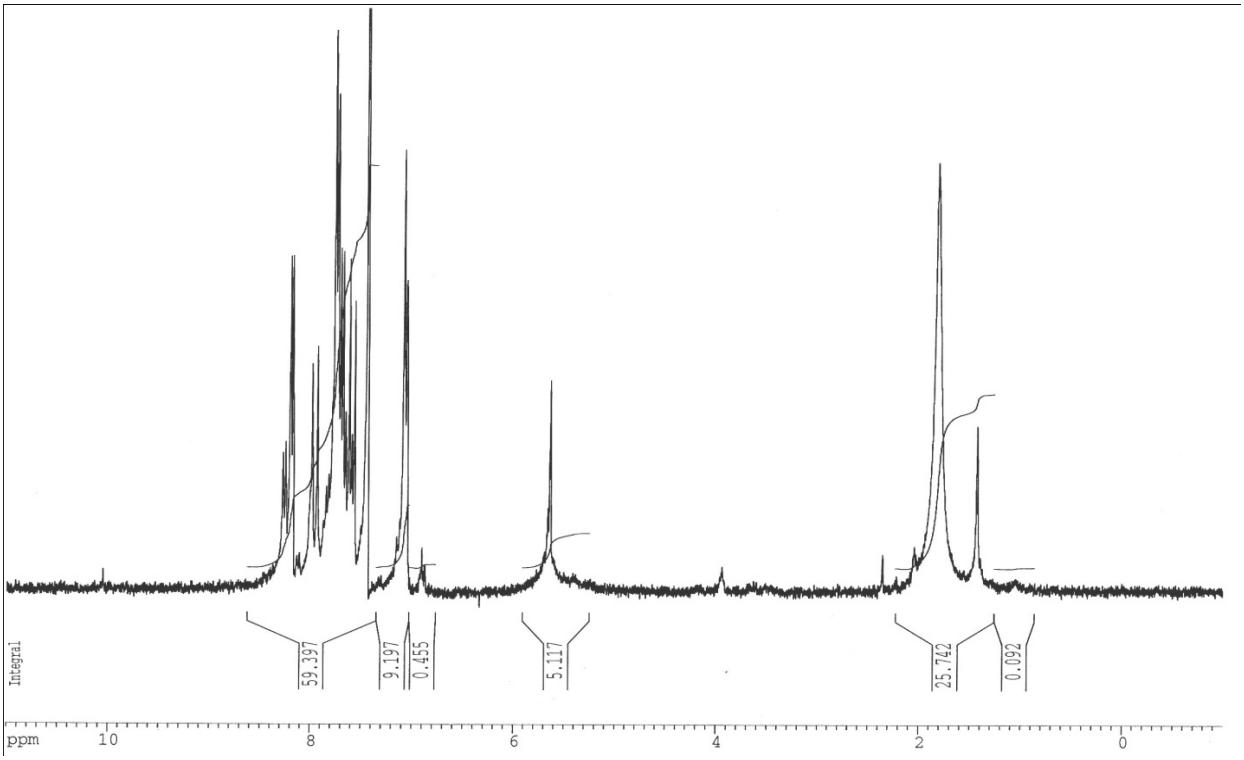

Figure 4.15a – ^{1}H NMR of 4-Hydroxychalcone Exposed to 300 nm UV Light in THF Solvent

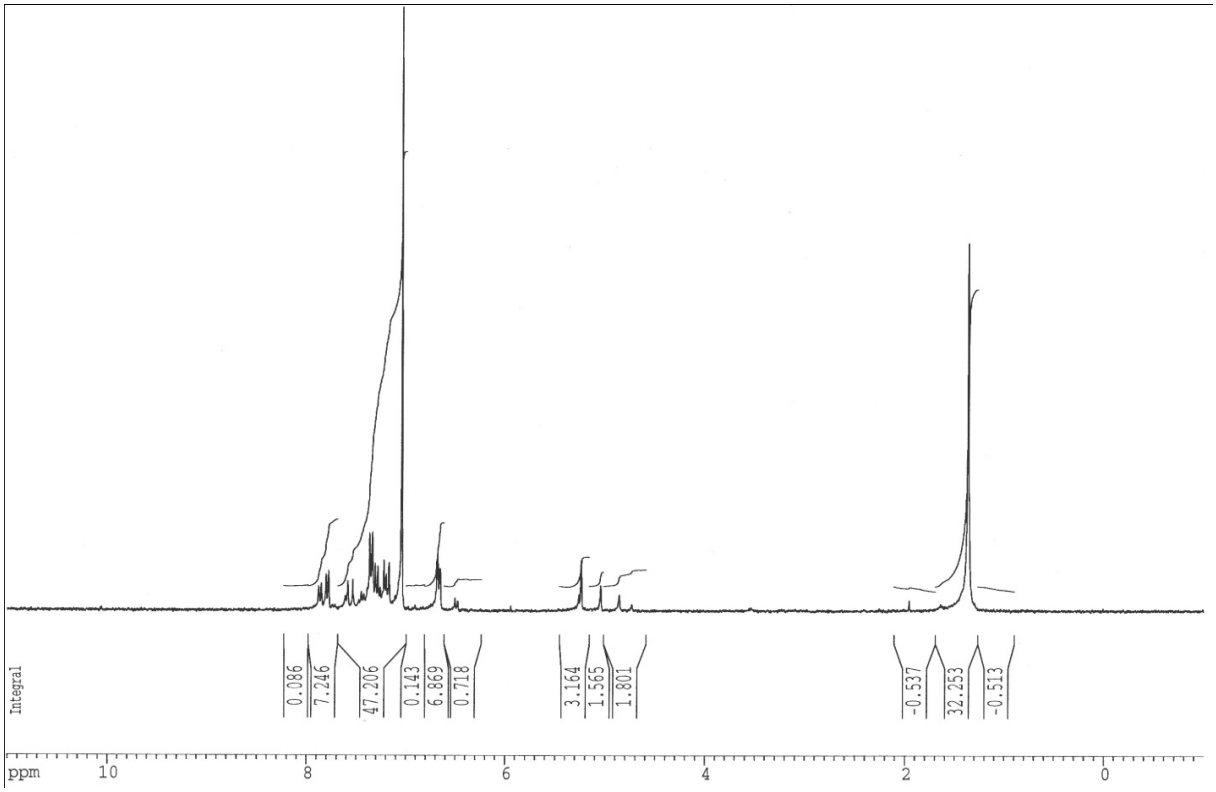

Figure 4.15b – ^{1}H NMR of 4-Hydroxychalcone Exposed to 366 nm UV Light in THF Solvent

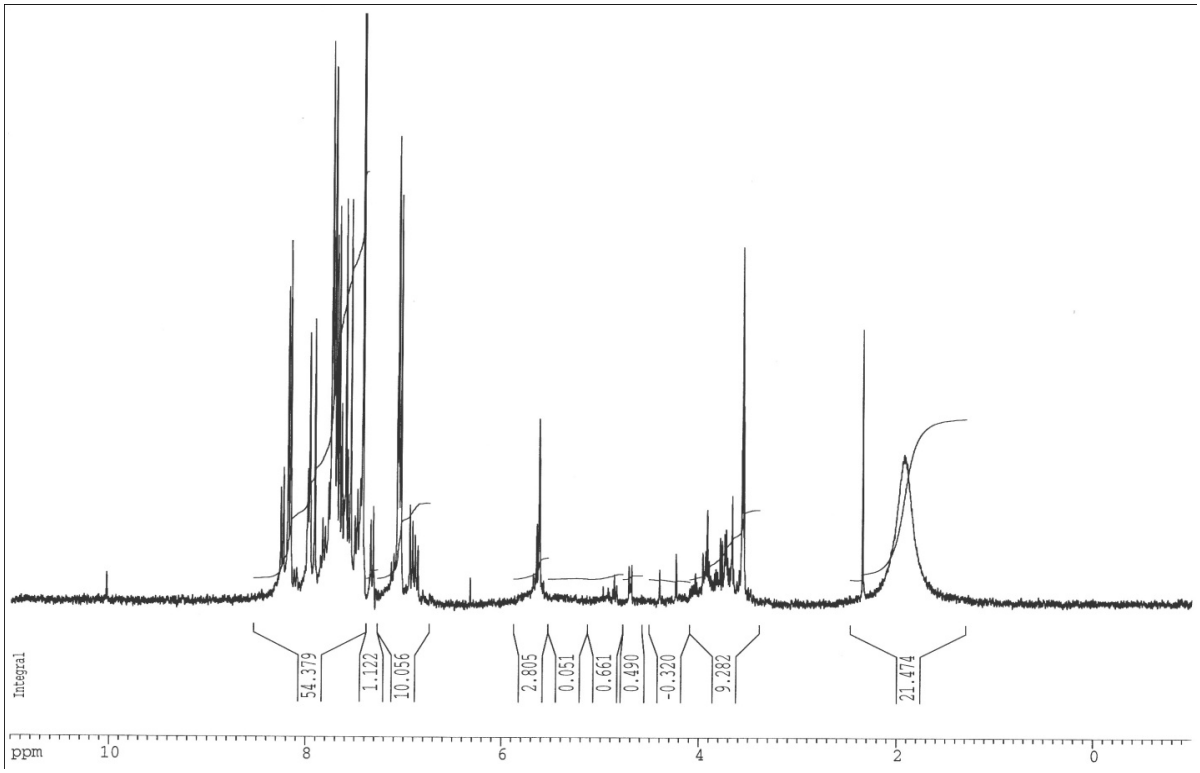

Figure 4.16a – ^{1}H NMR of 4-Hydroxychalcone Exposed to 300 nm UV Light in 2ME Solvent

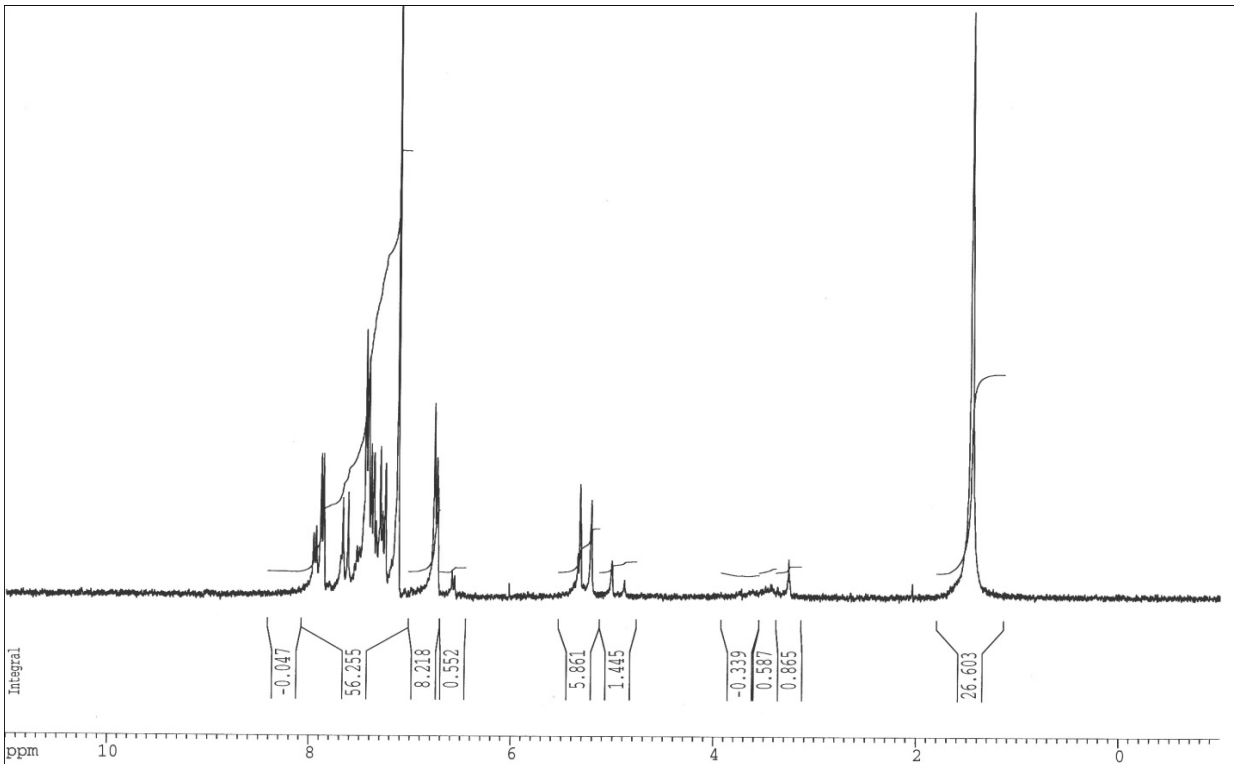

Figure 4.16b – ^{1}H NMR of 4-Hydroxychalcone Exposed to 366 nm UV Light in 2ME Solvent

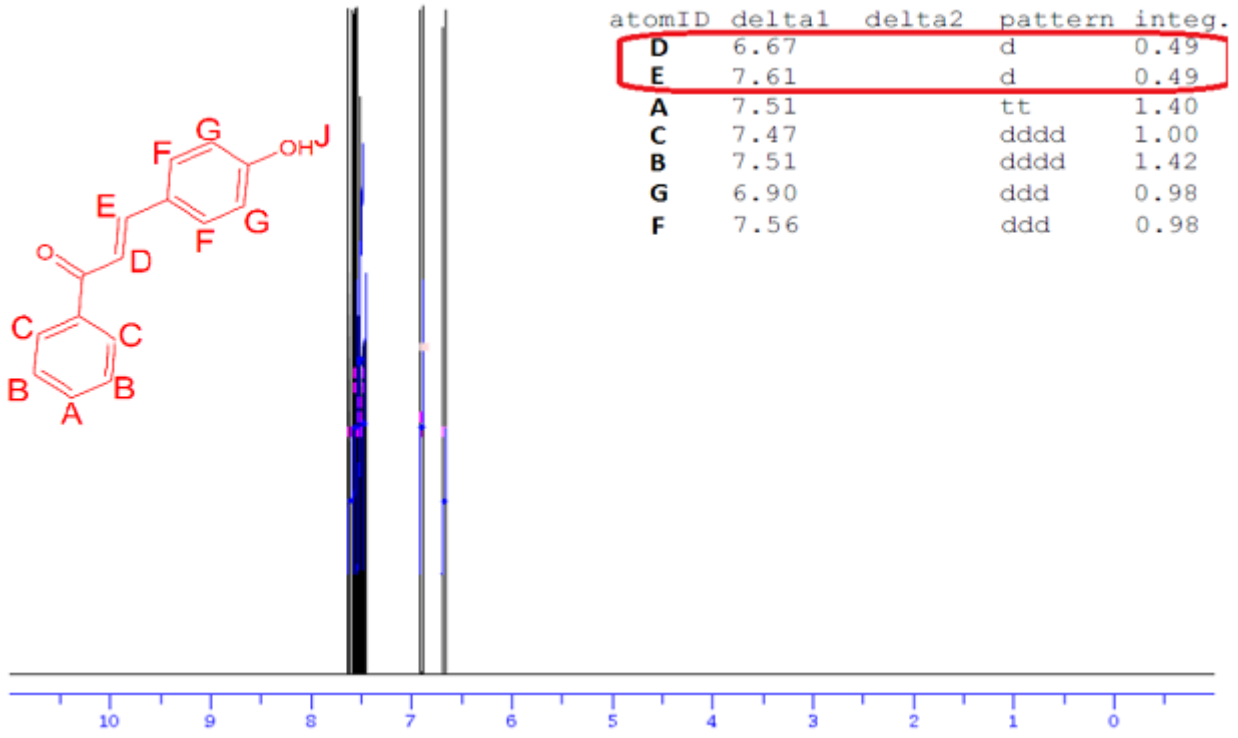

atomID	delta1	delta2	pattern	integ.
D	6.67		d	0.49
E	7.61		d	0.49
A	7.51		tt	1.40
C	7.47		dddd	1.00
B	7.51		dddd	1.42
G	6.90		ddd	0.98
F	7.56		ddd	0.98

Figure 4.17a – Predicted ^{1}H NMR of 4-Hydroxychalcone

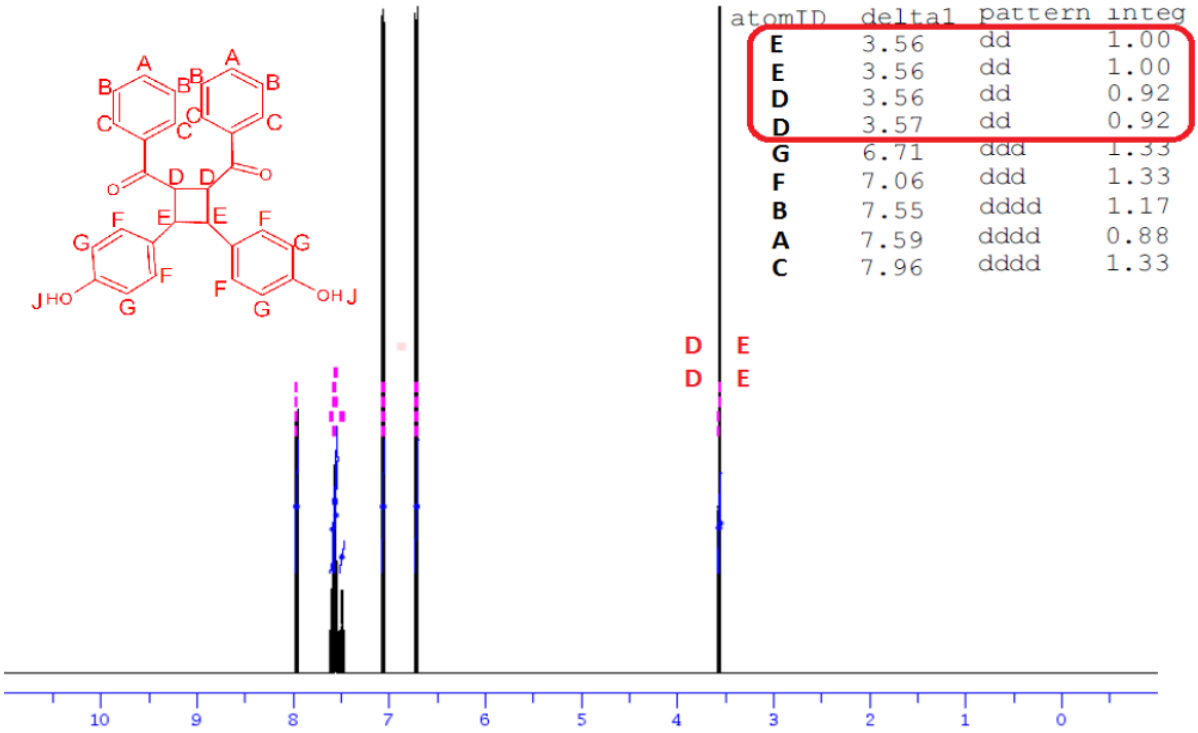

Figure 4.17b – Predicted [1]H NMR of UV Exposed 4-Hydroxychalcone; Cis- Isomer

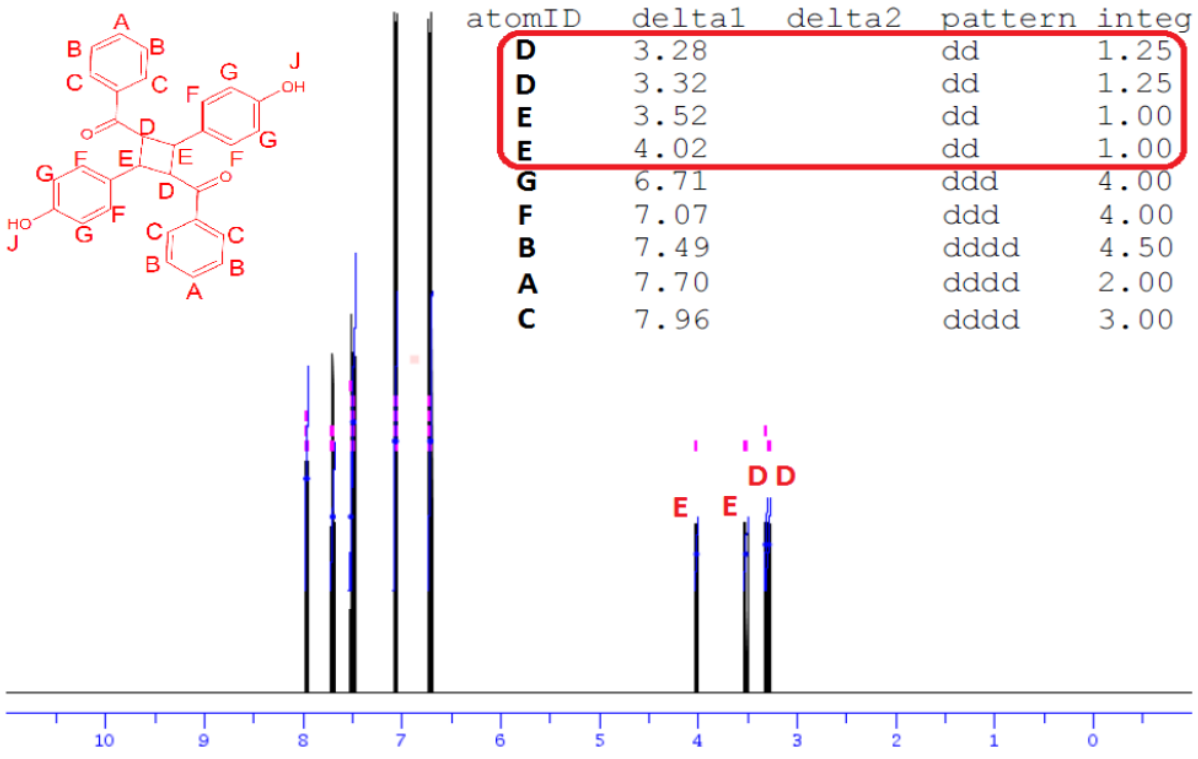

Figure 4.17c – Predicted [1]H NMR of UV Exposed 4-Hydroxychalcone; Trans- Isomer

4.3.1.2 Fourier Transform-Infrared Spectroscopy

FT-IR spectra were obtained for 4-hydroxychalcone exposed to two different UV light wavelengths; 300 nm and 366 nm, with five different solvent mediums; NMP, DMAc, DMF, THF and 2ME, as shown in Figs. 4.18-4.22. Fixed peak at 1658 cm^{-1} for C=O served as an internal standard reference. Peaks of interest and the expected changes in peak intensities are as shown in following Table 4.1. Table 4.1 also summarizes the observed results for residues from solution exposed to 300 nm and 366 nm UV light. As implicated, only 300 nm UV light is effective for dimerization of 4-hydroxychalcone. For all the solutions exposed to 300 nm light, the intensities of solvent effectiveness varied in the order of NMP > DMAc > THF > 2ME > DMF.

Table 4.1 – Summary of FT-IR Results for UV Light Wavelength Optimization

Functional Group	**Molecular Bond (Molecular Motion)**	**Expected Results**		**Observed Results**			
				300 nm		**366 nm**	
		Wavenumber[47] (cm^{-1})	**Trend**	**Wavenumber (cm^{-1})**	**Trend**	**Wavenumber (cm^{-1})**	**Trend**
Alkene	C = C (Conjugated)	1610-1640	Should Decrease	1600	Decreased	1600	Indifferent
	= C – H (bend-monosubstituted)	990 & 910	Should Decrease	970 & 900	Decreased	970 & 900	Indifferent
Alkane	C – H (Stretch)	2800-3000	Should Increase	2935	Slight Increase	2935	Indifferent

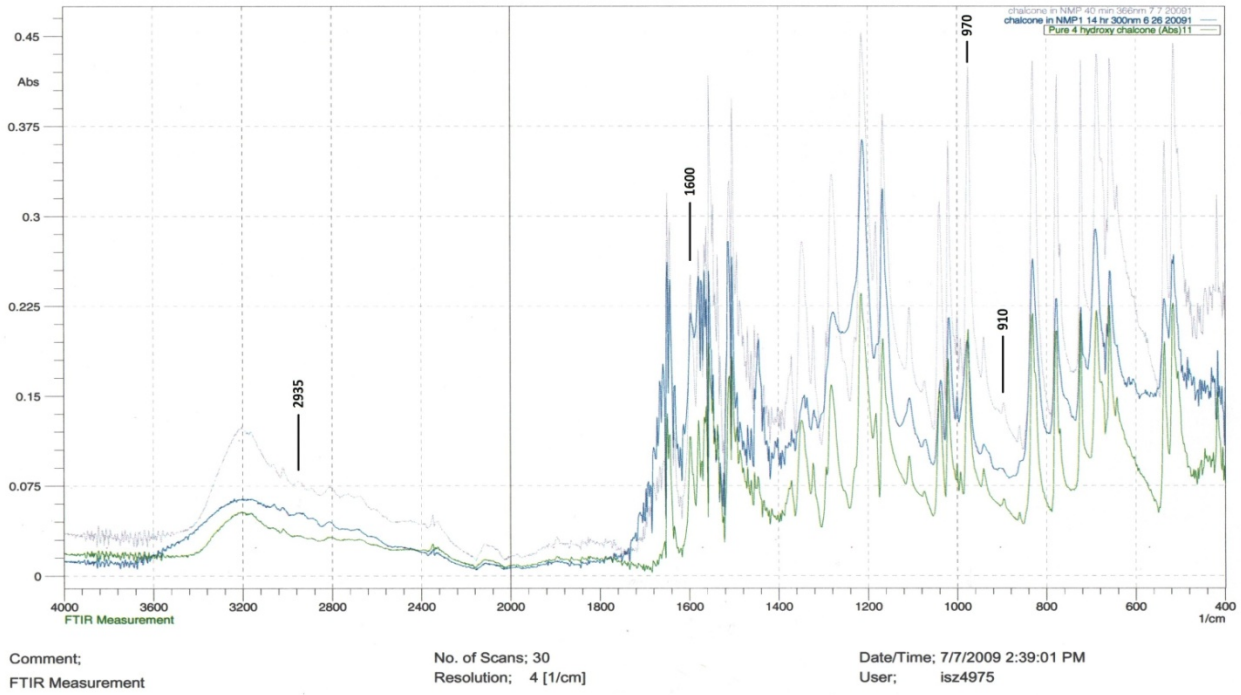

Figure 4.18 – Overlapping FT-IR Spectra of Unexposed 4-Hydroxychalcone, 4-Hydroxychalcone Exposed to 300 nm and 366 nm UV Light in NMP Solvent. (Int. Std. Ref. - 1658 cm^{-1}, C=O).

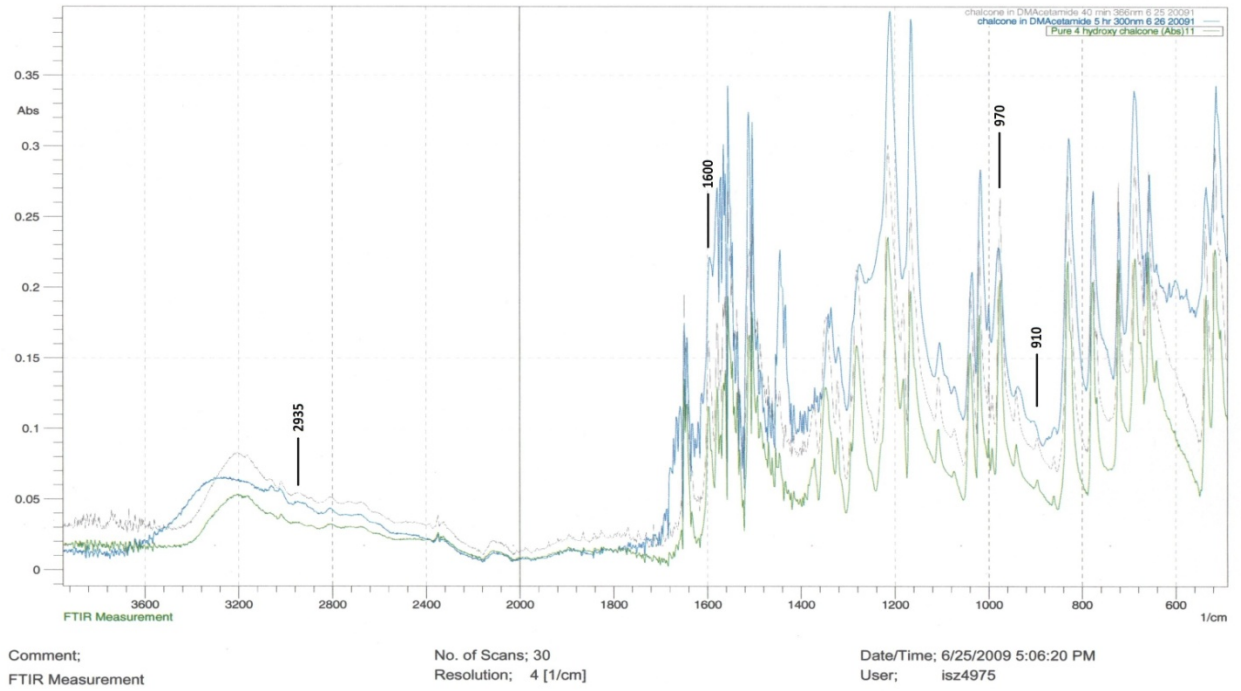

Figure 4.19 – Overlapping FT-IR Spectra of Unexposed 4-Hydroxychalcone, 4-Hydroxychalcone Exposed to 300 nm and 366 nm UV Light in DMAc Solvent. (Int. Std. Ref. - 1658 cm^{-1}, C=O).

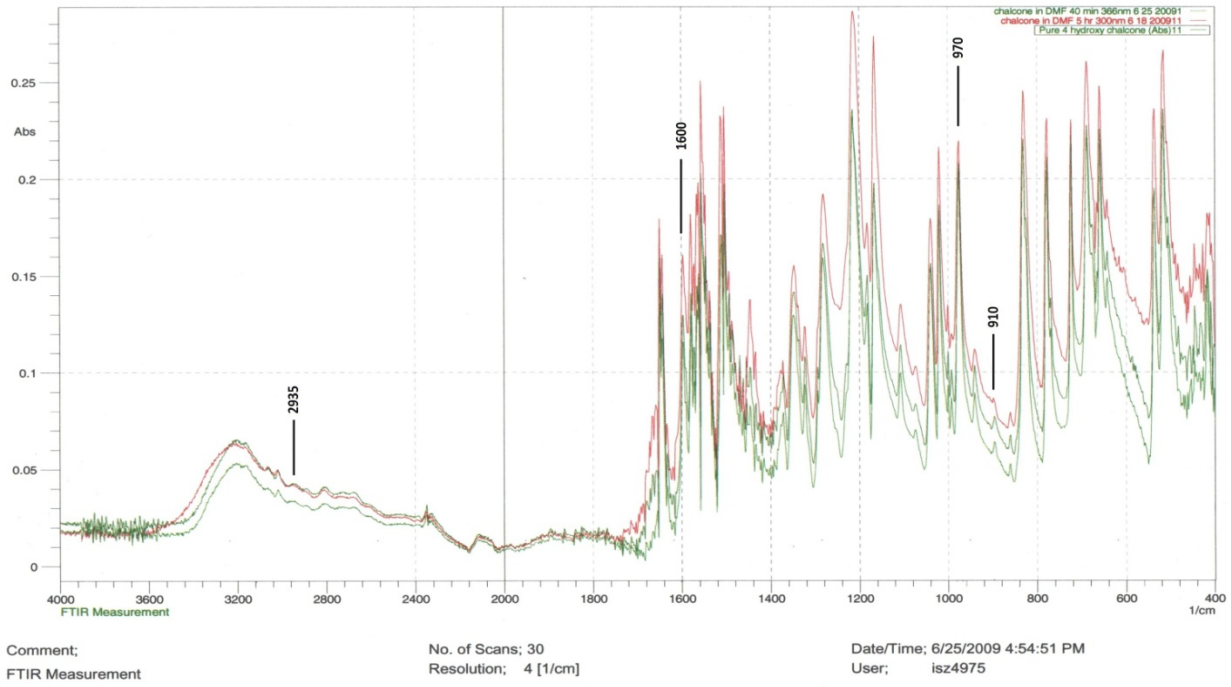

Figure 4.20 – Overlapping FT-IR Spectra of Unexposed 4-Hydroxychalcone, 4-Hydroxychalcone Exposed to 300 nm and 366 nm UV Light in DMF Solvent. (Int. Std. Ref. - 1658 cm^{-1}, C=O).

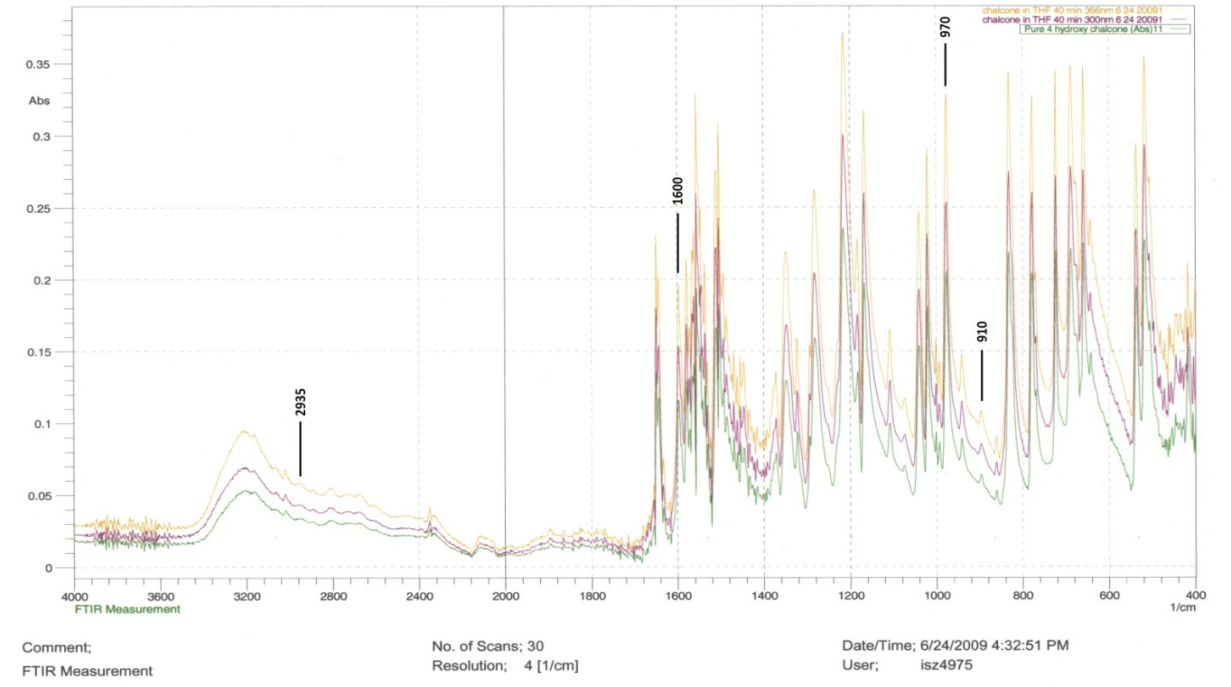

Figure 4.21 – Overlapping FT-IR Spectra of Unexposed 4-Hydroxychalcone, 4-Hydroxychalcone Exposed to 300 nm and 366 nm UV Light in THF Solvent. (Int. Std. Ref. - 1658 cm^{-1}, C=O).

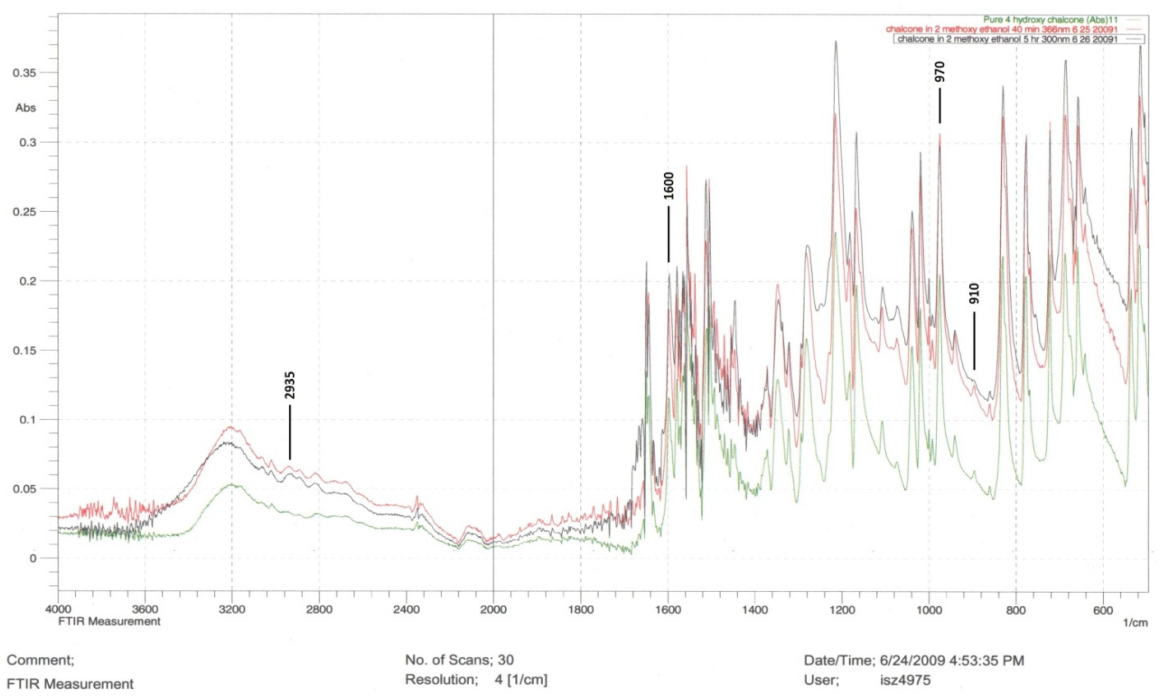

Figure 4.22 – Overlapping FT-IR Spectra of Unexposed 4-Hydroxychalcone, 4-Hydroxychalcone Exposed to 300 nm and 366 nm UV Light in 2ME Solvent. (Int. Std. Ref. - 1658 cm^{-1}, C=O).

4.3.1.3 Liquid Chromatography-Mass Spectroscopy

Mass spectroscopy was performed on samples of 4-hydroxychalcone exposed to two different UV light wavelengths in five different solvent mediums. 4-Hydroxychalcone upon UV exposure tends to form dimer via (2π+2π) cyclo-addition reaction at the bridging C=C bond. Hence, the UV-light – Solvent pair which demonstrated the most prominent peak intensity peak for molecular weight corresponding to dimer (~ 450-470 amu) with small-or-no intensity peak associated with 4-hydroxychalcone (~ 225-230 amu) indicating maximized conversion, was the obvious choice for study of mechanical properties and for final UV exposures down-the-road. Figs. 4.23-4.27 present mass spectra for the 300 nm and 366 nm pair of wavelengths in each solvent. It was evident that 366 nm UV did not trigger the cyclo-addition reaction as compared to 300 nm UV light, thus supporting the observations made by ^{1}H NMR and FT-IR. The effectiveness of solvent medium for UV exposure was also in accordance with results obtained from ^{1}H

NMR and FT-IR characterizations. The general trend of effectiveness can be stated as NMP > DMAc > DMF > THF > 2ME.

4.3.1.4 Ultraviolet-Visible Spectroscopy

UV-Visible Spectroscopy was lastly performed to consolidate the selection of solvent medium and UV light wavelength as derived from results of ^{1}H NMR, FT-IR and LC-MS. Typically when 4-hydroxychalcone is exposed to UV light, absorption at 348 nm corresponding to C=C, decreases drastically. Also a gradual increment at 240 nm is observed indicating increasing C-C bond formation. Increased absorption at 240 nm is also associated with cis-trans isomerism of chalcone unit.[29-30, 32, 45] Fig. 48 presents the UV-visible spectra for 300 nm and 366 nm UV light sources, respectively.

To interpret these spectrograms for effectiveness of solvent-UV light pair, the ratio of absorption peak heights at 343 nm-to-240 nm was determined for each solvent-UV light system. Table 4.2 summarizes the results. Again it was clearly inferred that 366 nm is ineffective and should not be considered for final UV exposures. Amongst all the solvents under consideration, smallest ratios obtained for NMP and DMAc further gave evidence of successful dimerization reaction to the maximum extent.

Table 4.2 – Effectiveness Ratio for 4-Hydroxychalcone for Each Solvent-UV Wavelength Pair

Solvent	**UV light Source**	
	300 nm	**366 nm**
Unexposed 4-hydroxychalcone	5.03	5.03
NMP	2.00	4.50
DMAc	2.37	5.03
DMF	3.50	4.83
THF	4.56	4.68
2ME	5.00	4.43

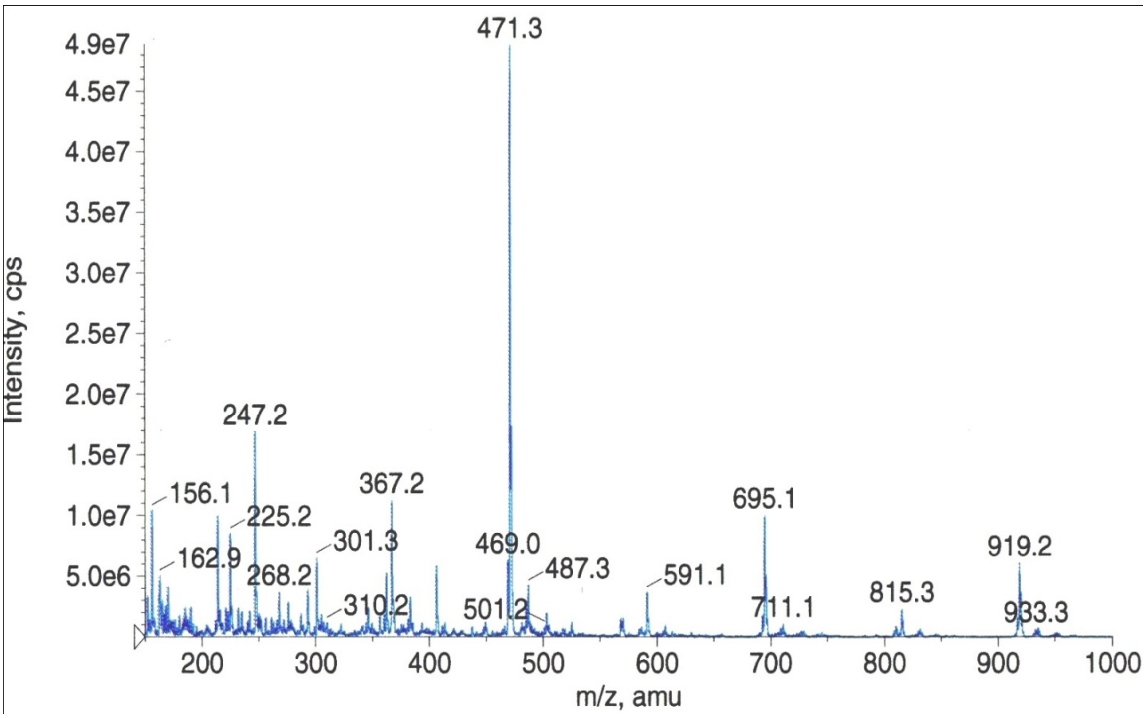

Figure 4.23a – LC-MS of 4-Hydroxychalcone Exposed to 300 nm UV Light in NMP Solvent

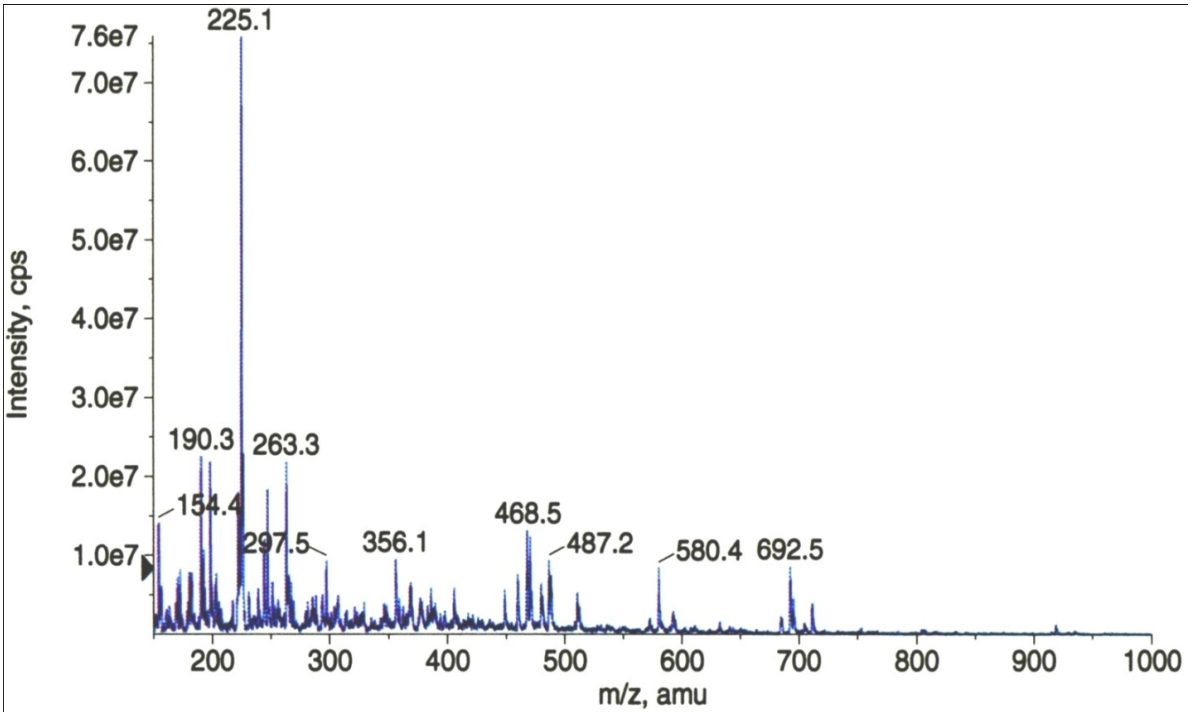

Figure 4.23b – LC-MS of 4-Hydroxychalcone Exposed to 366 nm UV Light in NMP Solvent

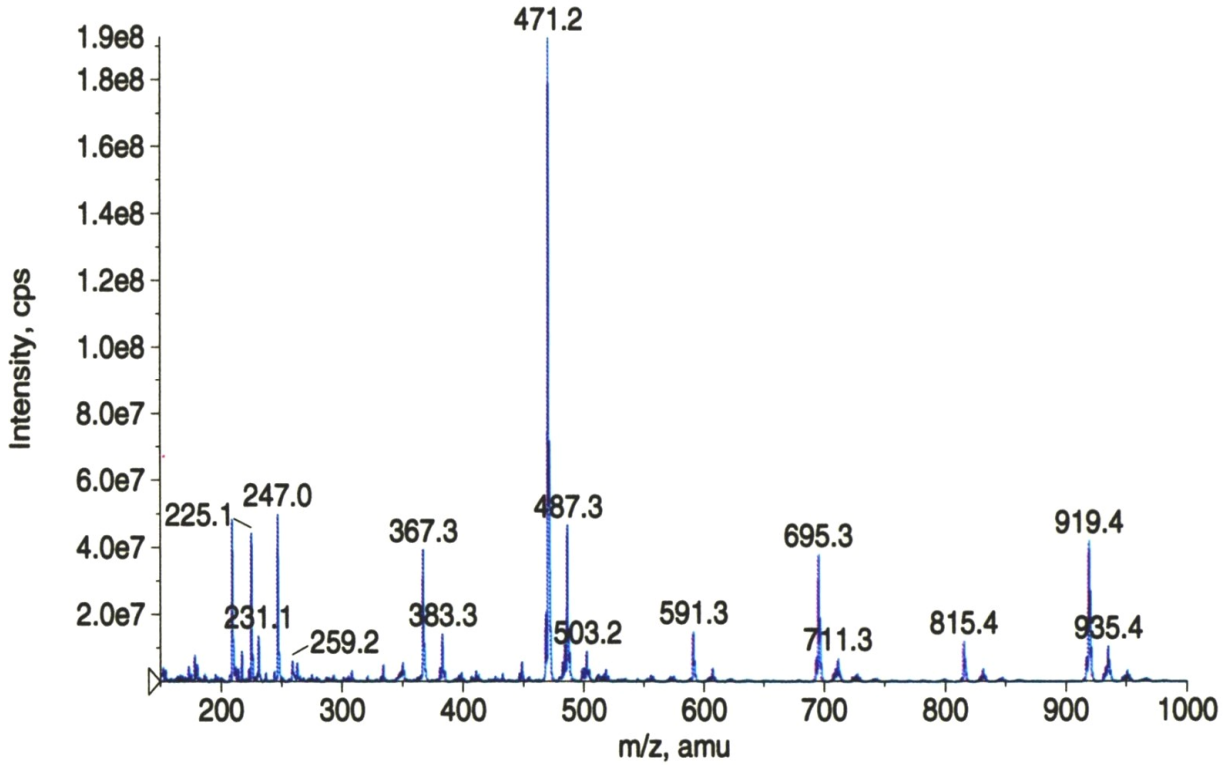

Figure 4.24a – LC-MS of 4-Hydroxychalcone Exposed to 300 nm UV Light in DMAc Solvent

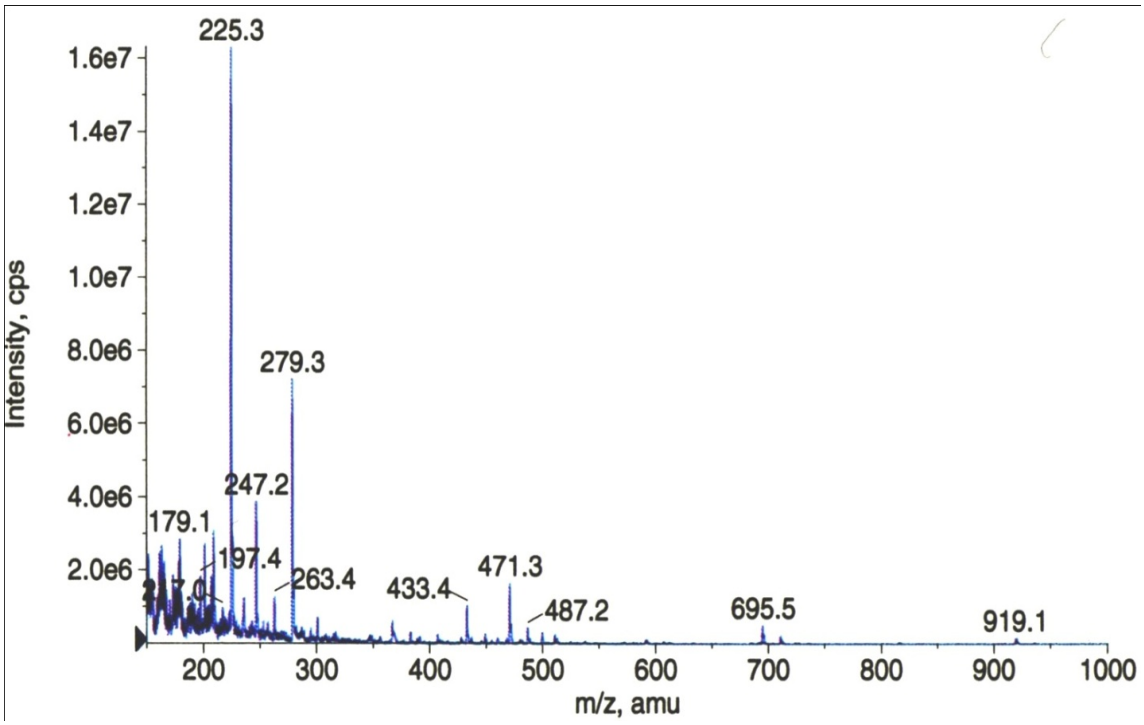

Figure 4.24b – LC-MS of 4-Hydroxychalcone Exposed to 366 nm UV Light in DMAc Solvent

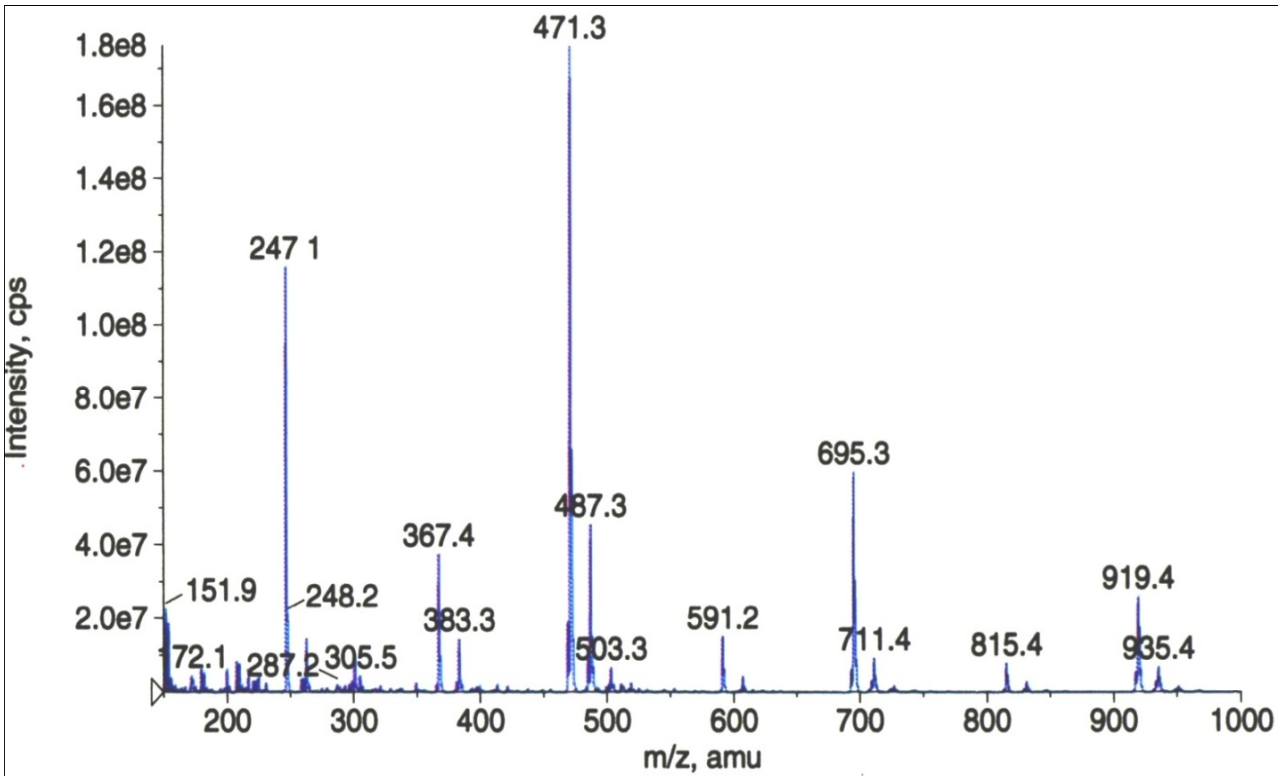

Figure 4.25a – LC-MS of 4-Hydroxychalcone Exposed to 300 nm UV Light in DMF Solvent

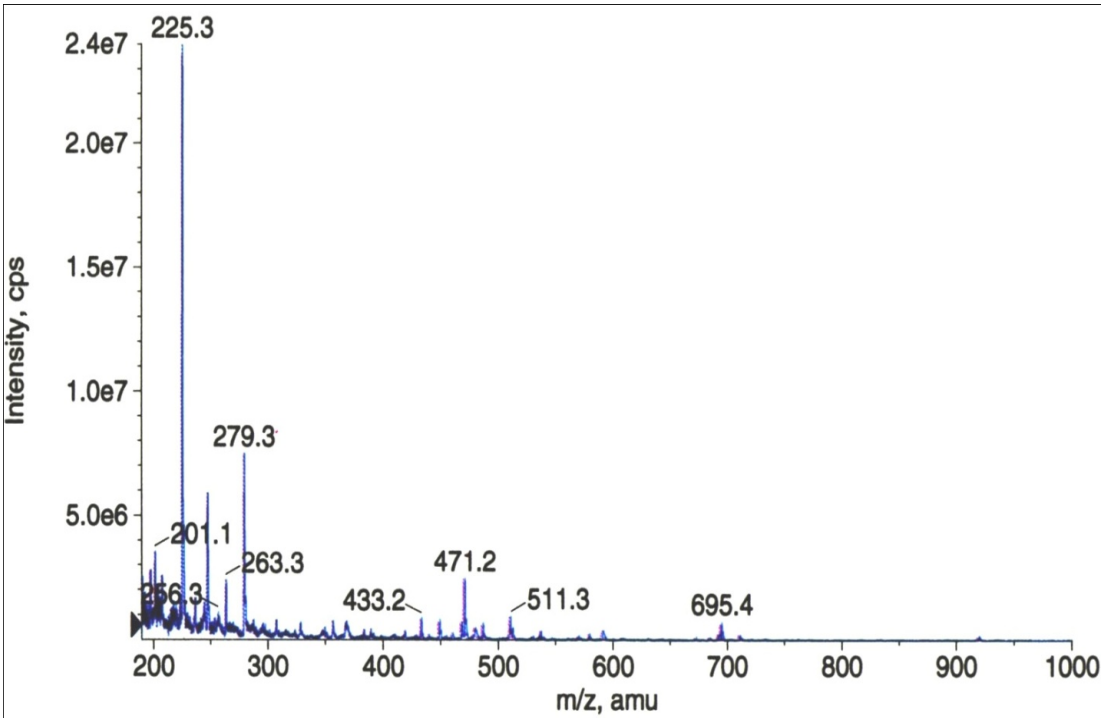

Figure 4.25b – LC-MS of 4-Hydroxychalcone Exposed to 366 nm UV Light in DMF Solvent

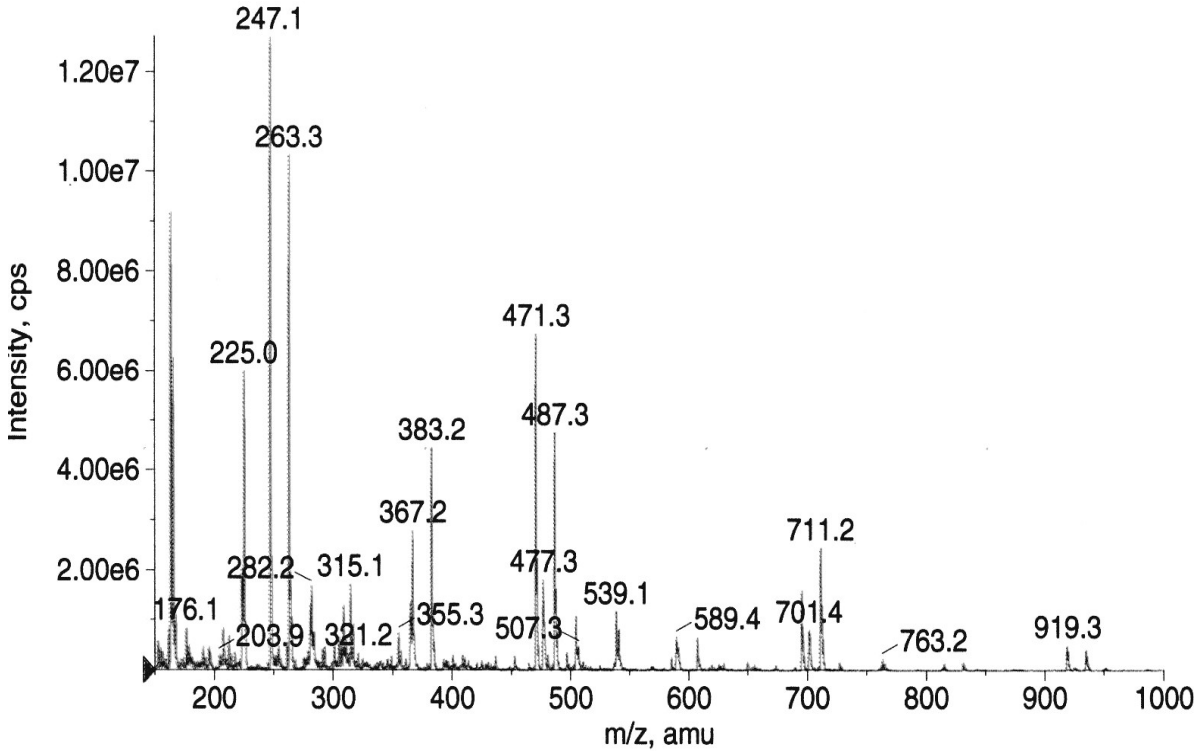

Figure 4.26a – LC-MS of 4-Hydroxychalcone Exposed to 300 nm UV Light in THF Solvent

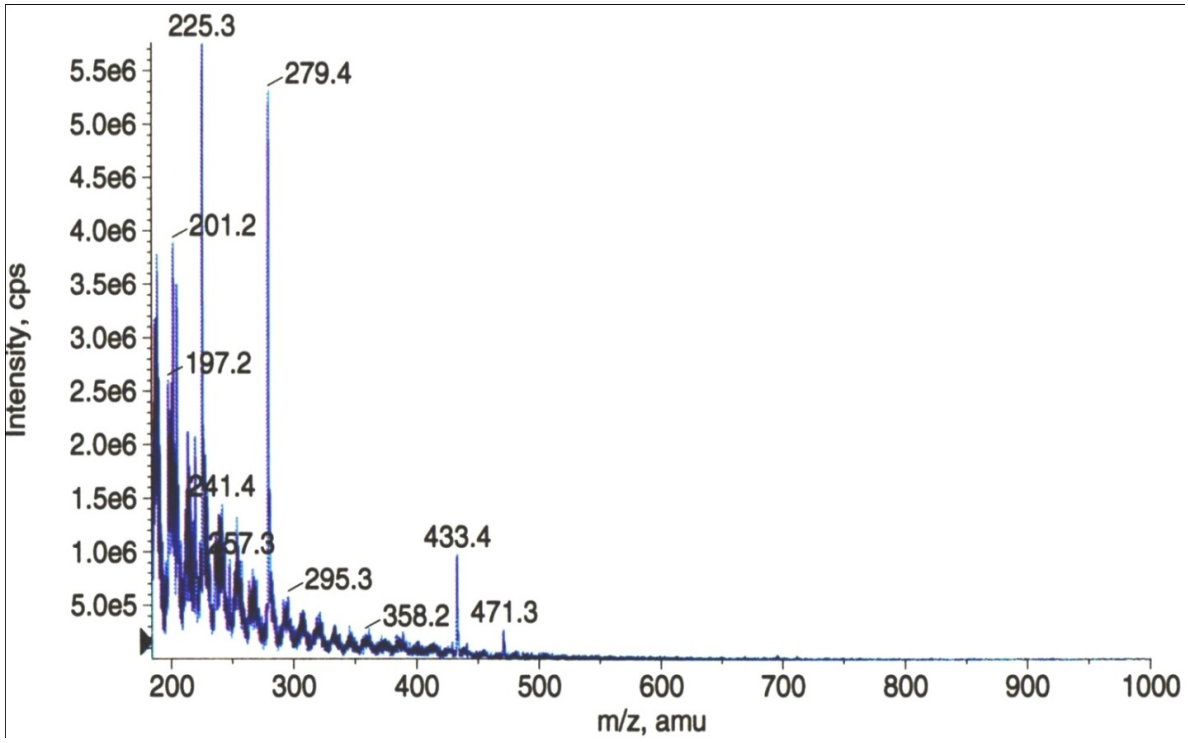

Figure 4.26b – LC-MS of 4-Hydroxychalcone Exposed to 366 nm UV Light in THF Solvent

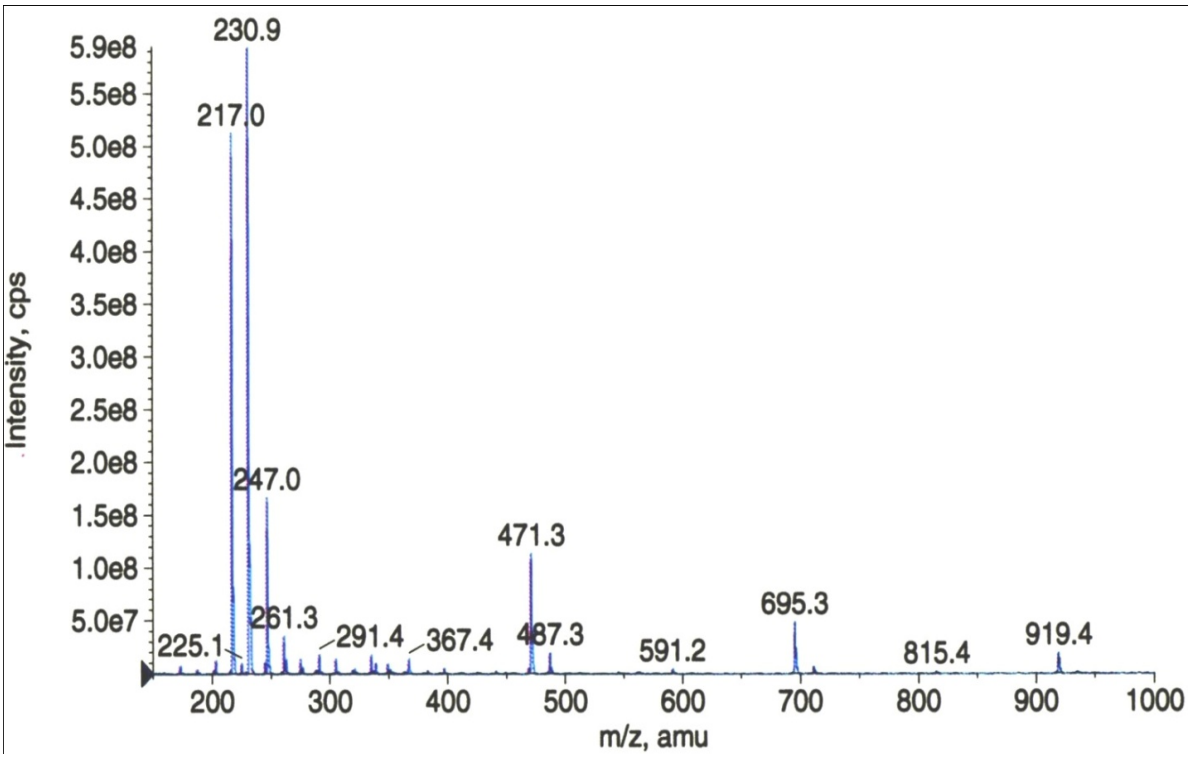

Figure 4.27a – LC-MS of 4-Hydroxychalcone Exposed to 300 nm UV Light in 2ME Solvent

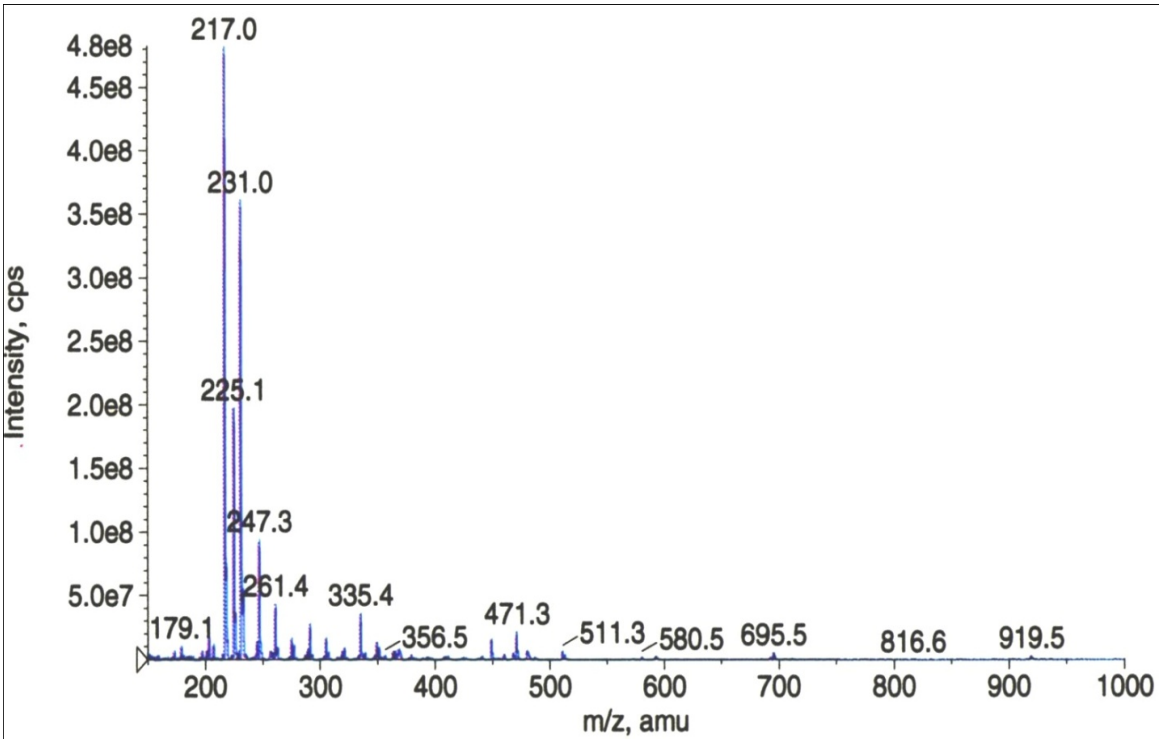

Figure 4.27b – LC-MS of 4-Hydroxychalcone Exposed to 366 nm UV Light in 2ME Solvent

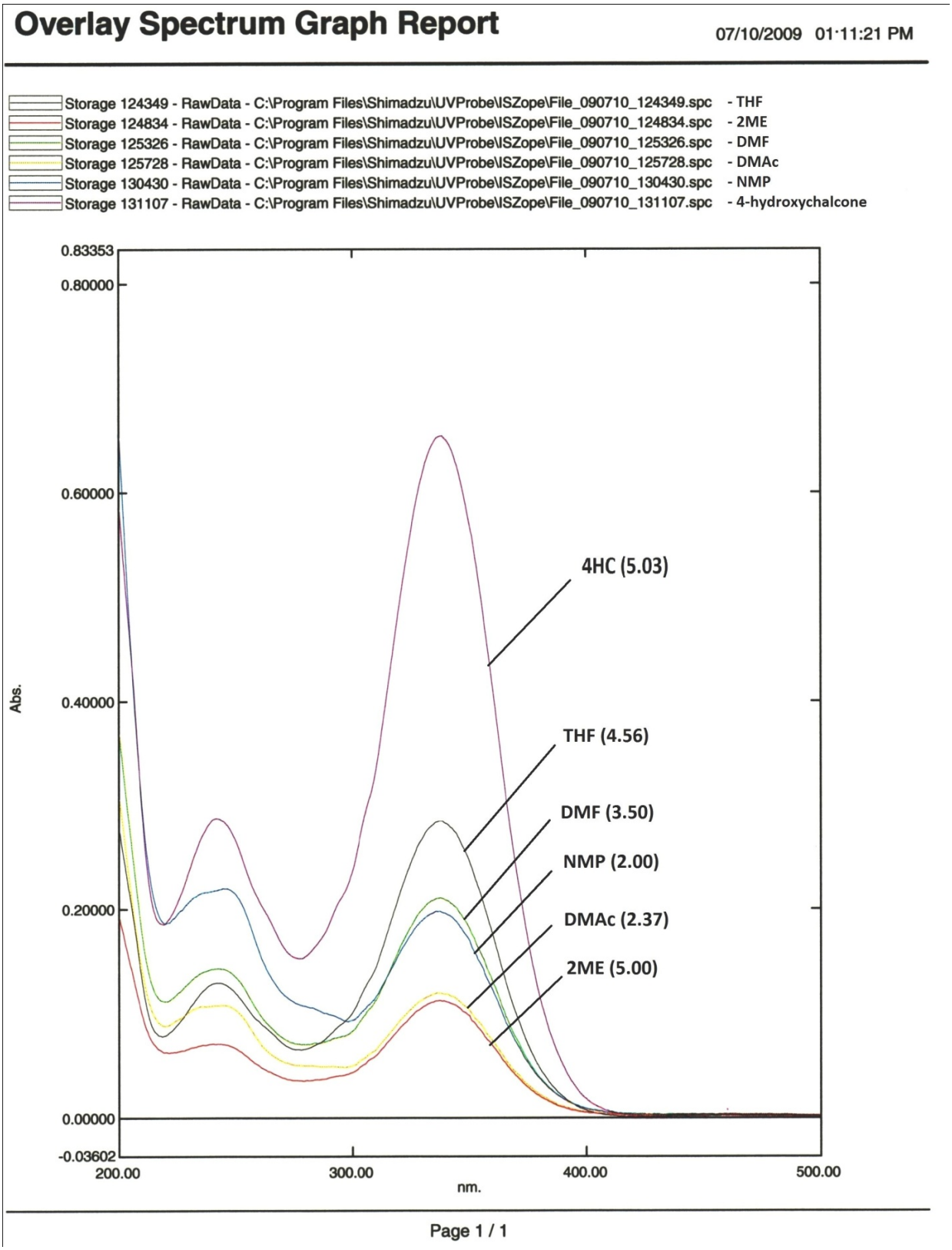

Figure 4.28a – UV-Vis of 4-Hydroxychalcone Exposed to 300 nm UV Light in NMP, DMAc, DMF, THF and 2ME

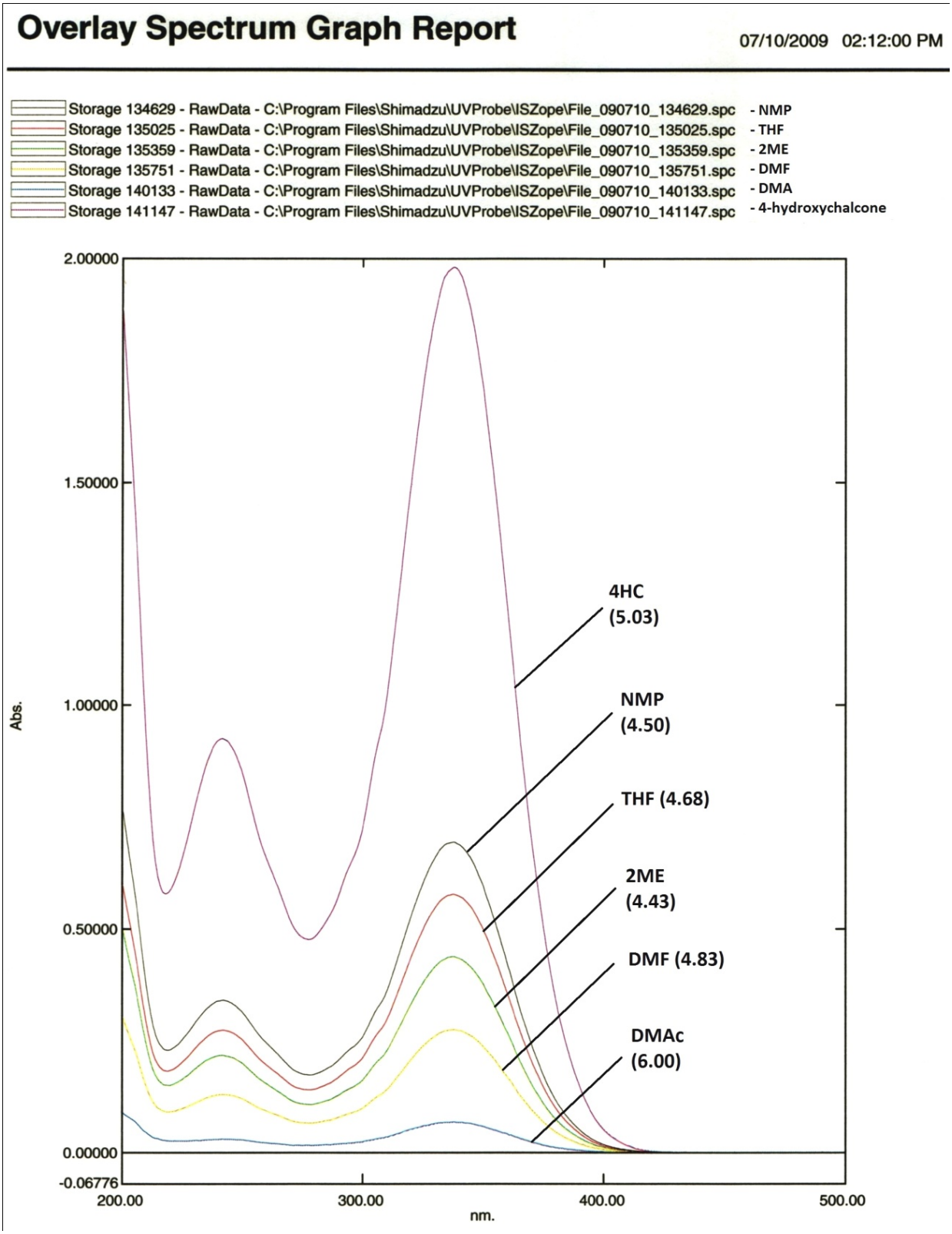

Figure 4.28b – UV-Vis of 4-Hydroxychalcone Exposed to 366 nm UV Light in NMP, DMAc, DMF, THF and 2ME

4.3.2 Solution Concentration

Established the fact that, for 4-hydroxychalcone, NMP proved to be the most effective solvent when used in combination with 300 nm UV light for UV exposure, the pair was used to study the effect of solution concentration on degree of polymerization. Instead of using 4-hydroxychalcone, the photo-cross-linkable component of Model Compound, the complete Model Compound was used to optimize the system for solution concentration.

4.3.2.1 Fourier Transform-Infrared Spectroscopy

FT-IR spectra for Model Compound dissolved in NMP, exposed to 300 nm UV light with different solution concentrations, 0.5 w%, 5 w%, 10 w%, 15 w% and 20 w%, can be seen in Fig. 4.29. Fig. 4.4 of unexposed Model Compound is repeated for the purpose of easier comparison. Since 4-hydroxychalcone is still the cross-linkable component in the Model Compound, IR absorption peaks to be studied here remain same as for 4-hydroxychalcone alone. Peaks at 1600 cm^{-1} (C=C, conjugated), 970 & 900 cm^{-1} (=C-H, bend) and 2935 cm^{-1} (C-H, stretch) were analyzed. The peak at 1172 cm^{-1} (C-O, ether linkage) served as the invariant internal reference for each spectrum of each concentration. Maximum reduction of the 1600 cm^{-1} peak was observed for lower concentrations, 0.5 w% followed by 5 w%. Analysis of the almost-overlapping spectra for 10 w%, 15 w% and 20 w% concentrations along with lesser reduction of the 1600 cm^{-1} peak and smaller increment of the 2935 cm^{-1} peak as against the 0.5 w% sample led to the conclusion that low solution concentrations for UV exposure yielded higher degree of polymerization of Model Compound via cyclo-addition reactions on each side.

4.3.2.2 Ultraviolet-Visible Spectroscopy

UV-visible spectroscopy was carried out to verify the conclusion derived from FT-IR characterization. Overlapping UV-Vis spectrum for each concentration of exposed Model Compound is seen in Fig. 4.30. Spectra obtained showed two absorption peaks, one at 343 nm for C=C and other at 246 nm for C-C, as observed for 4-hydroxychalcone. All samples showed large reduction of absorption at 343

nm along with slight increment in absorption at 246 nm, confirming the occurrence of photo-induced cyclo-addition reaction at C=C sites to form aliphatic four-member ring linkages between Model Compound monomers, ultimately leading to oligomeric/polymeric chains. It was observed that the 0.5 w% sample exhibited highest conversion followed by the 5 w% sample. Very small increment in conversion of monomer-to-polymer was observed for samples of concentrations greater than 5 w%.

It was concluded that, lower concentration solutions of Model Compound in NMP for UV exposure yielded best results, probably because of easy mobility of bulky molecules which in-turn facilitate higher chances of finding neighboring cross-linking site at right location and at right time. Bulkier nature of model compound monomer poses restrictions of mobility after initial rapid addition reaction. Considering the aspect of eventual requirement of film-casting for mechanical studies, 5 w% solution concentration was selected.

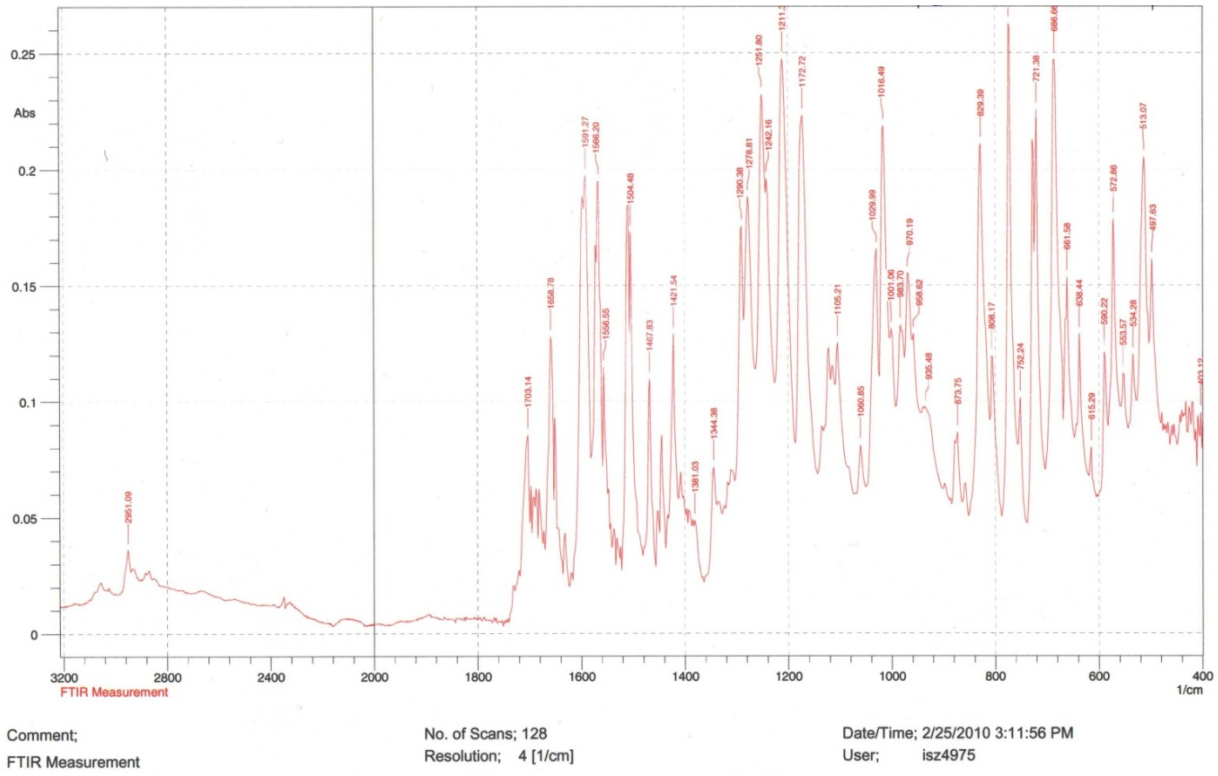

Figure 4.4 – FTIR of Terephthalic Acid-based, UV Cross-linkable Model Compound

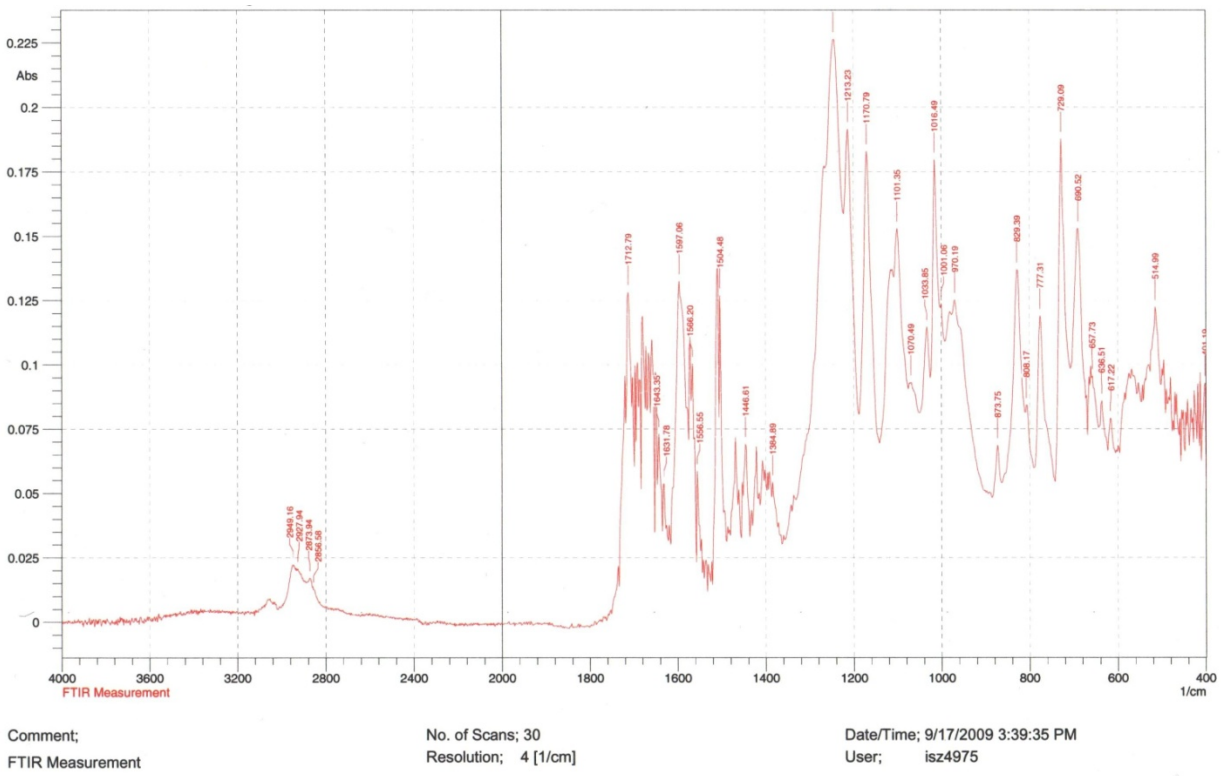

Figure 4.29a – FTIR of 0.5 w% Solution of Model Compound Exposed to 300 nm UV Light in NMP Solvent

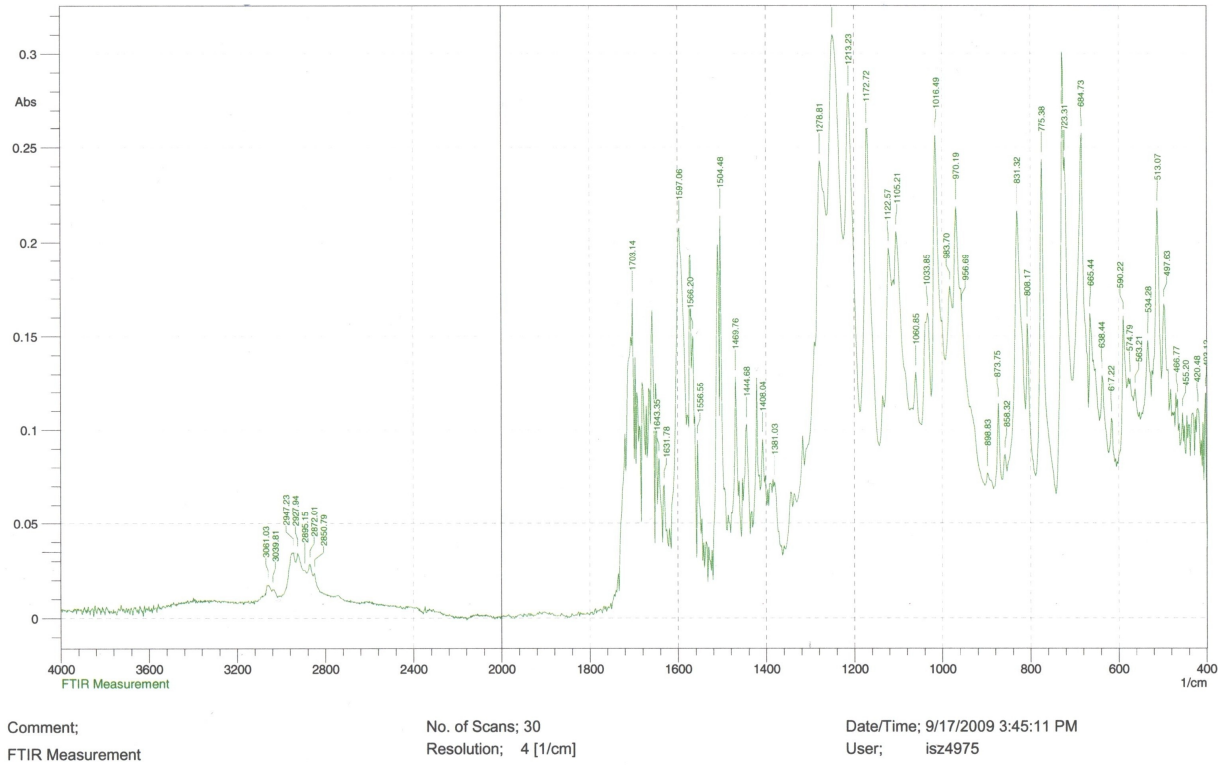

Figure 4.29b – FTIR of 5 w% Solution of Model Compound Exposed to 300 nm UV Light in NMP Solvent

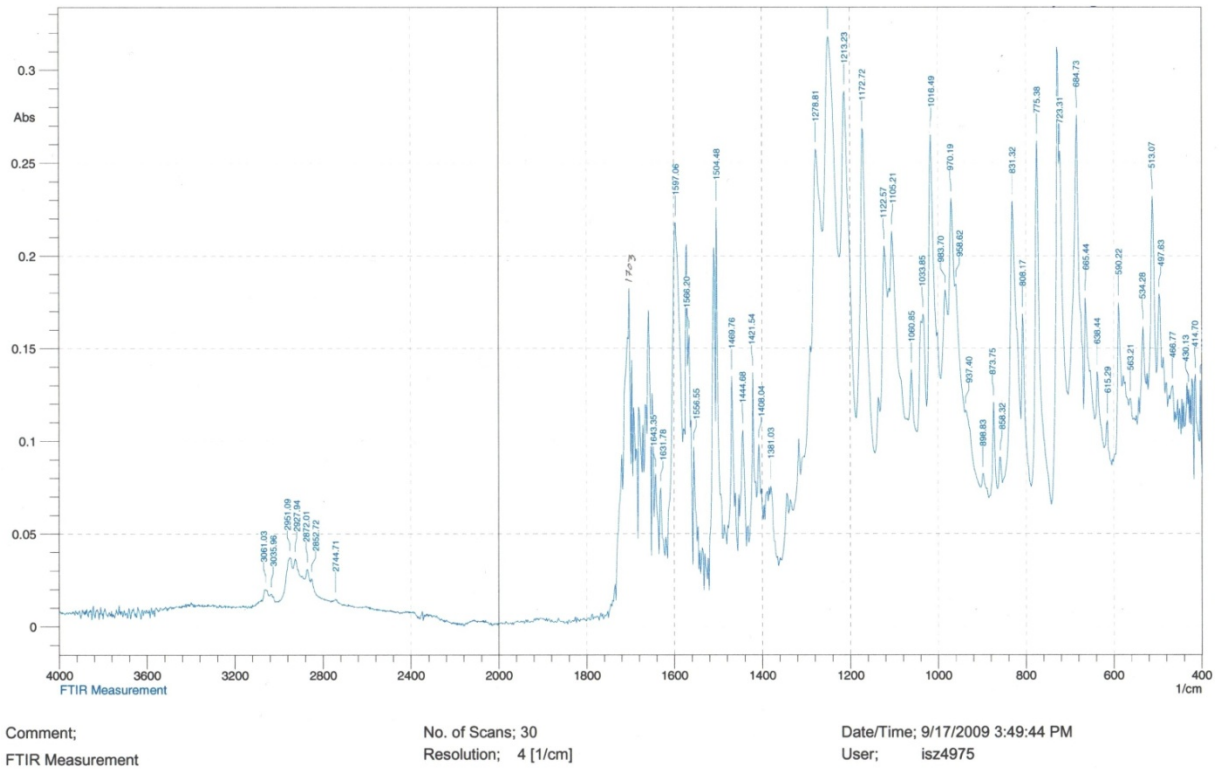

Figure 4.29c – FTIR of 10 w% Solution of Model Compound Exposed to 300 nm UV Light in NMP Solvent

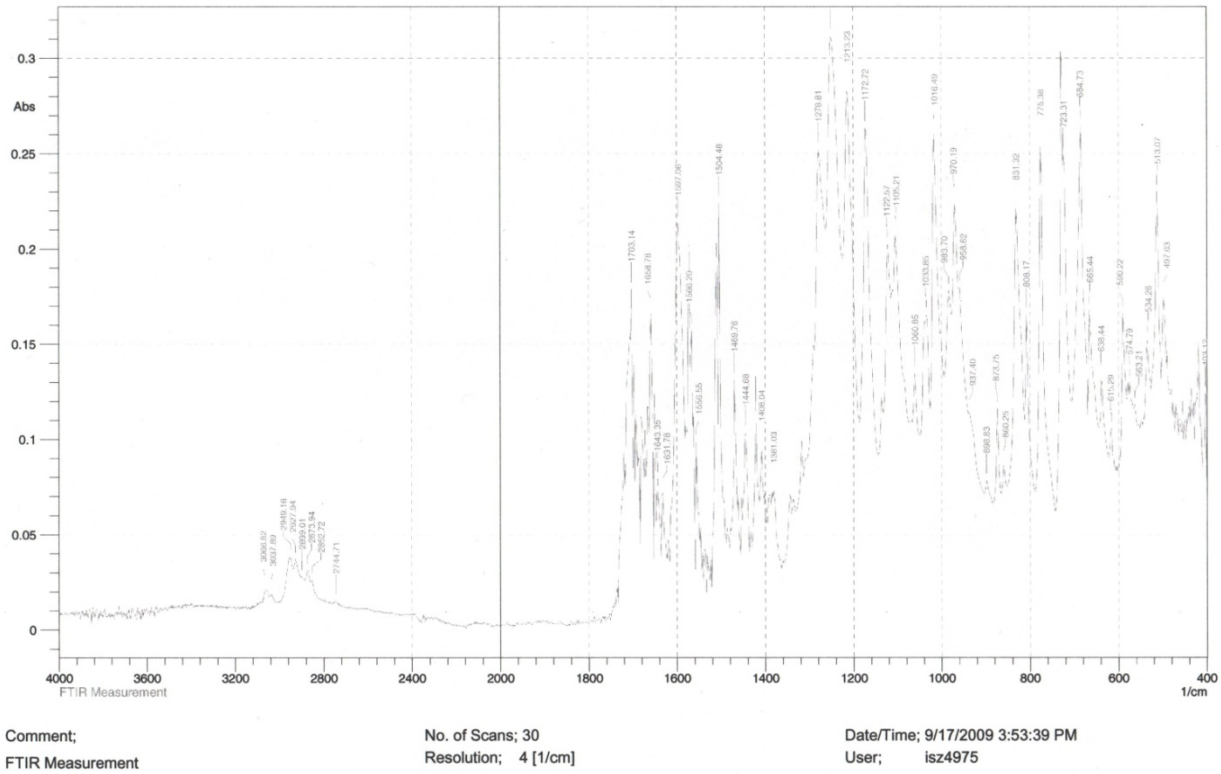

Figure 4.29d – FTIR of 15 w% Solution of Model Compound Exposed to 300 nm UV Light in NMP Solvent

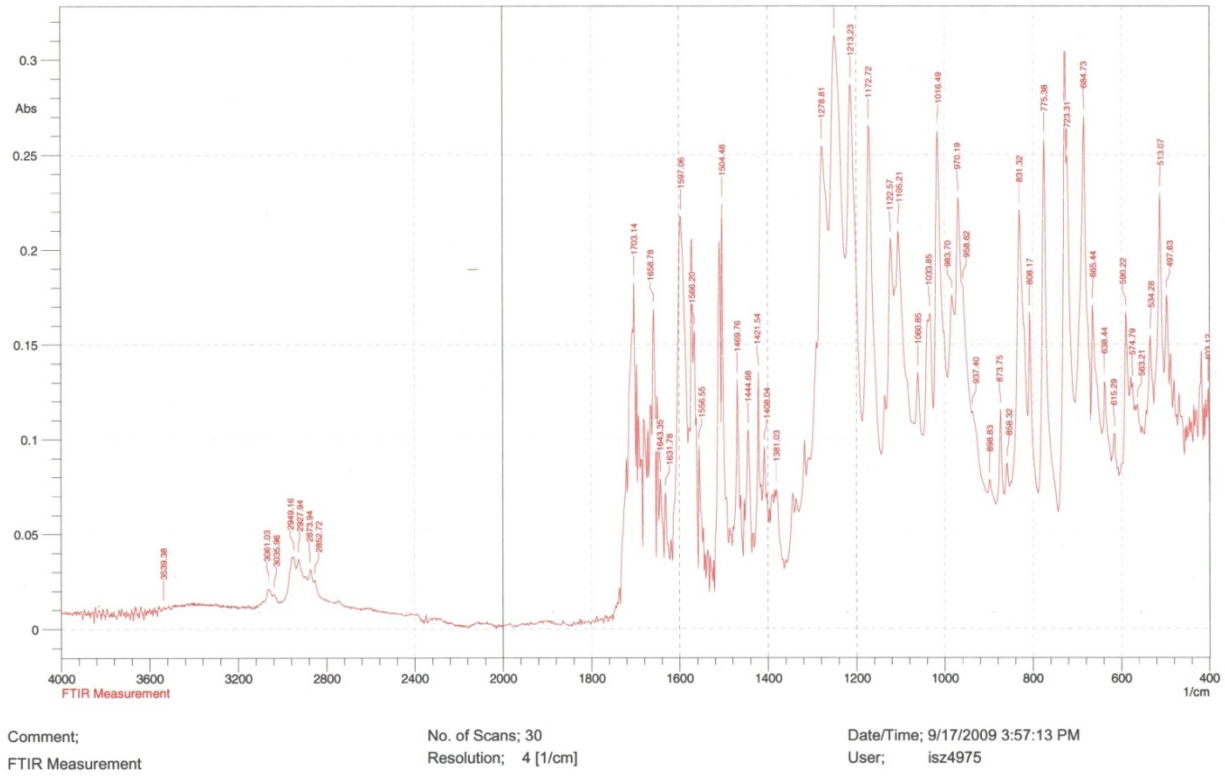

Figure 4.29e – FTIR of 20 w% Solution of Model Compound Exposed to 300 nm UV Light in NMP Solvent

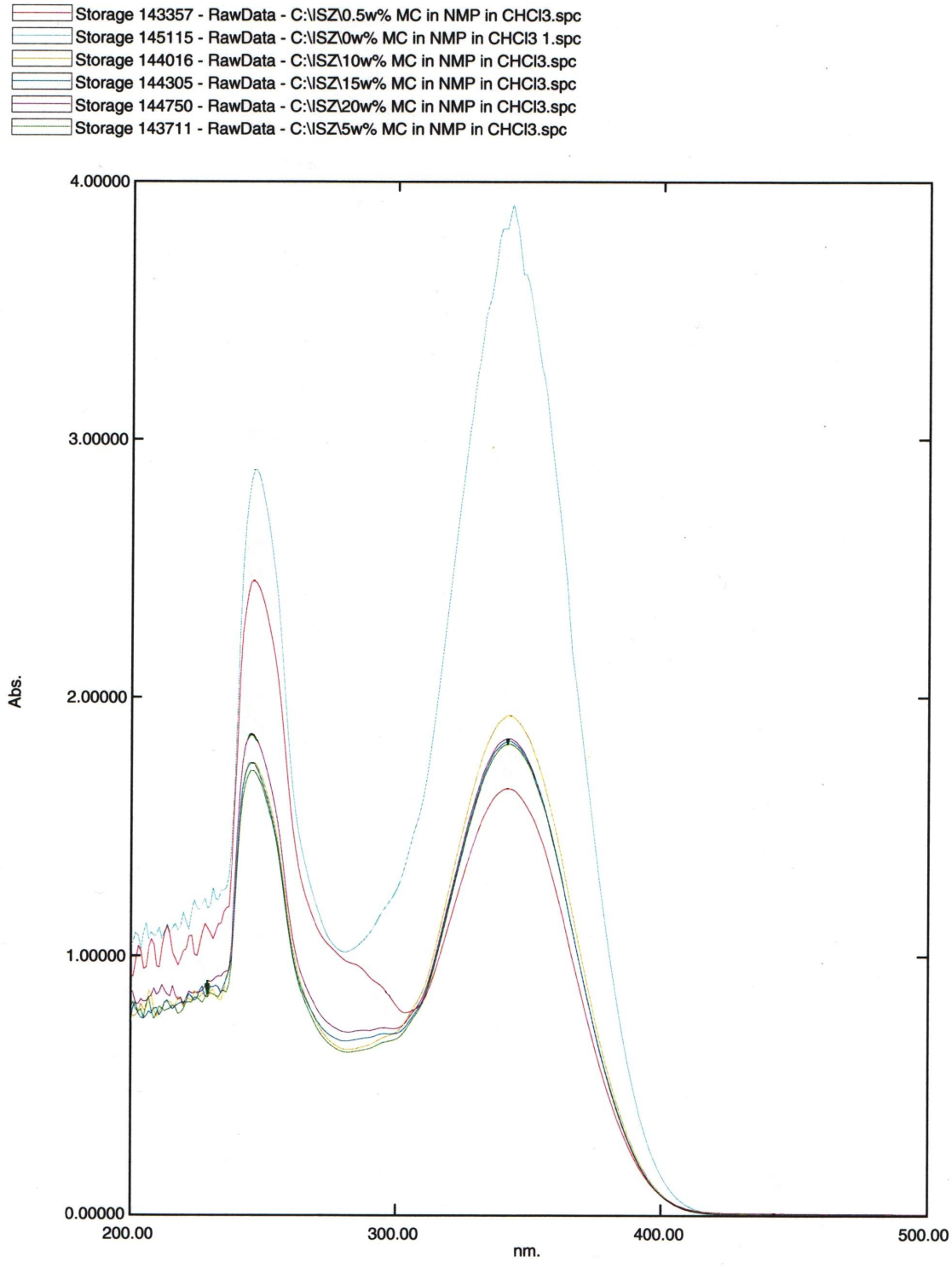

Figure 4.30 – UV-Vis for Optimization of Solution Concentration

4.3.3 Optimization – Result Summery

After extensive experimentation for system optimization for UV light source, Solvent medium and Solution concentration, results are summarized as follows,

- UV light Source – 300nm
- Solvent medium – NMP/DMAc/THF
- Solution concentration – 5w%

Experimental data obtained was lastly compared with literature work before concluding optimization. Table 4.3 summarizes the finding for all three works.

Table 4.3 – Comparison Between Experimental Data and Literature Work

Parameter under consideration that might affect rate of photo-cross-linking reaction for Chalcone in side-chain.		**Results by P. Selvam et.al.[40]**	**Results by A. Rehab et.al.[32]**	**Results of this study.**
Effect of UV Light Wavelength	UV light wavelength used	-	-	300 nm, 366 nm
	Conclusion	-	-	Photo-sensitivity varies for different materials.
Effect of Solvent Medium	Solvents used	$CHCl_3$, 1,4-dioxane, THF, DMF, DMSO	$CHCl_3$, CCl_4, dioxane, DMF, dichloromethane	NMP, DMAc, DMF, THF, 2-methoxyethanol
	Conclusion	Rate of reaction as well as extent of reaction are affected by solvent medium	Initial rate is unaffected but final extent of reaction is affected by solvent medium	Only extent of reaction is studied which is affected by solvent medium
Effect of Solution Concentration	Concentration domain	0.021 g/L – 0.166 g/L	0.0108 g/L – 0.036 g/L	6.25 g/L – 258.3 g/L
	Conclusion	Rate increases with increase in concentration	Rate decreases with increase in concentration	Rate decreases with increase in concentration

4.4 Blend of PI[6FDA/Bis-AP-AF] and UV Cross-linker

4.4.1 Selection Criteria - Polyimide

Requirement of an external polymer base for good film formation made analysis of polyimide and UV cross-linker blends more critical. Compatibility and possible hindrance during UV exposure were two main issues to be addressed.

4.4.1.1 Compatibility

Selection of PI[6FDA/Bis-AP-AF] as a base polymer was based on the fact that both PI[6FDA/Bis-AP-AF] and UV cross-linker are proposed components of same novel UV cross-linkable MADA-containing non-linear optical pendent polyimide (Fig. 2.1). To test this, Polyimide and UV cross-linker were dissolved in both NMP as well as THF solvent and as expected, both the solutions were perfectly clear (brownish-red color) without any visible trace of phase separation.

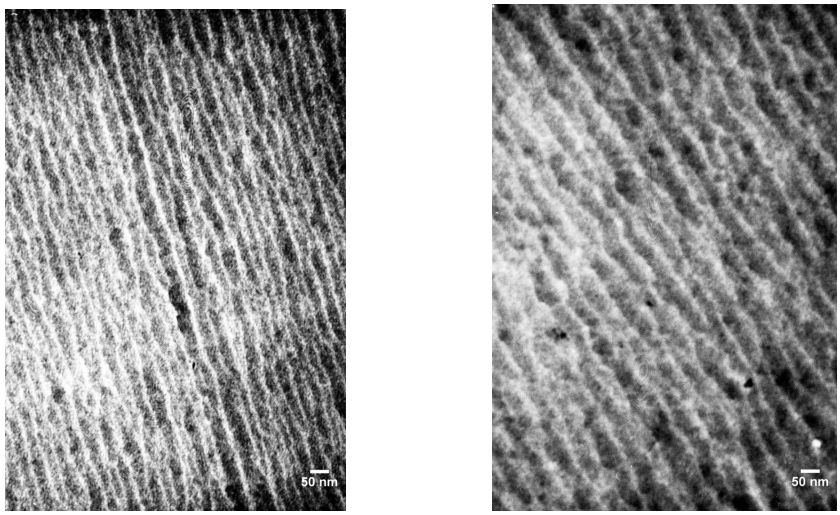

Figure 4.31 – TEM of Unexposed Blend Film (left) and 45 Minutes UV Exposed Blend Film (right)

Further TEM spectroscopy was carried out on unexposed and 45 min UV exposed blend films to check for compatibility. It was confirmed that no distinct phase separation occurred at 50 nm

magnification as observed in Fig 4.31. Ripples were concluded to be irremovable effect of sample preparation.

4.4.1.2 Hindrance During UV Exposure

UV spectroscopy was primarily used to study the hindrance effect posed by polyimide, which may restrict efficient polymerization of model compound upon UV exposure in blend solution. UV spectroscopy was performed for exposed/unexposed model compound, exposed/unexposed polyimide and exposed/unexposed blend of polyimide-model compound as shown in Figs. 4.32-4.34. From UV-Vis spectrum for polyimide, it was evident that polyimide does not absorb UV wavelengths above 300 nm as seen in Fig. 4.32. Earlier experimental work well established the fact that upon UV exposure, the absorption peak at 343nm (C=C) for model compound drastically decreases, and is again verified in Fig. 4.33. By comparing exposed and unexposed blends of polyimide-UV cross-linker in Fig. 4.34, it was clearly established that polyimide does not pose UV exposure hindrance.

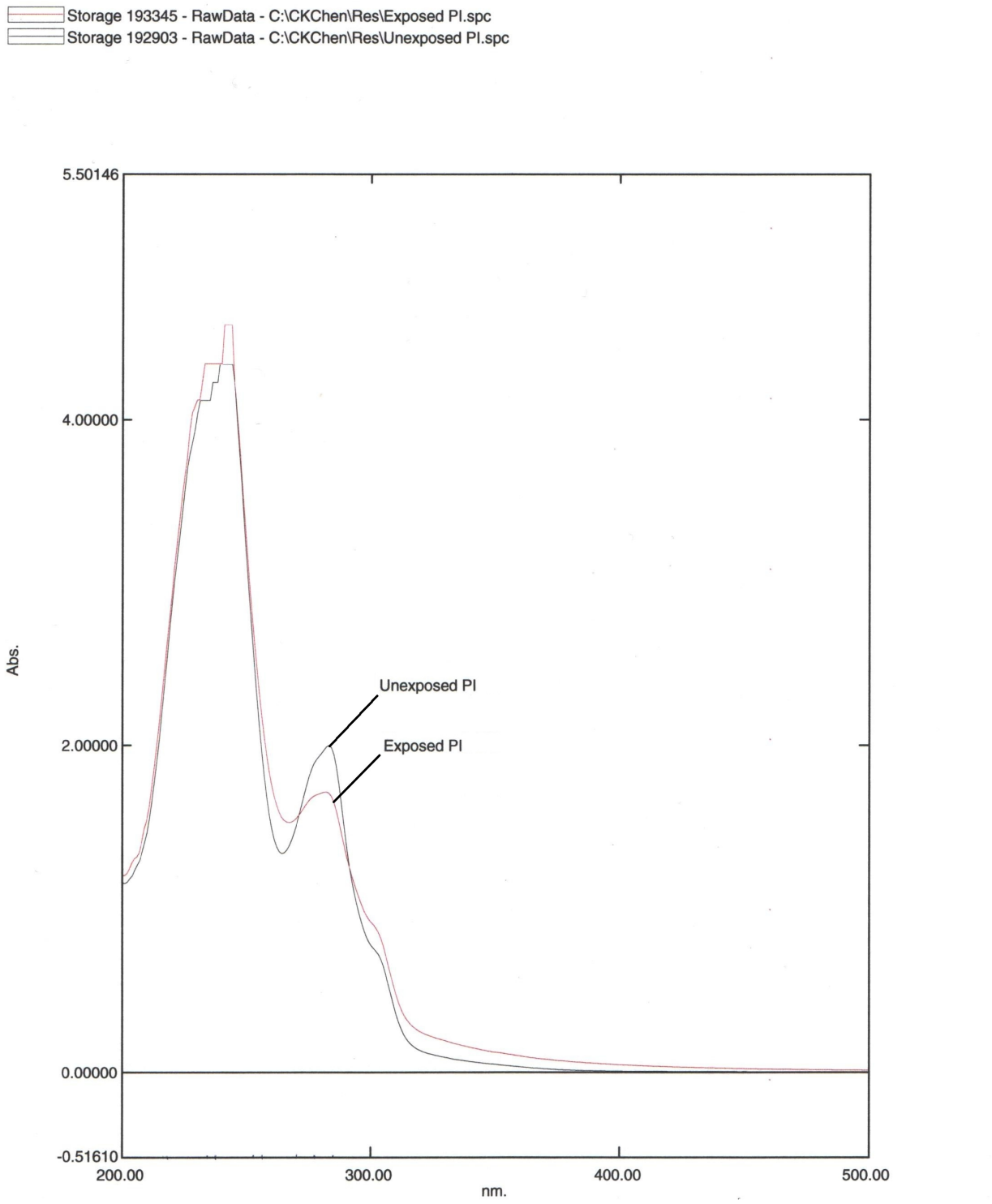

Figure 4.32 – UV-Vis of Unexposed and UV Exposed Polyimide

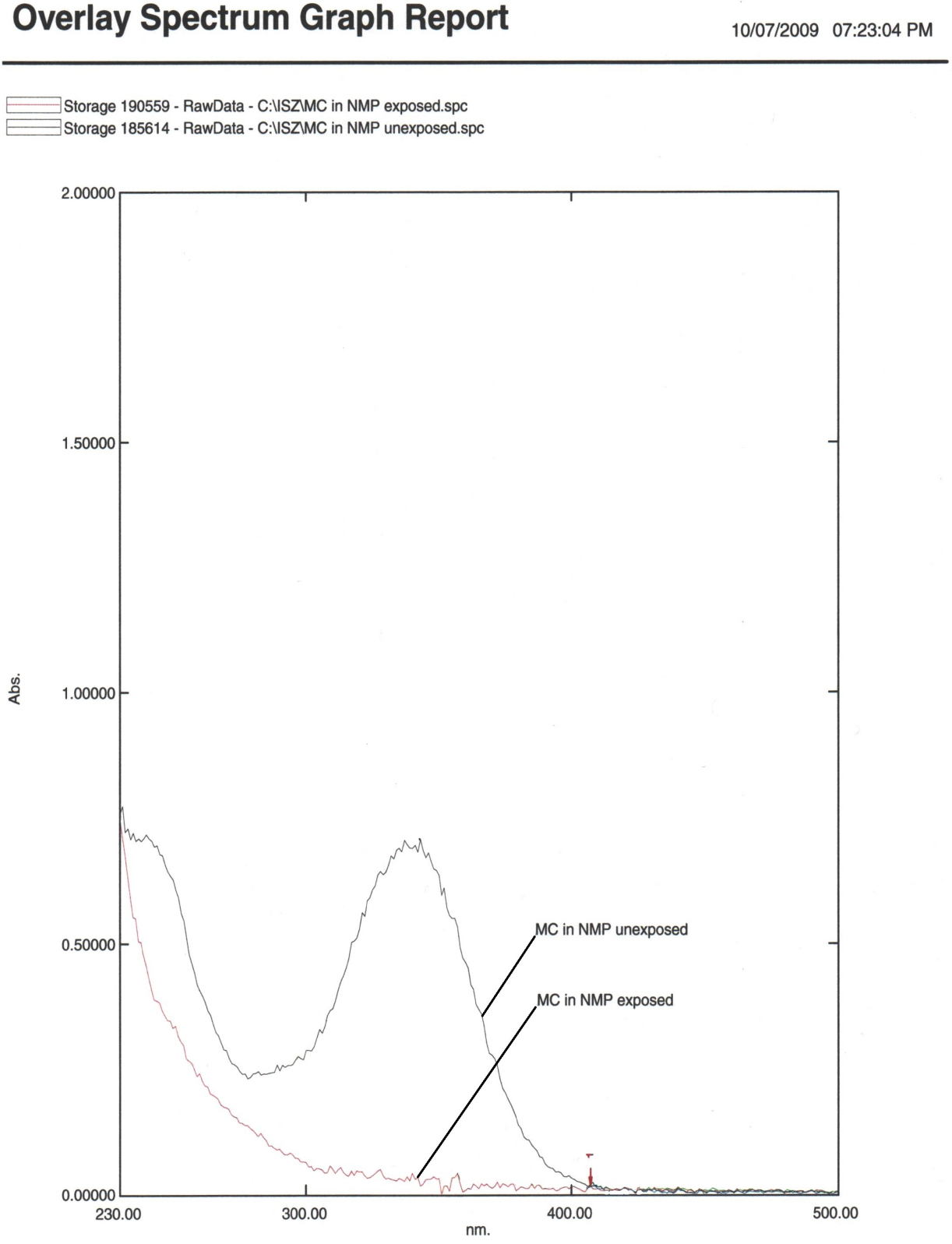

Figure 4.33 – UV-Vis of Unexposed and UV Exposed Model Compound

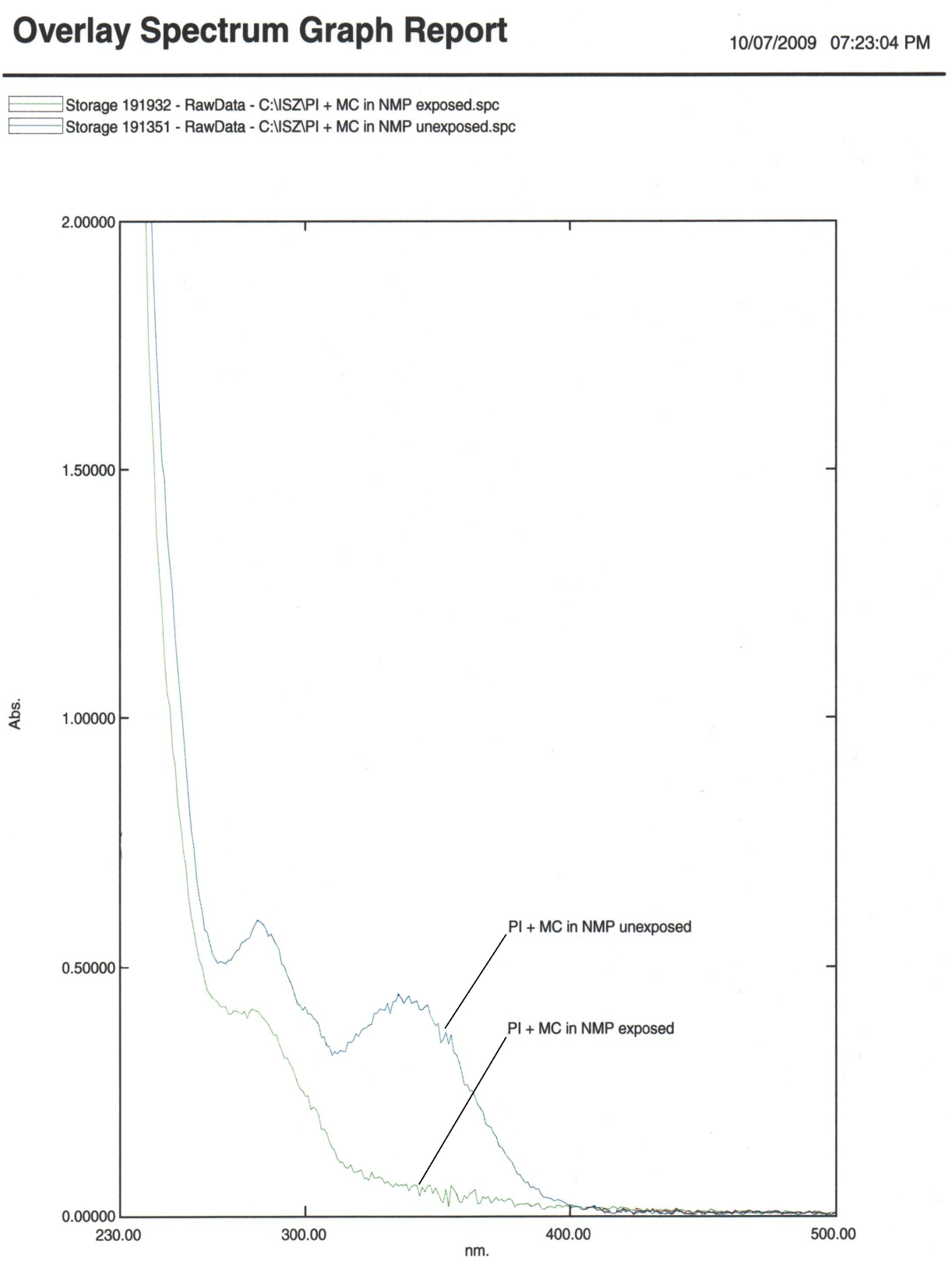

Figure 4.34 – UV-Vis of Unexposed and UV Exposed Polyimide and Model Compound Blend

4.4.2 Blend Characterization

4.4.2.1 Fourier Transform-Infrared Spectroscopy

FT-IR was used to characterize two main points regarding Polyimide and Model Compound blends,

1) Establish the presence of both components, Model Compound & Polyimide, in blend - Qualitatively.
2) Check and verify the occurrence of cyclo-addition reaction for model compound in blend as well.

A comparative study of major absorption peaks for Model Compound, Polyimide, Unexposed Blend, Blend exposed in NMP and Blend exposed in THF was used for this purpose.

To confirm the presence of both components in the blends, IR spectra for Model compound, Polyimide and unexposed Blend are compared, see Figs. 4.4, 4.8, 4.35, and important peaks are summarized in Table 4.4. This study, thus, established the presence of Model Compound in the Polyimide matrix.

Table 4.4 – Typical IR Peaks for Model Compound, Polyimide and their Blend

Functional Group	**Model Compound (cm^{-1})**	**Polyimide (cm^{-1})**	**Polyimide and Model Compound Blend (cm^{-1})**
-(CO)-O-	1703 (s)	-	1703 (s)
C=C	1599	-	1600
-C-O-C-	1278, 1018	-	1280, 1018
-CH2- bend	775	-	777
-(CO)-	1658	1658	1658
-(CO)- (imides)	-	1788, 1726, 723	1788, 1726, 723
-CN- (imides)	-	1371	1371
-C-OH-	-	1105	1105
-CF-	-	1205, 1180	1203, 1190

The occurrence of cyclo-addition reaction for model compound in blend was studied by performing comparative study of FT-IR spectra of Unexposed Blend, Blend exposed in NMP and Blend exposed in THF, refer to Figs. 4.35-4.37. It was observed that the peak at 1600 cm^{-1} corresponding to C=C, conjugated was decreased, positively establishing the occurrence of cyclo-addition reaction for model compound in mixture for both solvent mediums, NMP and THF. NMP was decidedly better for exposure purposes. Also, the increase in peaks at 2916 and 2848 cm^{-1}, corresponding to C-H alkane stretching, verify the cyclo-addition reaction.

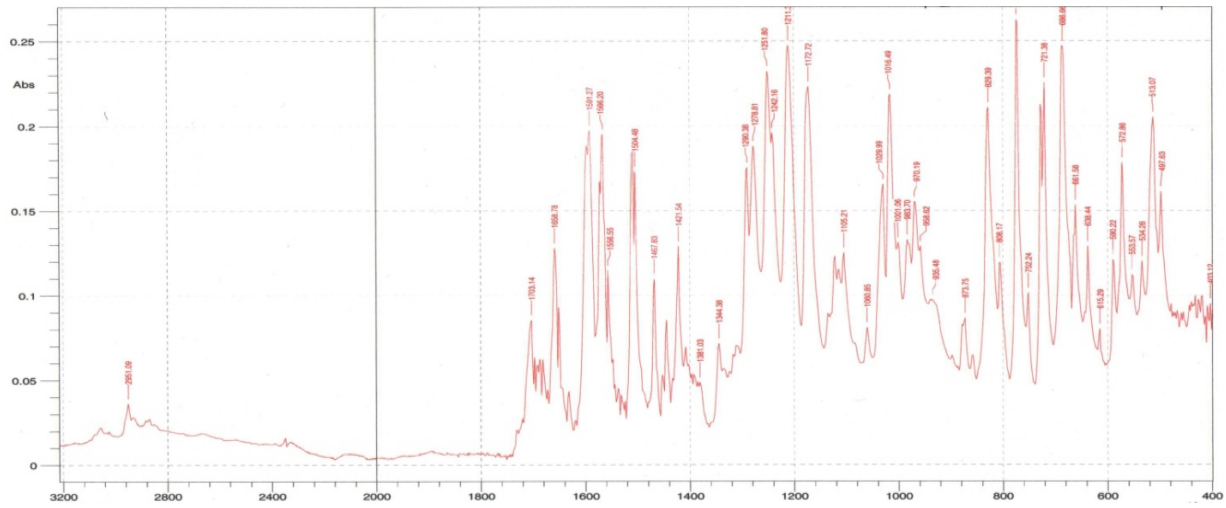

Figure 4.4 – FTIR of Terephthalic Acid-based, UV Cross-linkable Model Compound

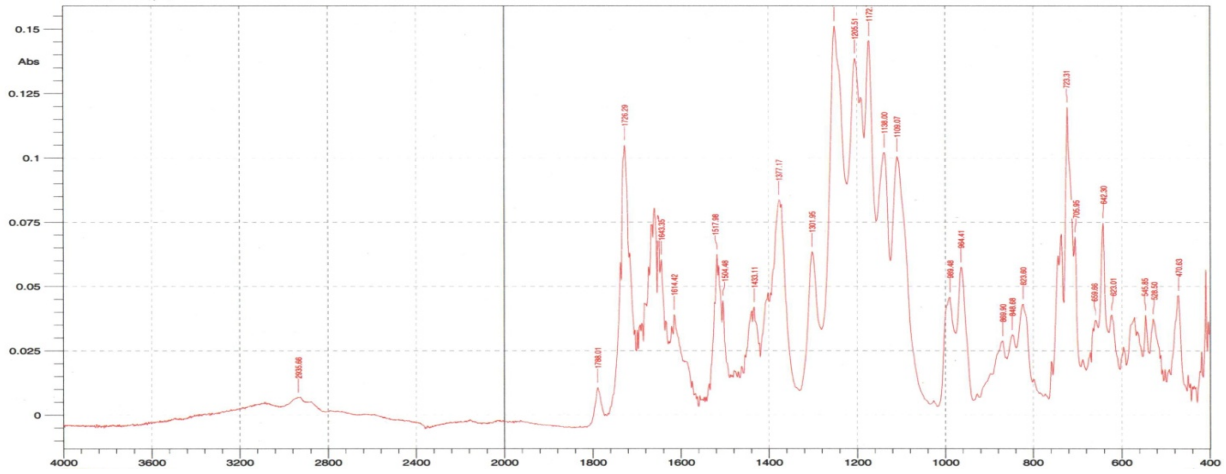

Figure 4.8 – FTIR of Polyimide

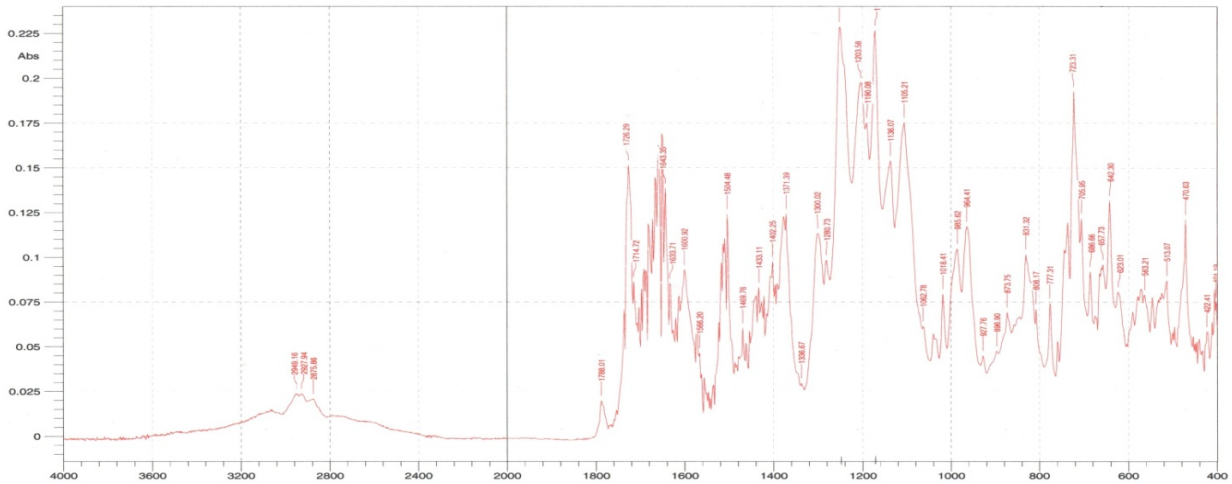

Figure 4.35 – FTIR of Unexposed Polyimide-Model Compound Blend

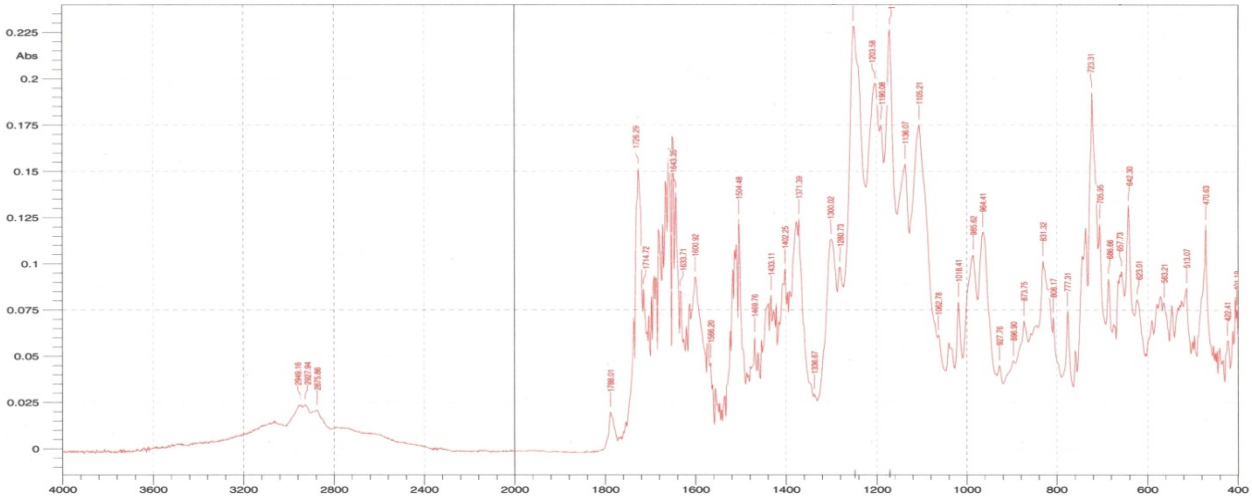

Figure 4.35 – FTIR of Unexposed Polyimide-Model Compound Blend

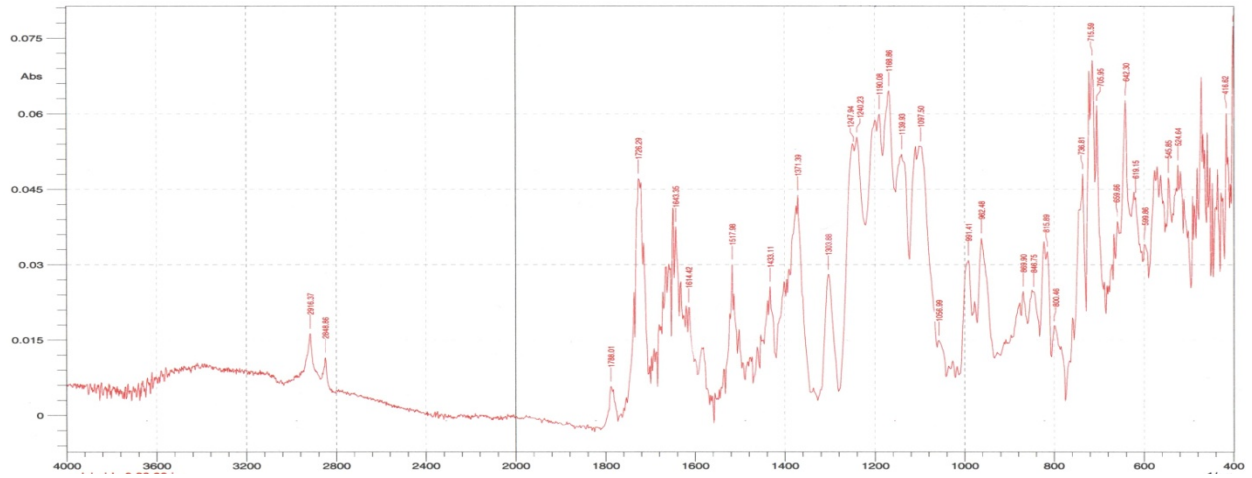

Figure 4.36 – FTIR of Polyimide-Model Compound Blend Exposed to 300 nm UV Light in NMP Solvent

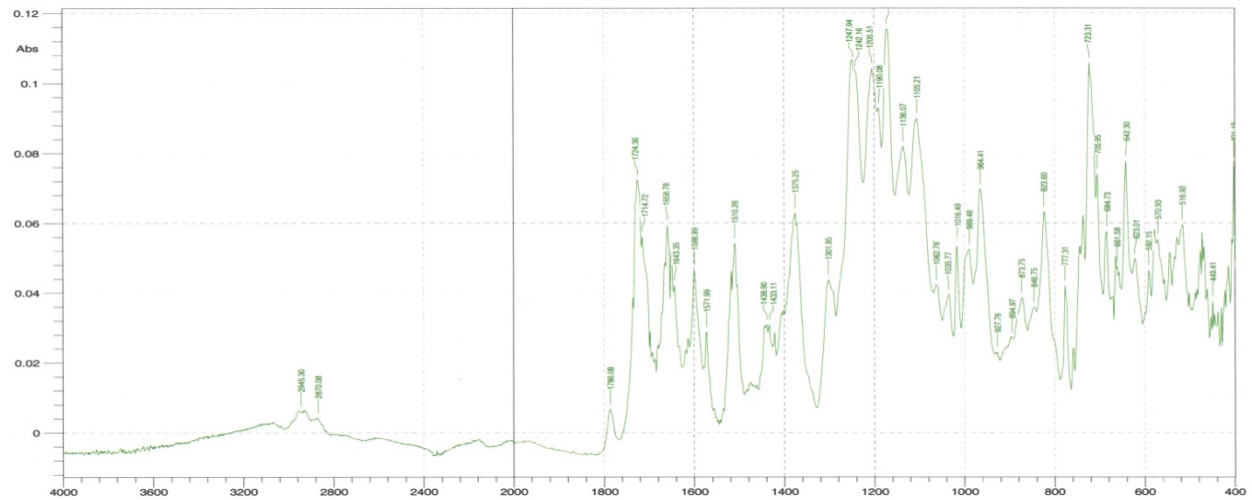

Figure 4.37 – FTIR of Polyimide-Model Compound Blend Exposed to 300 nm UV Light in THF Solvent

4.4.2.2 Thermo-gravimetric Analysis

TGA was also used to confirm the presence of Model Compound in the blend mixture. Fig. 4.38 illustrates the thermograms for model compound, polyimide and blend exposed in THF. Comparing the weight loss around 230^0C for all three products, it was evident that a dominant weight loss event for the model compound was also observed in blend mixture confirming the blend components.

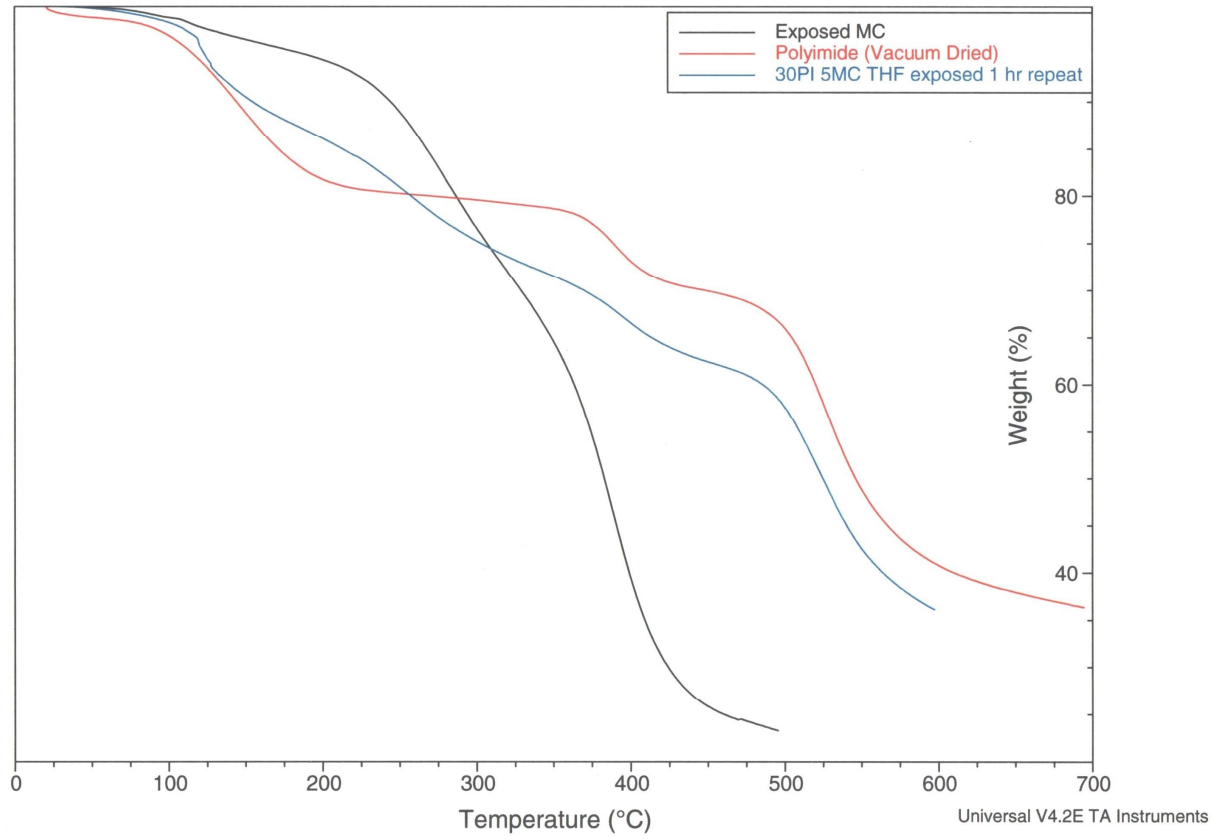

Figure 4.38 – Overlapping TGA Thermograms of Exposed Model Compound, Polyimide and Exposed Blend in THF Solvent

4.5 Tensile Properties Measurements

In order to study the effect of UV exposure time on the tensile property of Polyimide-Model Compound blend, Tensile Testing was performed using Universal Testing Machine. Figs. 4.39-4.44 represent instrument output for the mechanical behavior of blend films under tensile load.

As expected, very low elongations were obtained for all the film samples owing to the brittleness of base polymer, PI[Bis-AP-AF/6FDA] polyimide. Consistent results for Tensile Breaking Strength and Young's Modulus were obtained with standard deviations of < 10 MPa and ≤ 0.2 GPa, respectively. Individual Means and Standard Deviations for each set of samples are summarized in Table 4.5. Results for each sample for each exposure time are tabulated in Appendix C.

Figs. 4.45-4.47 demonstrate the effect of UV exposure time on Tensile Breaking Strength, Tensile Modulus and % Elongation respectively. The trend observed was in accordance with expected results.

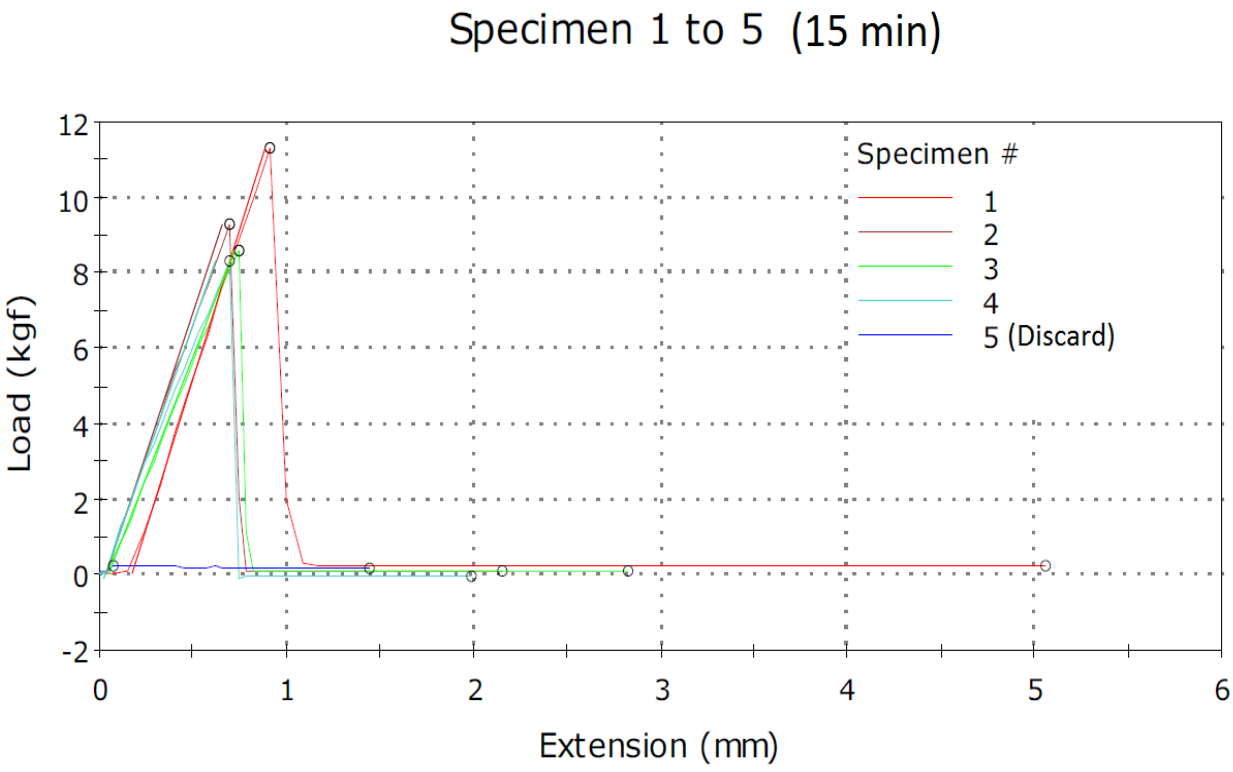

Figure 4.39 – Load-Extension Plot for Tensile Test – 15 Minutes Exposed Samples

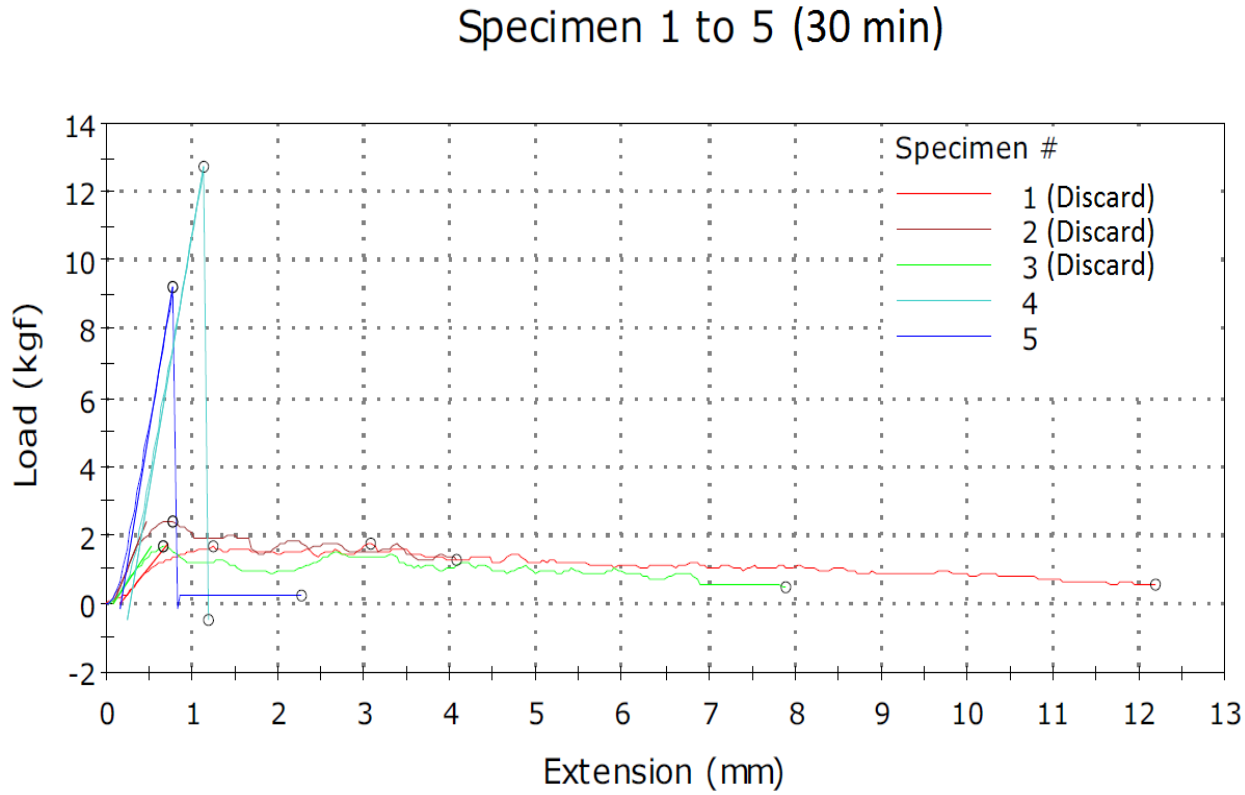

Figure 4.40a – Load-Extension Plot for Tensile Test – 30 Minutes Exposed Samples

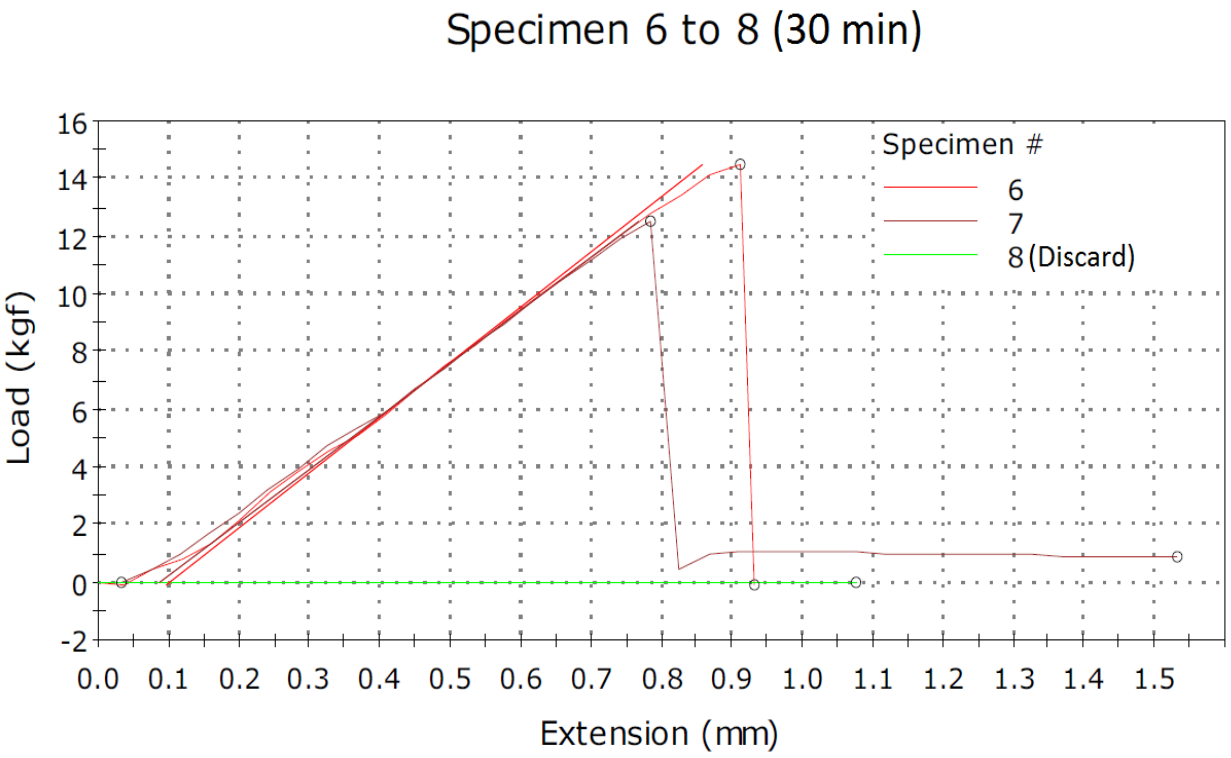

Figure 4.40b – Load-Extension Plot for Tensile Test – 30 Minutes Exposed Samples: Continued

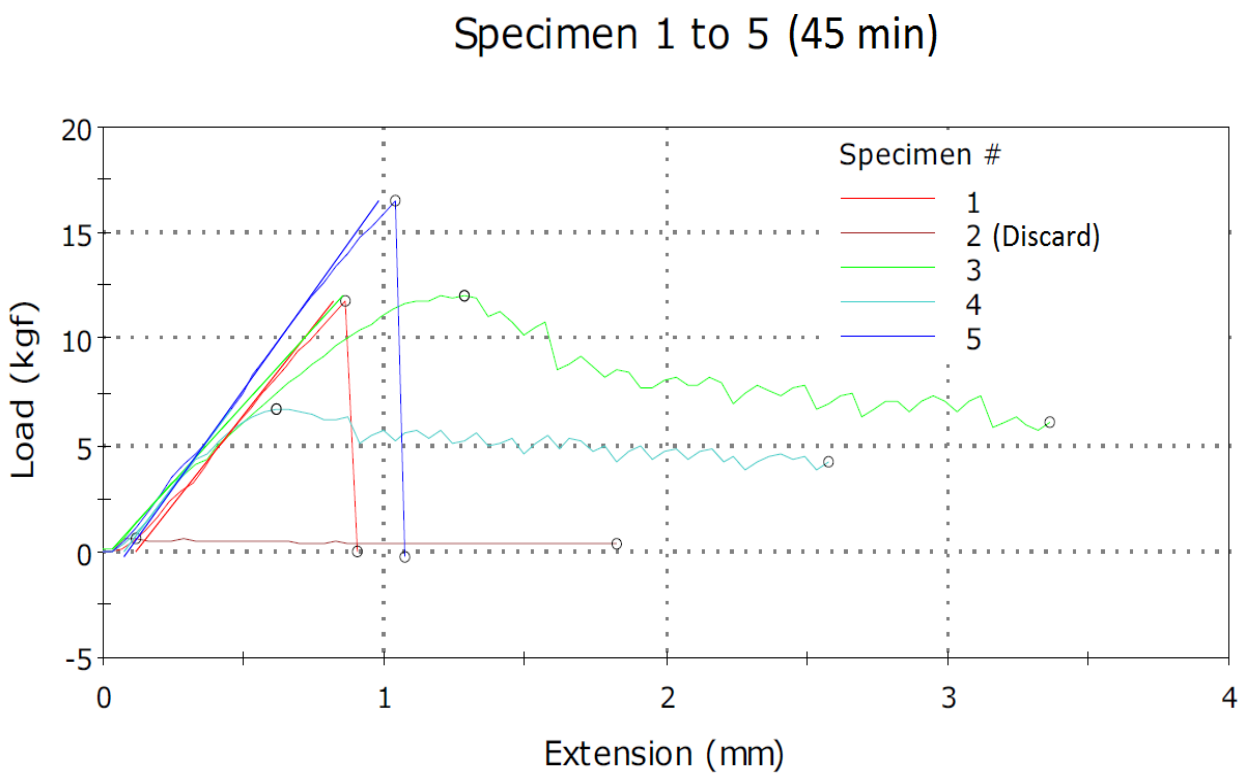

Figure 4.41a – Load-Extension Plot for Tensile Test – 45 Minutes Exposed Samples

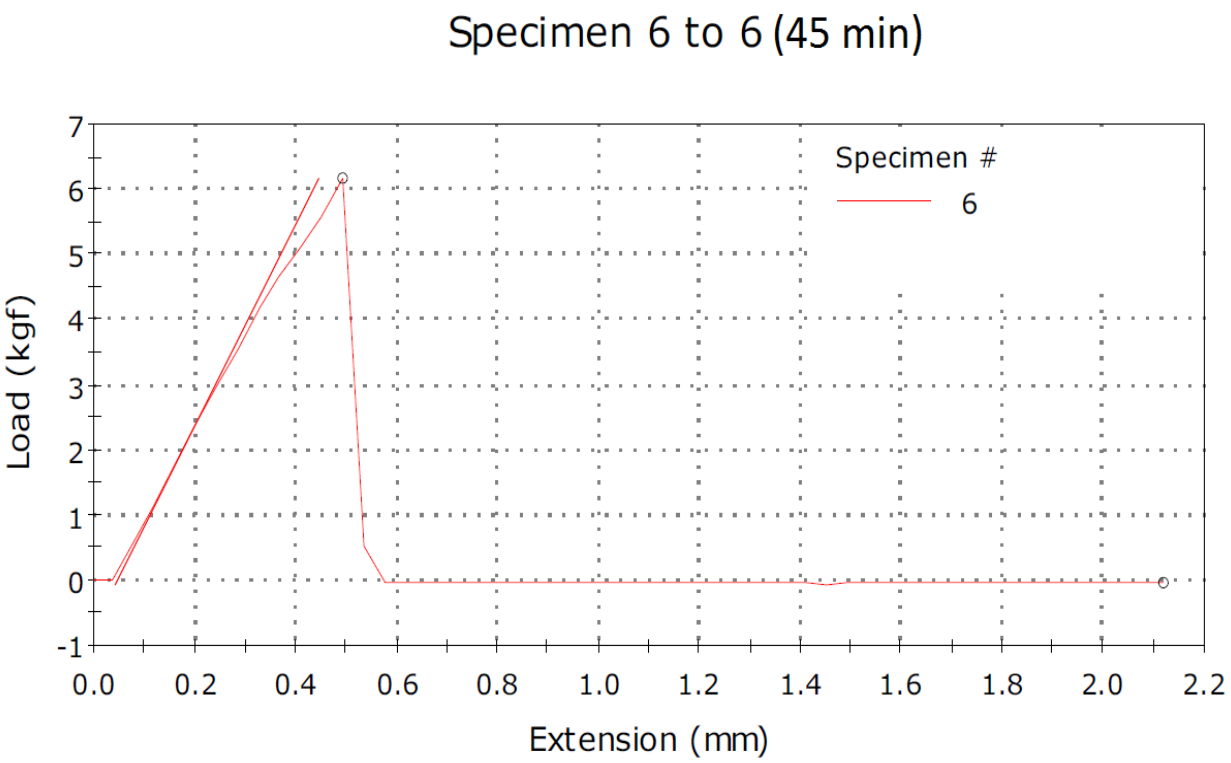

Figure 4.41b – Load-Extension Plot for Tensile Test – 45 Minutes Exposed Samples: Continued

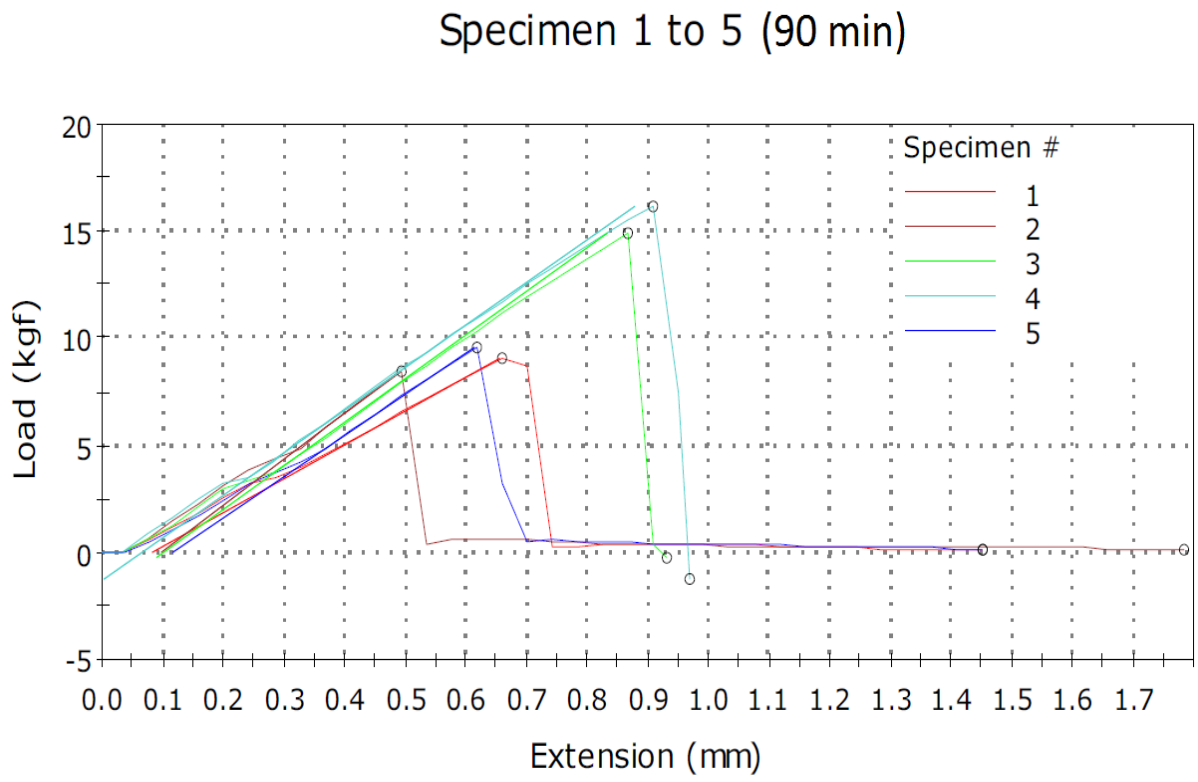

Figure 4.42 – Load-Extension Plot for Tensile Test – 90 Minutes Exposed Samples

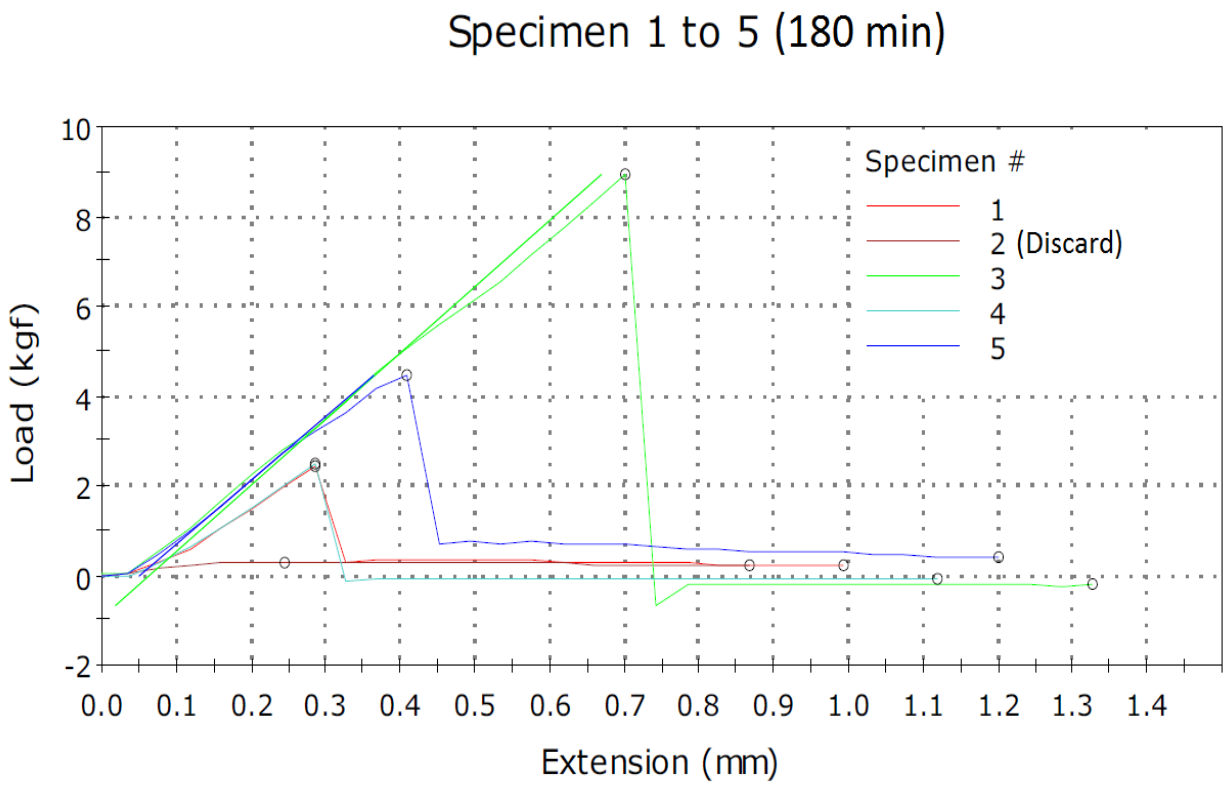

Figure 4.43 – Load-Extension Plot for Tensile Test – 180 Minutes Exposed Samples

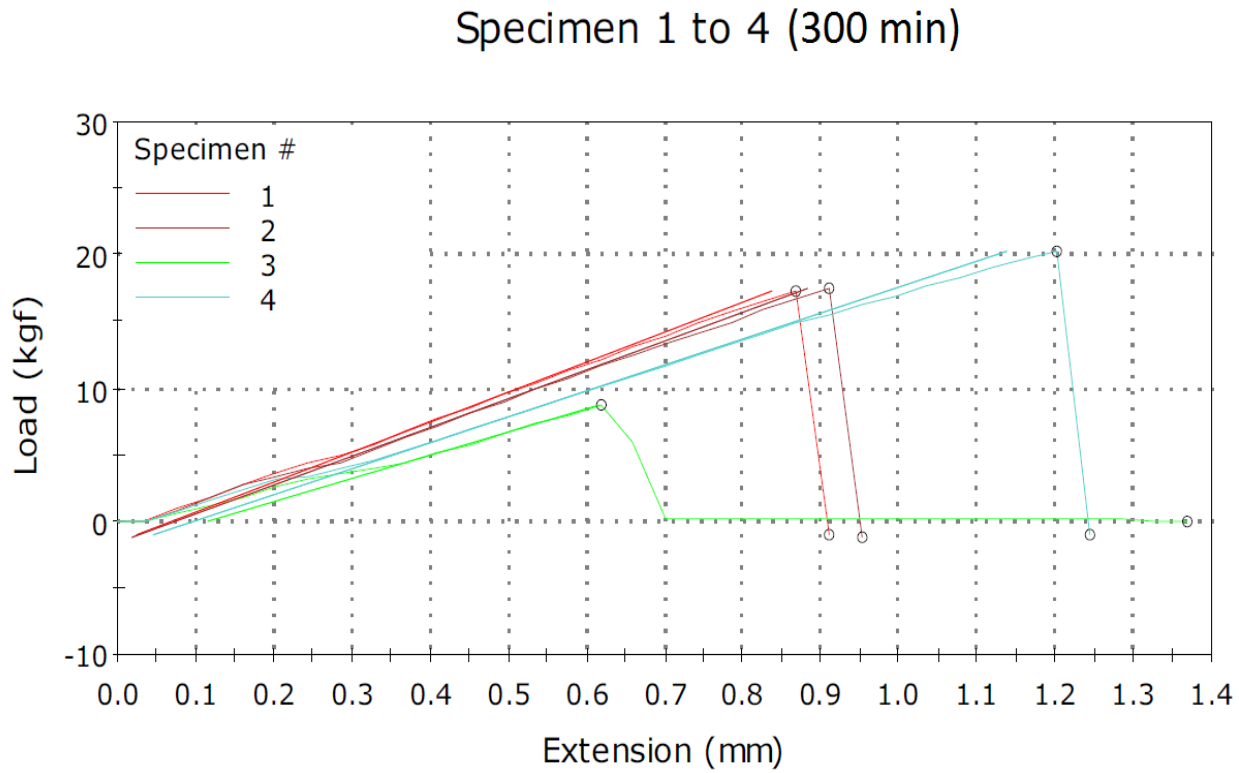

Figure 4.44 – Load-Extension Plot for Tensile Test – 300 Minutes Exposed Samples

Table 4.5 – Summary of Tensile Test Results

UV Exposure Time (Min)	Number of Samples	Tensile Strength (MPa)		Young's Modulus (GPa)		% Elongation	
		Mean	Standard Deviation	Mean	Standard Deviation	Mean	Standard Deviation
15	4	11.643	1.7551	0.7707	0.0411	1.51	0.202
30	4	14.8661	2.3115	0.8472	0.16	1.785	0.34
45	5	19.1387	5.7837	1.1646	0.1923	1.691	0.625
90	5	19.5235	5.0716	1.4002	0.1339	1.398	0.344
180	4	21.0506	9.3644	1.4393	0.6403	1.641	0.468
300	4	24.8	7.8372	1.3852	0.225	1.772	0.472

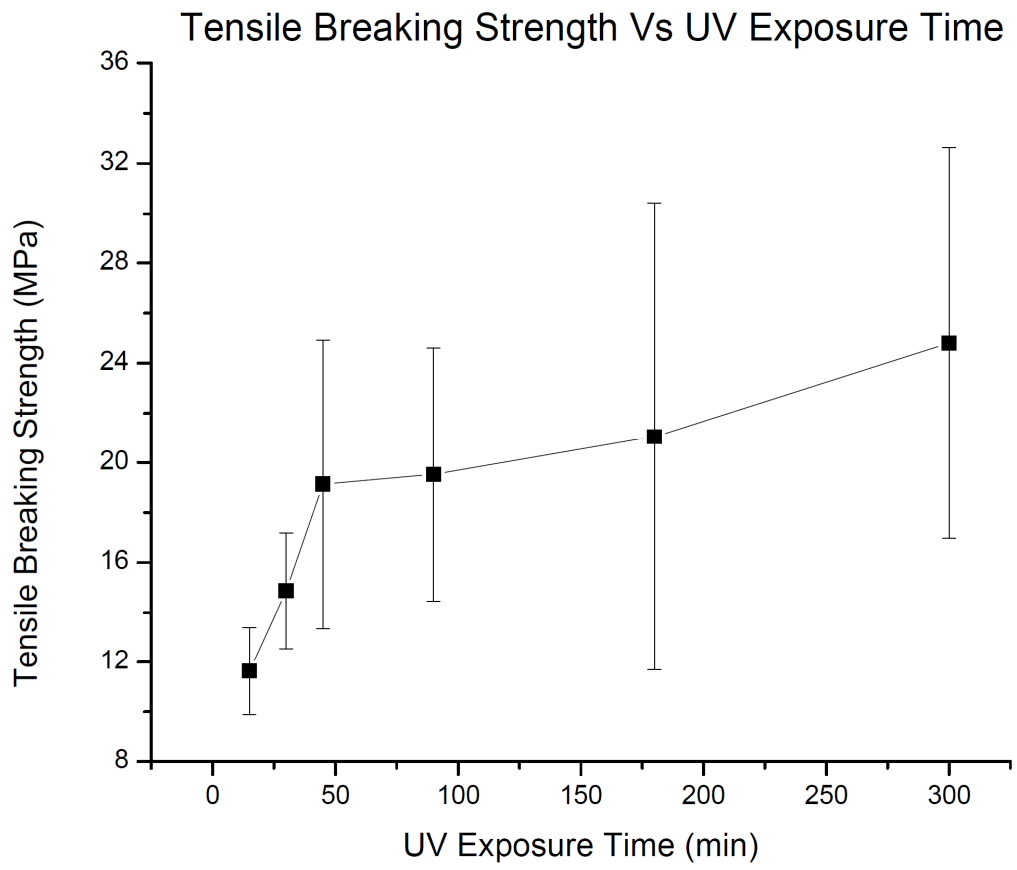

Figure 4.45 – Effect of UV Exposure Time on Tensile Breaking Strength

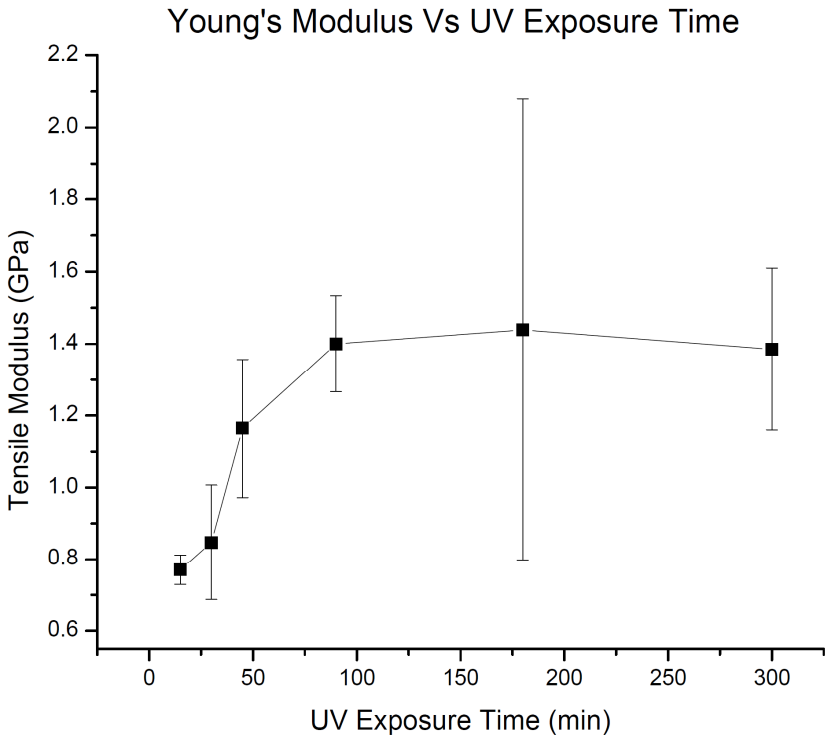

Figure 4.46 – Effect of UV Exposure Time on Young's Modulus

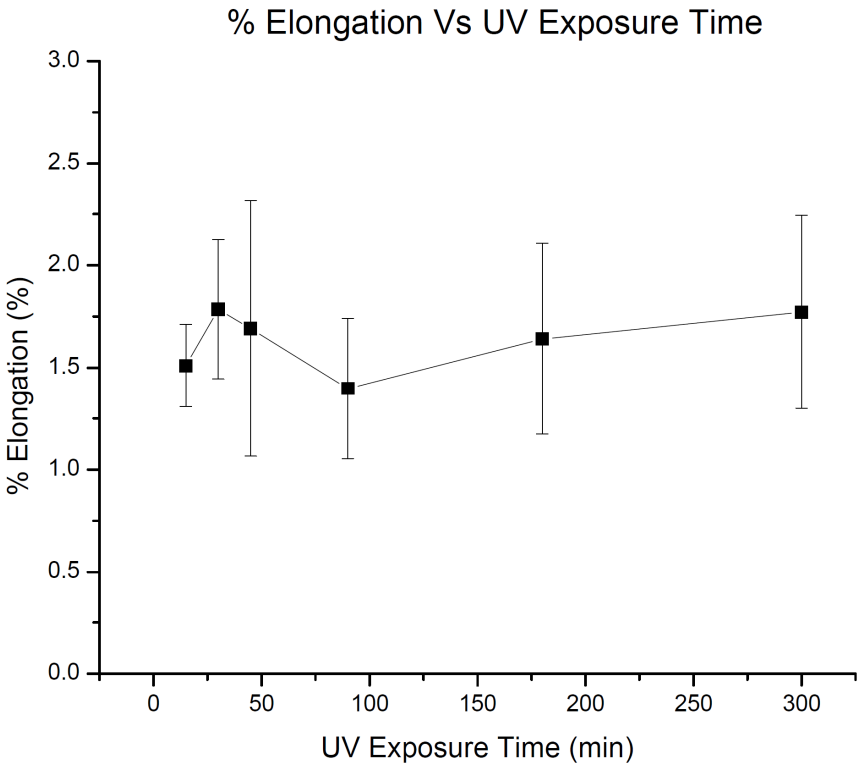

Figure 4.47 – Effect of UV Exposure Time on % Elongation

4.6 Dynamic Mechanical Analysis Measurements

The effect of UV exposure time on the visco-elastic property of Polyimide-Model Compound blends was studied using DMA. Storage Modulus (E'), Loss Modulus (E") and tan δ were analyzed for this purpose. Figs. 4.48-4.53 represent instrument output for E', E" and tan δ for each set of samples exposed to UV light for six different durations.

All the tests were performed at room temperature and at four different frequencies; 0.1 Hz, 1 Hz, 10 Hz and 20 Hz. Results for all samples along with their mean and standard deviations are tabulated in Appendix D. Figs. 4.54-4.56 represent the change in individual properties with increase in UV exposure times. DMA results are in congruence with expected results and results obtained by Tensile Tests. Results obtained by DMA are summarized in Table 4.6.

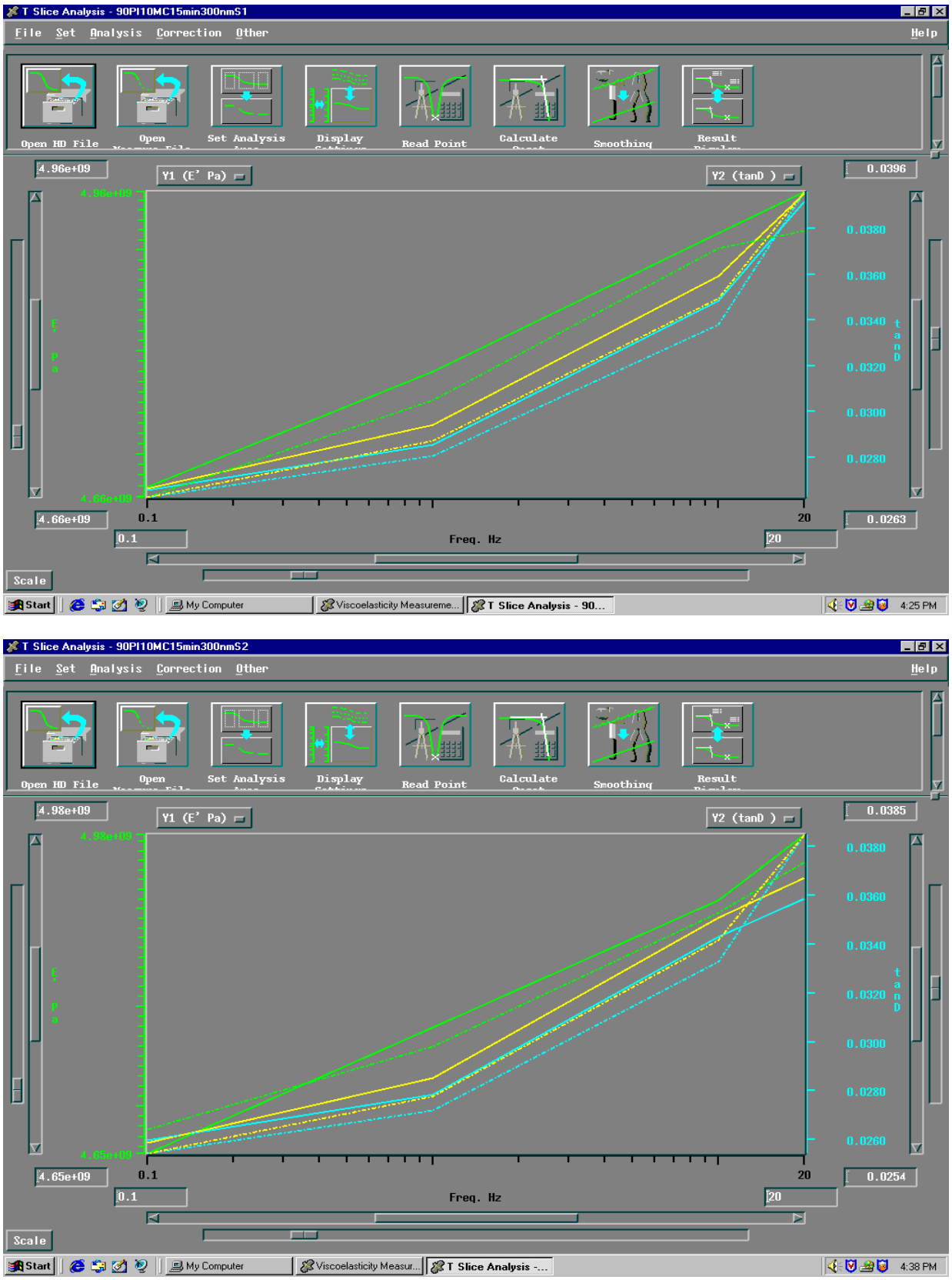

Figure 4.48 – DMA Instrument Output – 15 Minutes Exposed Blend, Samples 1 & 2

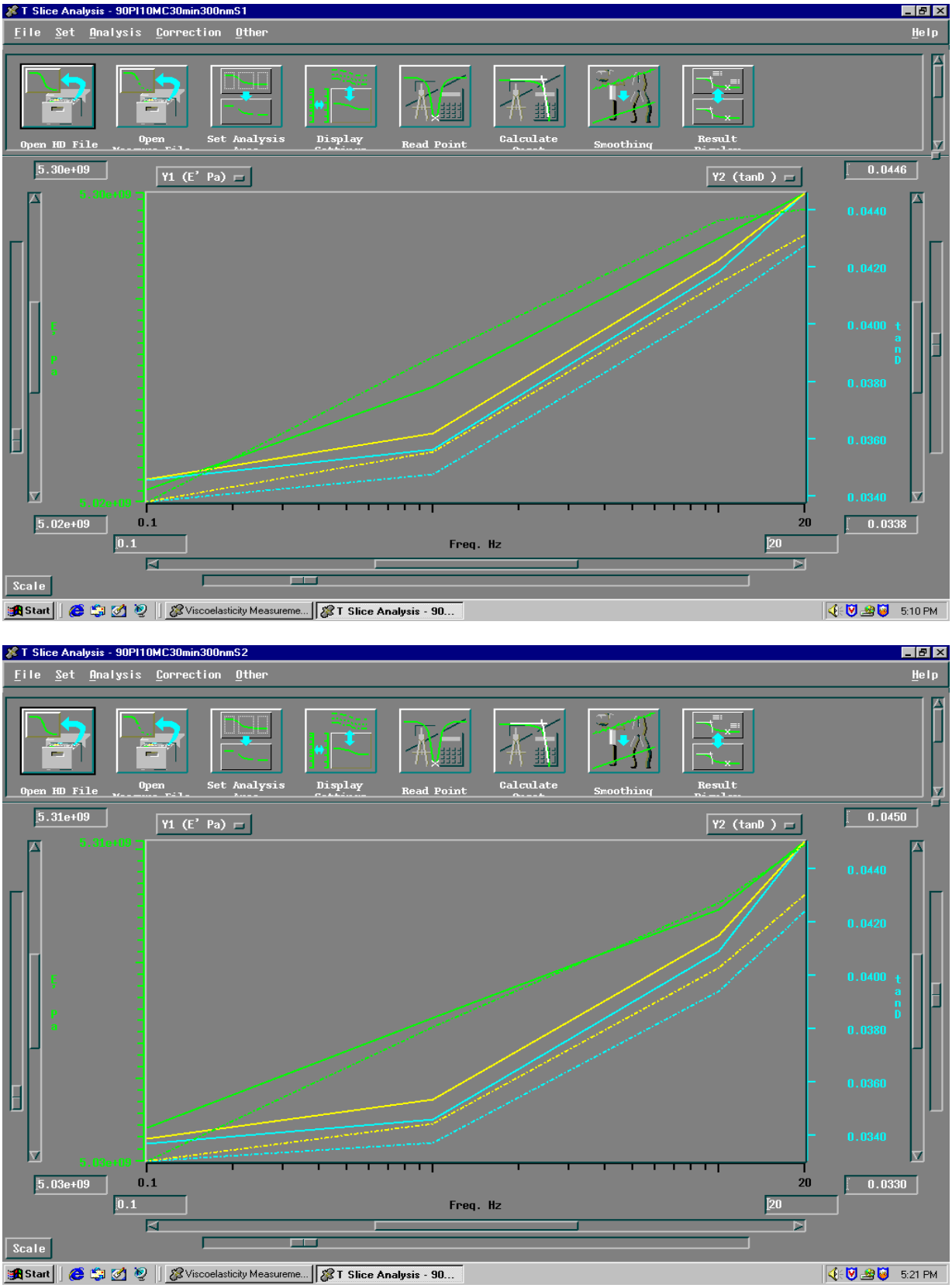

Figure 4.49 – DMA Instrument Output – 30 Minutes Exposed Blend, Samples 1 & 2

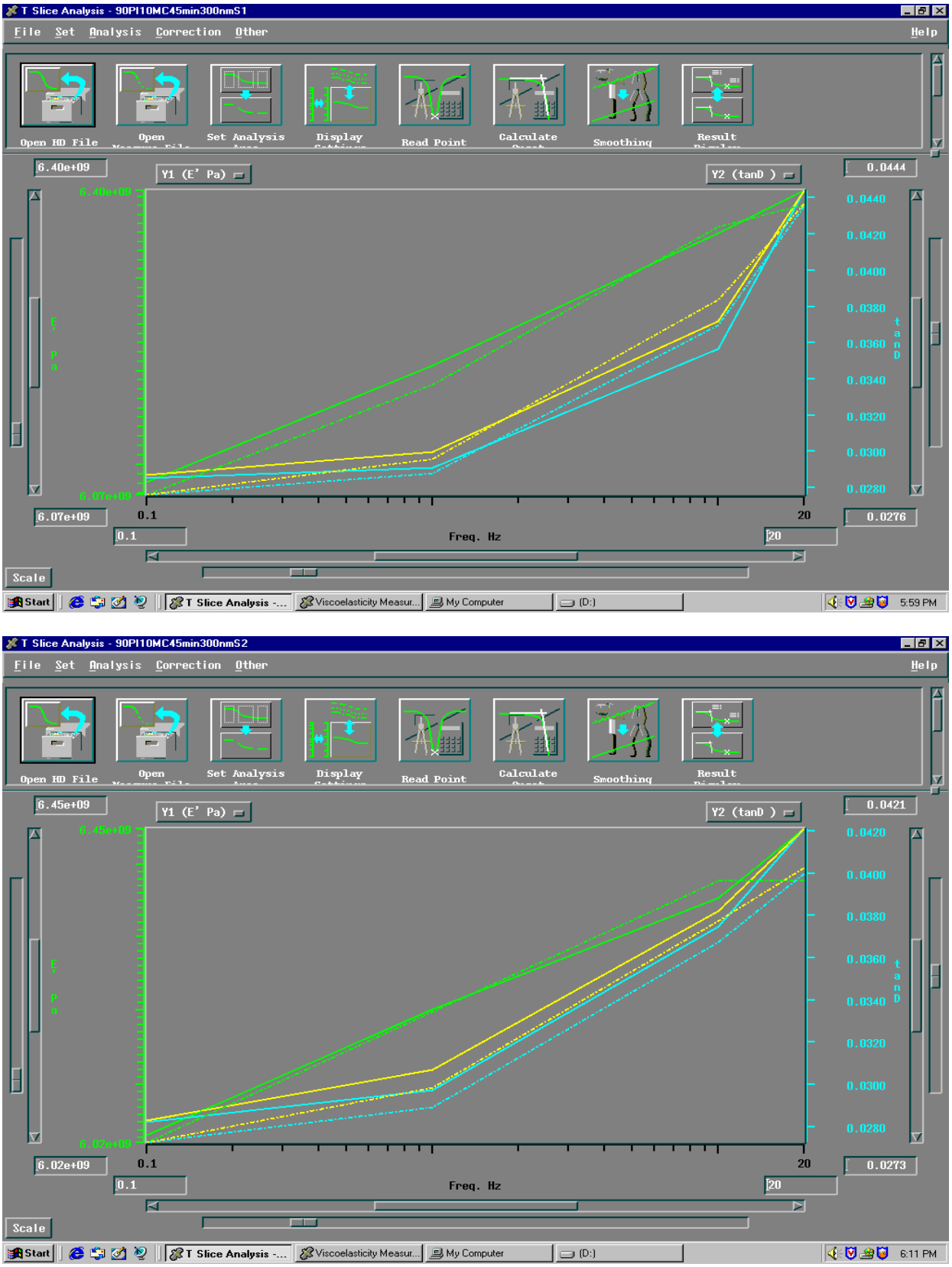

Figure 4.50 – DMA Instrument Output – 45 Minutes Exposed Blend, Samples 1 & 2

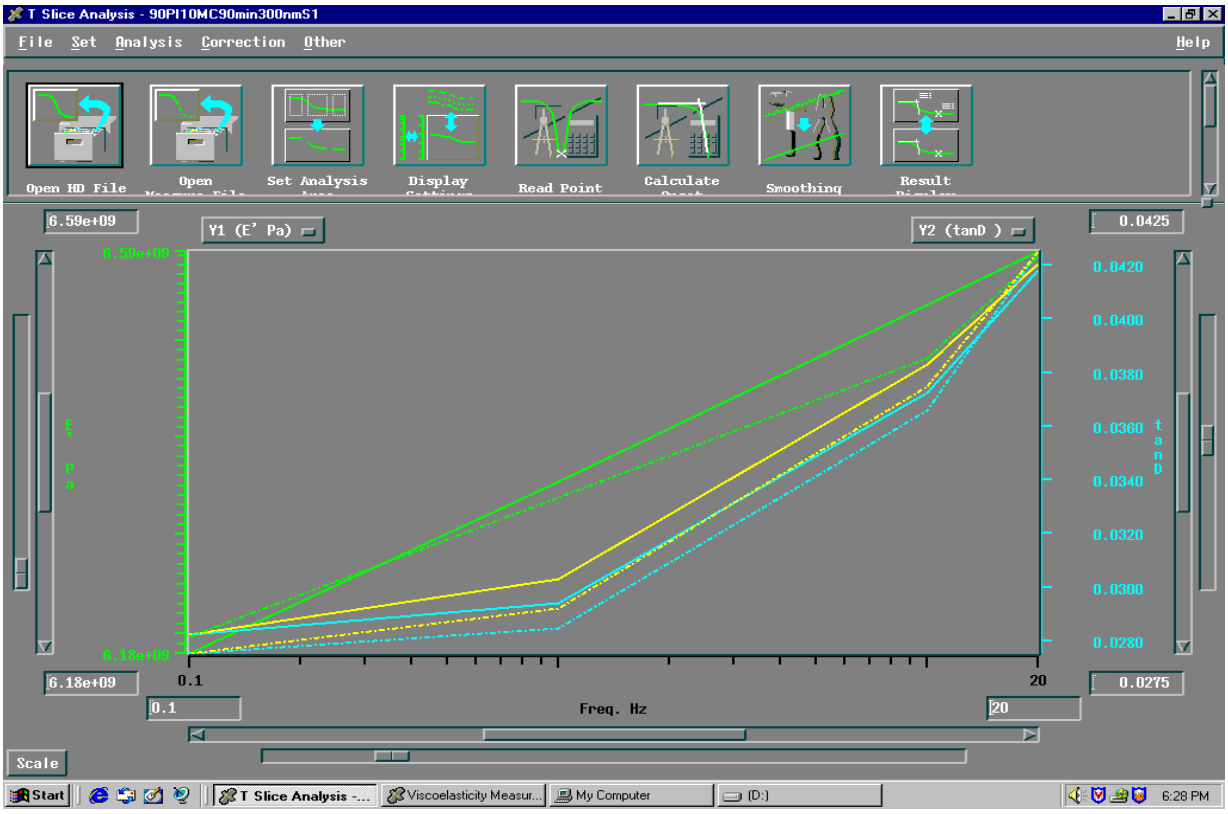

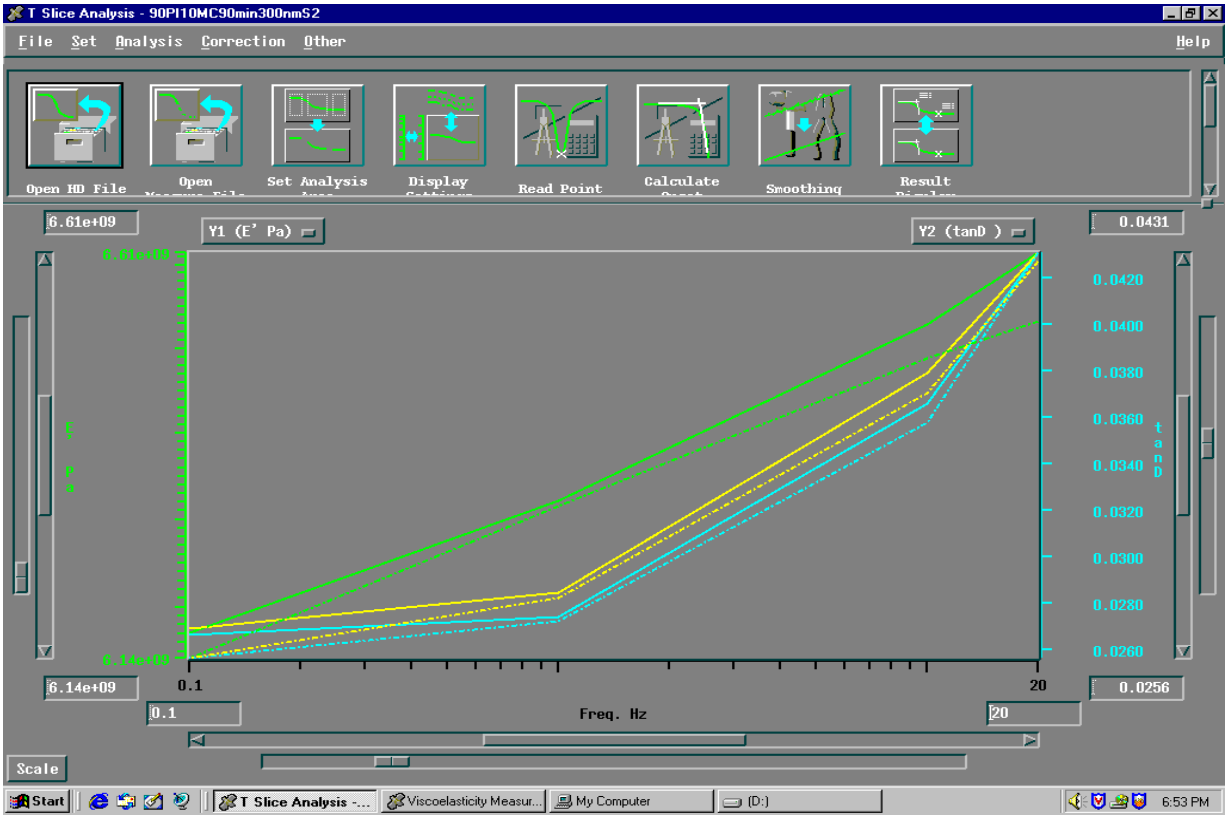

Figure 4.51 – DMA Instrument Output – 90 Minutes Exposed Blend, Samples 1 & 2

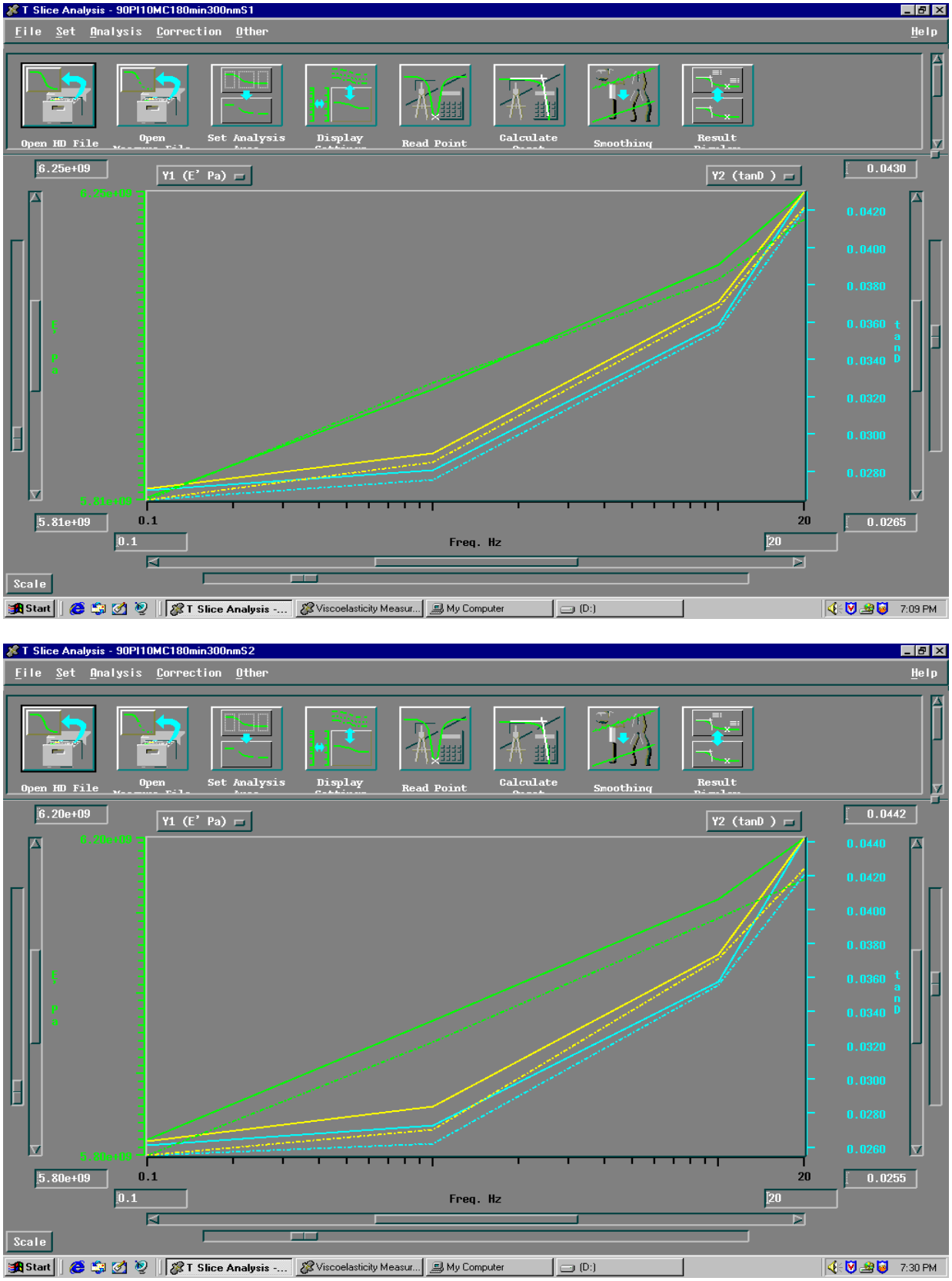

Figure 4.52 – DMA Instrument Output – 180 Minutes Exposed Blend, Samples 1 & 2

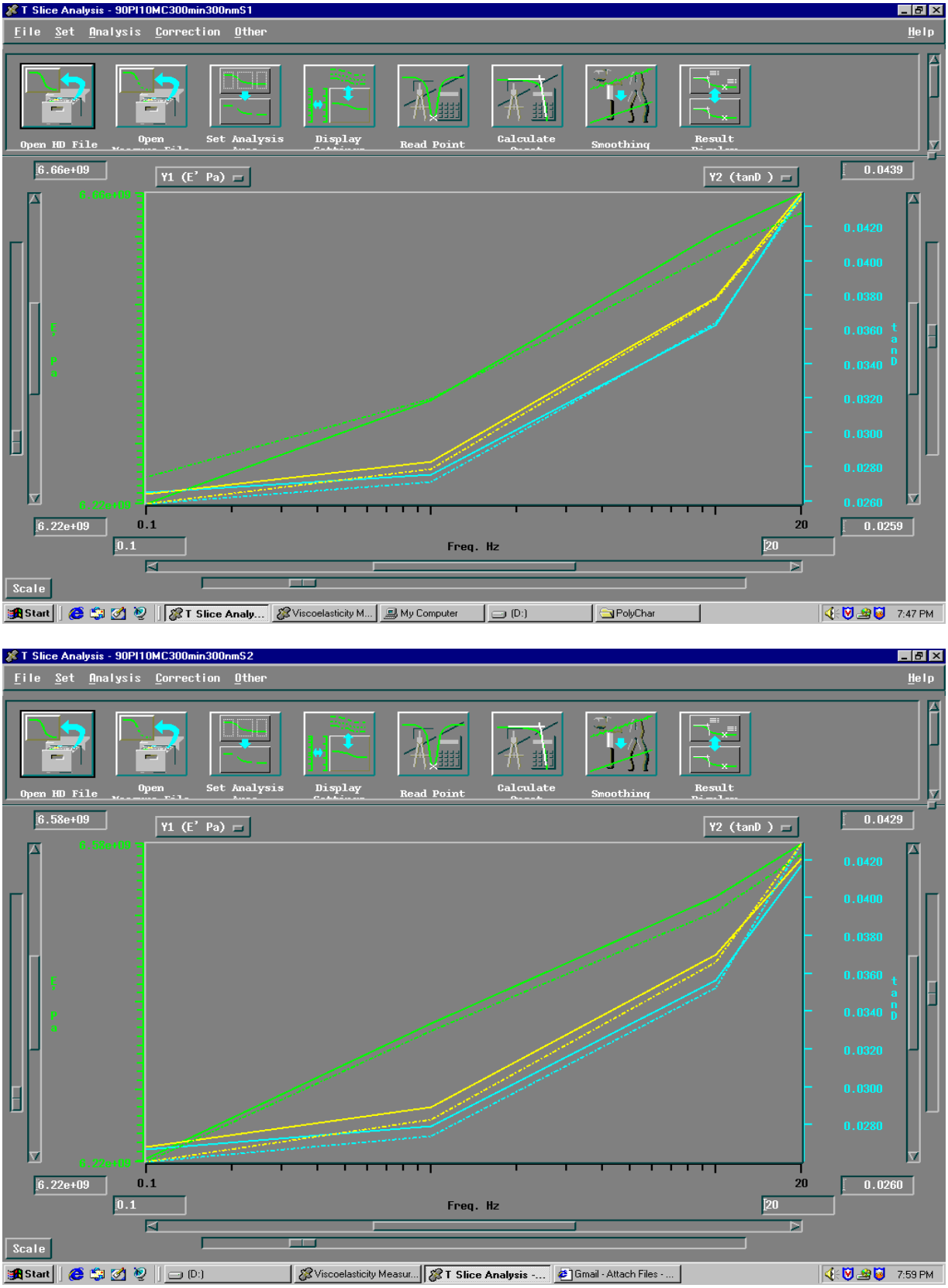

Figure 4.53 – DMA Instrument Output – 300 Minutes Exposed Blend, Samples 1 & 2

Table 4.6 – Summary of DMA Results

Frequency (Hz)	UV Exposure Time (Min)	E` (GPa)		E" (GPa)		tan δ	
		Mean	Standard Deviation	Mean	Standard Deviation	Mean	Standard Deviation
0.1	15	4.66	0.0129	0.1216	0.00246	0.0261	0.0005
	30	5.03	0.0164	0.1699	0.0031	0.0338	0.0006
	45	6.05	0.0294	0.1693	0.00439	0.0280	0.0007
	90	6.17	0.0250	0.1670	0.00736	0.0271	0.0011
	180	5.81	0.0082	0.1528	0.00355	0.0263	0.0006
	300	6.23	0.0150	0.1641	0.00325	0.0264	0.0005
1	15	4.77	0.0144	0.1334	0.00223	0.0280	0.0005
	30	5.14	0.0133	0.1783	0.0036	0.0347	0.0008
	45	6.19	0.0108	0.1812	0.00194	0.0293	0.0003
	90	6.33	0.0222	0.1786	0.00669	0.0282	0.0010
	180	5.96	0.0141	0.1628	0.00517	0.0273	0.0008
	300	6.37	0.0048	0.1756	0.00219	0.0276	0.0003
10	15	4.90	0.0115	0.1671	0.00328	0.0341	0.0007
	30	5.26	0.0105	0.2140	0.00505	0.0407	0.0010
	45	6.36	0.0118	0.2341	0.00509	0.0368	0.0008
	90	6.46	0.0648	0.2366	0.00506	0.0366	0.0006
	180	6.12	0.0206	0.2186	0.00174	0.0357	0.0002
	300	6.56	0.0512	0.2354	0.00469	0.0359	0.0005
20	15	4.95	0.0250	0.1895	0.00752	0.0383	0.0017
	30	5.30	0.0141	0.2317	0.0065	0.0437	0.0013
	45	6.40	0.0343	0.2719	0.01236	0.0425	0.0019
	90	6.56	0.0814	0.2785	0.00434	0.0425	0.0007
	180	6.20	0.0450	0.2653	0.00685	0.0428	0.0011
	300	6.61	0.0443	0.2854	0.00833	0.0432	0.0010

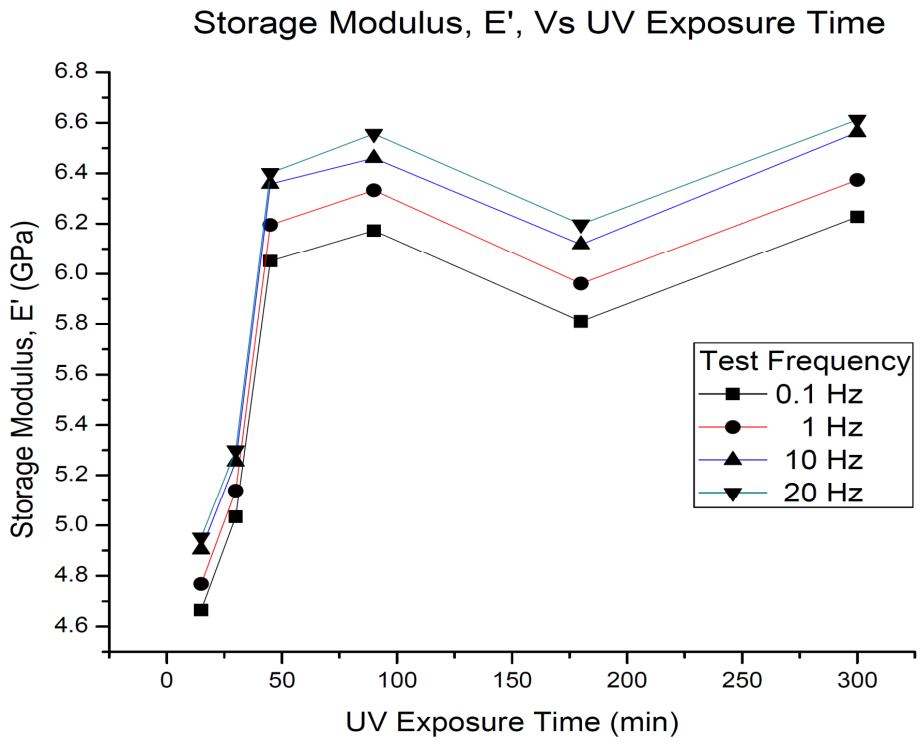

Figure 4.54 – Effect of UV Exposure Time on Storage Modulus, E'

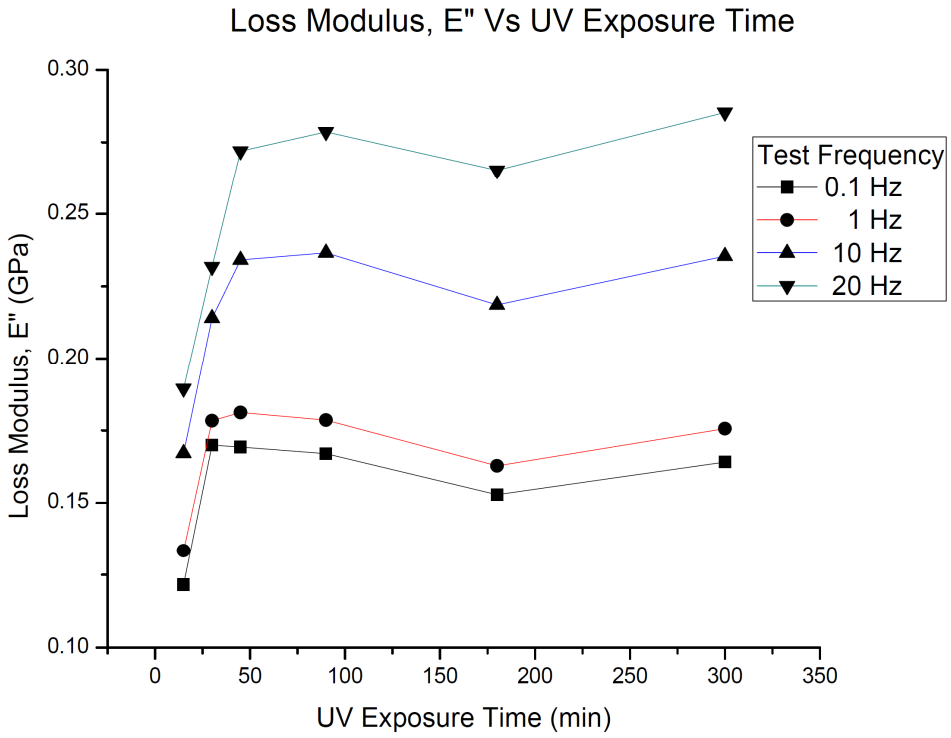

Figure 4.55 – Effect of UV Exposure Time on Loss Modulus, E"

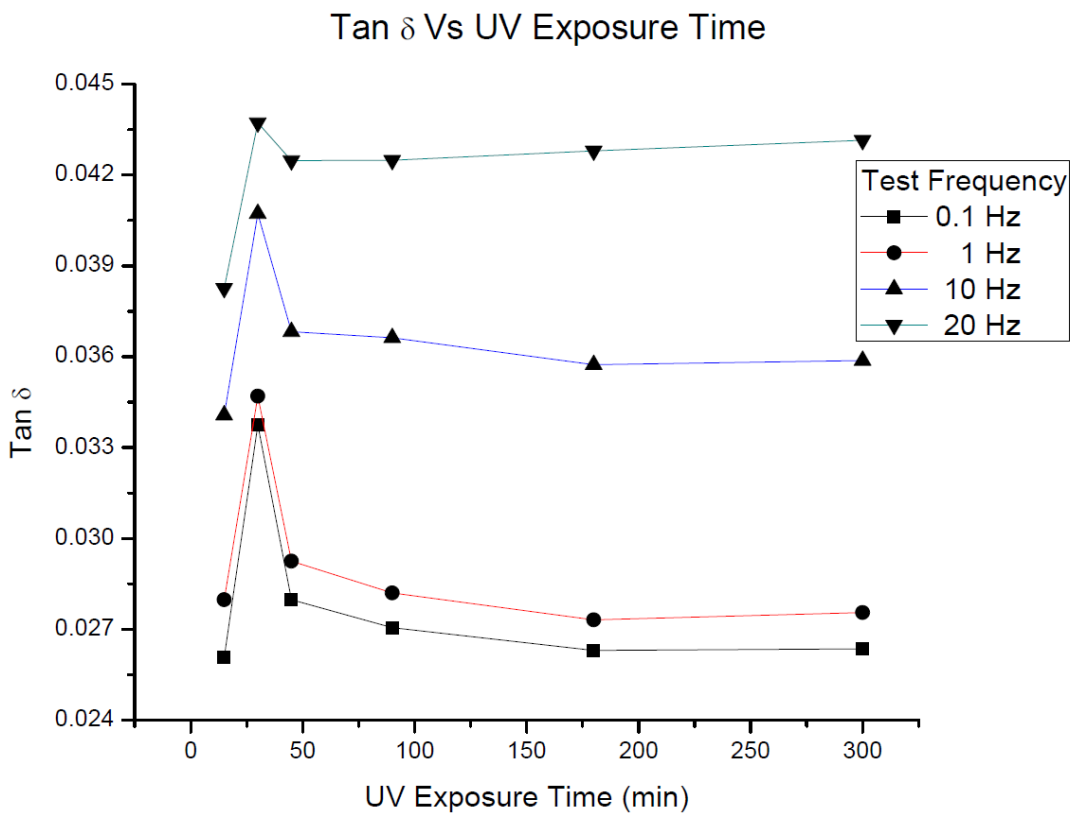

Figure 4.56 – Effect of UV Exposure Time on Tan δ

4.7 Viscosity Measurements

The effect of UV exposure on viscosity of UV irradiated blend solutions was studied using Ubbelohde viscometric technique. The primary advantage of solution viscometry for characterization was to establish the viability of proposed experimentation during the early stages of project work. Calculation and plotting of the normalized viscosity ratio, as defined earlier, not only eliminated the need of knowing the material parameters but also nullified the effect of usage of secondary solution for characterization as it eliminates the effect on solvent medium.

With increase in exposure time, a rapid increase in solution viscosity was observed initially, while prolonged exposure times showed very gradual viscosity rise as shown in Fig. 4.57. Viscometric data, including individual means and standard deviations for solutions for all exposure times, are summarized in Table 4.7. Detailed results are tabulated in Appendix E.

Table 4.7 – Summary of Viscometry Results

UV Exposure Time (Min)	Number of Readings	Normalized Viscosity	
		Mean	Standard Deviation
0	5	5.58857	0.02911
15	7	5.77714	0.02059
30	7	6.23429	0.0207
45	7	6.58857	0.041
90	7	6.68429	0.02149
180	7	6.74286	0.06651
300	7	6.75857	0.05305

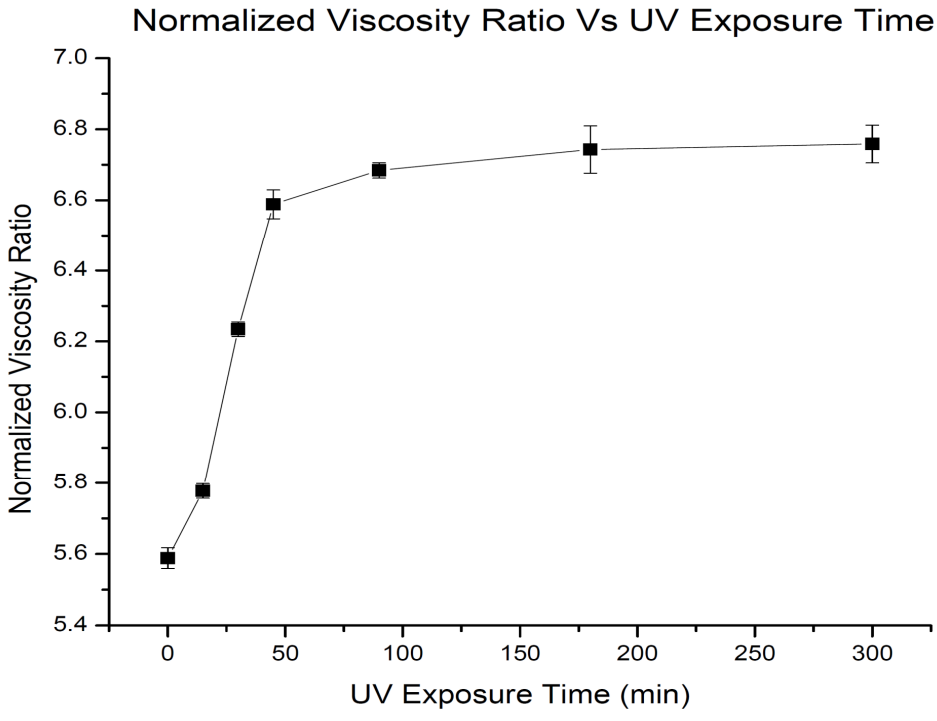

Figure 4.57 – Effect of UV Exposure Time on Blend Solution Viscosity

CHAPTER 5:
DISCUSSION

5 DISCUSSION

The purpose of this study was to estimate the exposure time to be used for UV irradiation of the final pendent co-polyimide with NLO groups and cross-linkers attached. This exposure will not only lock in the aligned NLO orientation but also provide enough mechanical strength to withstand the mechanical forces during operational lifespan at elevated working temperatures, for maximized productive output. To achieve this target, the effects of duration of UV exposure on tensile, visco-elastic and viscometric property were studied for a Model Compound using a Polyimide as a base polymer. Because the mobility of chalcone groups in this system might be different from that in the pendent NLO polymer, the optimum exposure time represents the lower time limit for UV exposure of pendent NLO polymer. A detailed discussion of results obtained with possible explanations is as follows.

5.1 Blend of PI[Bis-AP-AF/6FDA] and UV Cross-linker

The Model Compound (or cross-linker) used for this study was designed to be a monomeric unit with functionality 2 and, thus, would be able to form polymeric chains upon UV exposure. With increase in UV exposure time, it was predicated that these chains would lengthen. If so, the presence of these polymeric chains in Polyimide base would not only affect the tensile property of the blend mixture, but also the extent of affection would be dependent on the length of polymeric chains. Increase or decrease in blend properties is a function of blend compatibility and miscibility. Crudely speaking, in either case the extent of increase/decrease in strength, modulus or viscosity with increase in exposure time will yield chain length-sensitive results. But by performing a controlled comparative study, the limitation posed by blend related issues can be over-looked as they occur uniformly in all test specimens. Also selection of PI[Bis-AP-AF/6FDA] as a base polymer, based on its structural resemblance with one of the component of desired pendent NLO, UV cross-linkable co-polyimide, further reduced the possible blend incompatibility issues.

Consistent results with acceptable standard deviations obtained from Tensile Test, DMA and Viscosity test further solidified the theoretical assumption that selected blend properties would be prominently sensitive to Model Compound chain lengths.

5.2 Tensile Properties Measurements

With increase in UV exposure time, an expected trend followed by tensile breaking strength and Young's Modulus was demonstrated by Tensile Test results. The observed trend was divided into two zones, for explanation purpose; $M < M_c$ and $M > M_c$, where M is molecular weight of polymerized Model Compound and M_c is critical molecular weight corresponding to optimum UV exposure time, t_c, Refer to Fig. 5.1.

$M < M_c$: Initially, for increasing exposure duration, a rapid increase in degree of polymerization is achieved for model compound monomer. This increase in molecular weight with UV exposure, thus, results in sharp increment in tensile properties like, tensile strength by increased entanglements between polyimide and model compound polymeric chains.

$M > M_c$: This zone is beyond critical molecular weight which corresponds to UV exposure time of 45 min indicating a change-over point. Molecular weight attained is sufficient enough to cause restricted free motion of polymeric chain due to entanglement with high molecular weight polyimide chains as observed in typical chain polymerization reactions. It would take infinite time to attain complete polymerization. Hence, from practicality point, the critical exposure time associated with change-over point would yield acceptable balance between optimum mechanical strength and UV exposure time.

5.3 Dynamic Mechanical Analysis Measurements

Dynamic Mechanical Analysis of PI-MC blends were carried out to study the influence of UV exposure on both viscous and elastic components of blends separately. Instead of the more common temperature sweep, frequency sweep was carried out for all the specimens in-order to prevent any thermal polymerization of heat sensitive model compound during tests.

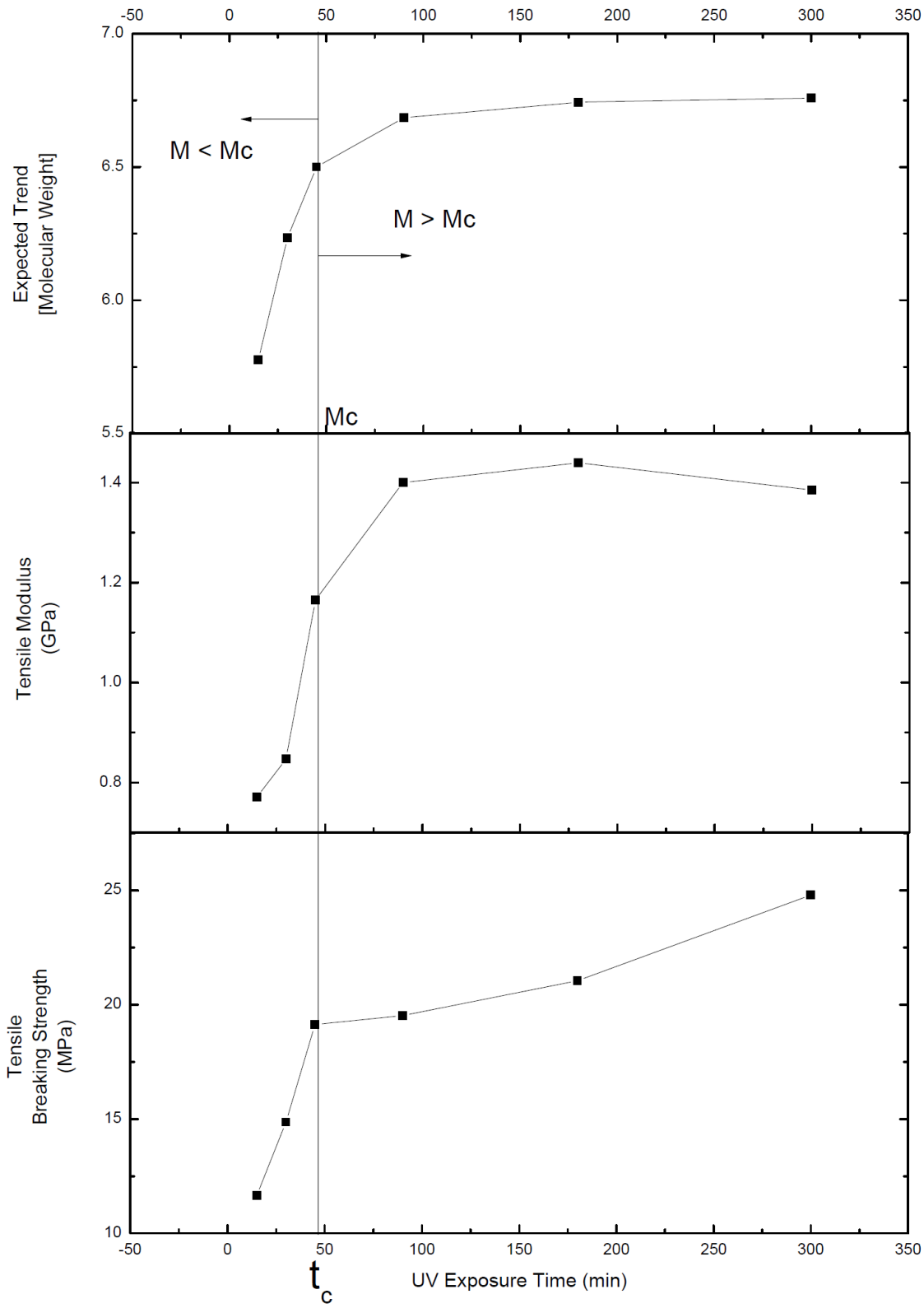

Figure 5.1 – Critical Molecular Weight and Critical UV Exposure Time

An increase in storage modulus with increase in test frequency can be associated with reduction in chain relaxation time. An unsuspected dip in storage modulus observed for specimens exposed to UV light for 180 minutes can be due to remaining microscopic traces of THF solvent in the blend matrix.

It was observed that loss modulus, which relates to "damping", increased with increase in UV exposure time, which proves the formation of low molecular weight polymeric chains of Model Compound, thus increasing the viscous component of blend. As loss modulus is stabilized after 45 min UV exposure, it can safely be assumed that model compound chain length is approaching its highest value with very little possibility of increment. Sharp increase in tan δ was observed for specimen exposed to UV light for 30 minutes. It can be interpreted as the minimum exposure time required to observe any significant change in blend strength caused by polymerization reaction of model compound. Rapid formation of oligomeric chains after 30 minutes of exposure adds to the viscous component of the blend and is prominently seen in result plots for Loss modulus. This clearly indicates that 15 minutes of exposure is very insufficient to cause any observable change while 45 minutes of exposure leads to near-saturation level for tensile properties. Thus, we can conclude that for the given system of polyimide-model compound blend, the UV exposure window is between 30 to 60 minutes.

5.4 Viscometric Measurements

Viscometric study was performed for UV exposed blend solution prior to film casting. Results obtained using Ubbelohde viscometry were congruent to those obtained upon mechanical testing. Sharp initial viscosity rise for solution exposed to UV light not only established the occurrence of polymerization via (2π+2π) cyclo-addition reaction for model compound but also demonstrated that polymeric chains formed are long enough to prominently affect the viscosity of blend solutions. The reduced rate of increase of normalized viscosity in viscosity-ratio plot after 45 minutes of UV exposure can be attributed to "almost" completion of polymerization reaction. Thus, it is concluded that UV

exposure for 45 minutes is sufficient to attain the maximum degree of polymerization for the cross-linker model compound in this system.

Lastly, considering the sensitivity of each of these methods to the degree of cross-linking, it was concluded that all three tests (Tensile, DMA, Viscosity) yield best possible results within their limitations. This research work, not only provided multiple confirmations for proposed theory, but also leads to a comparative study between different test methods, which can be used as a reference for future work for such systems.

CHAPTER 6:
CONCLUSIONS

6 CONCLUSIONS

It is established that,

- *UV cross-linker is sensitive to 300 nm wavelength UV light.*

  This conclusion is established by LC mass spectrography and UV-visible spectrography.

- *Optimum UV exposure time is around 45 minutes with a window of 30-60 minutes, depending on the system viscosity.*

  Each repeat unit of final NLO pendent co-polyimide is proposed to have different ratios of cross-linker to (Bis AP-AF/6FDA) polyimide ranging from (0.3 : 0.7) to (0.05 : 0.95). As 5MC-30PI blend used for this work have the ratio of (0.125 : 0.875) which is in range of proposed ratios, the applicability of the determined UV exposure time window, is justified and can be used for future reference purpose.

- *UV cross-linkable model compound does polymerize via a (2π+2π) cyclo-addition mechanism.*

  Although the actual requirement from UV cross-linker model compound once attached to final NLO pendent co-polyimide, is just to chemically bond with its neighboring clone forming a cross-link, it's capability of forming polymeric chains is demonstrated, which should answer any relevant questions regarding its cross-linkability in the presence of the PI[Bis-AP-AF/6FDA] structure.

- *Polymerized UV cross-linker is mechanically strong.*

  As prominent increase in mechanical strength was observed when UV cross-linker model compound in PI-MC blend was photo-polymerized, it can cautiously be concluded that cross-links generated by this UV cross-linker will also be strong enough, thus, to satisfy the goal of preserving NLO alignment.

CHAPTER 7:

FUTURE WORK

7 FUTURE WORK

- Study the effect of varying length of spacer group on mechanical properties of cross-linkable Model Compound.
- Study the cis-trans configuration observed for photo-cyclo-addition reaction. Mechanical properties of cis- and trans- isomers vary drastically; hence it is important to optimize the synthesis process for control of such isomerism.
- Attach the cross-linkable group to pendent NLO Polyimide backbone and study its mechanical properties upon cross-linking.

REFERENCES

REFERENCES

1. (a) Dalton; Larry, *Nonlinear optical polymeric materials: From chromophore design to commercial applications*. Springer: Berlin, Heidelberg, 2002; Vol. 158, p 86;

   (b) Cho, M. J.; Choi, D. H.; Sullivan, P. A.; Akelaitis, A. J. P.; Dalton, L. R., Recent progress in second-order nonlinear optical polymers and dendrimers. *PROG POLYM SCI* **2008,** *33* (11), 1013-1058;

   (c) Baehr-Jones, T.; Penkov, B.; Huang, J.; Sullivan, P.; Davies, J.; Takayesu, J.; Luo, J.; Kim, T.-D.; Dalton, L.; Jen, A.; Hochberg, M.; Scherer, A., Nonlinear polymer-clad silicon slot waveguide modulator with a half wave voltage of 0.25 V. *APPL PHYS LETT* **2008,** *92* (16), 163303-3.
2. (a) Kajzar, F.; Lee, K.-S.; Jen, A., Polymeric Materials and their Orientation Techniques for Second-Order Nonlinear Optics. In *ADV POLYM SCI*, Lee, K.-S., Ed. Springer Berlin / Heidelberg: 2003; Vol. 161, pp 1-85;

   (b) Schneider, A.; Stillhart, M.; Günter, P., High efficiency generation and detection of terahertz pulses using laser pulses at telecommunication wavelengths. *OPT EXPRESS* **2006,** *14* (12), 5376-5384.
3. (a) Dalton, L. R.; Harper, A. W.; Robinson, B. H., The role of London forces in defining noncentrosymmetric order of high dipole moment–high hyperpolarizability chromophores in electrically poled polymeric thin films. *PROC NATL ACAD SCI USA* **1997,** *94* (10), 4842-4847;

   (b) Vakhonina, T. A. S., Sirina M.; Ivanova, Nataliya V.; Fominykh, Olga D.; Smirnov, Nickolai N.; Yakimansky, Alexander V.; Balakina, Marina Yu., Second-order nonlinear optical response of the epoxy-based thin films with azo-chromophores. *PROC OF SPIE* **2010,** *7993*, 799307.
4. (a) Cho, Y.-S.; Lee, J.-S.; Cho, G.; Wada, T.; Sasabe, H., Nonlinear optical properties in novel crosslinked system with host-guest and side chain. *POLYMER* **2001,** *42* (23), 9379-9384;

   (b) Sui, Y.; Wang, D.; Yin, J.; Tan, G.-Z.; Zhu, Z.-K.; Wang, Z.-g., Side-chain second-order nonlinear optical poly(urethane-imide)/photosensitive polyimide blends with the improved dipole orientation stability by photo-crosslinking. *MATER LETT* **2002,** *52* (1-2), 53-56;

   (c) Shi, Z.; Liang, W.; Luo, J.; Huang, S.; Polishak, B. M.; Li, X.; Younkin, T. R.; Block, B. A.; Jen, A. K. Y., Tuning the Kinetics and Energetics of Diels−Alder Cycloaddition Reactions to Improve Poling Efficiency and Thermal Stability of High-Temperature Cross-Linked Electro-Optic Polymers. *CHEM MATER* **2010,** *22* (19), 5601-5608;

   (d) Hong, J.; Li, C.; Zhou, J.; Zhou, L.; Chen, S.; Chen, W. In *A cross-linked electro-optic polymer for second order nonlinear optical applications*, Hangzhou, China, Luo, Y.; Buus, J.; Koyama, F.; Lo, Y.-H., Eds. SPIE: Hangzhou, China, 2008; pp 713530-8.

5. Shi, Z.; Luo, J.; Huang, S.; Zhou, X.-H.; Kim, T.-D.; Cheng, Y.-J.; Polishak, B. M.; Younkin, T. R.; Block, B. A.; Jen, A. K. Y., Reinforced Site Isolation Leading to Remarkable Thermal Stability and High Electrooptic Activities in Cross-Linked Nonlinear Optical Dendrimers. *CHEM MATER* **2008,** *20* (20), 6372-6377.
6. (a) Miller, R. D.; Burland, D. M.; Jurich, M.; Lee, V. Y.; Moylan, C. R.; Thackara, J. I.; Twieg, R. J.; Verbiest, T.; Volksen, W., Donor-Embedded Nonlinear Optical Side Chain Polyimides Containing No Flexible Tether: Materials of Exceptional Thermal Stability for Electrooptic Applications. *MACROMOLECULES* **1995,** *28* (14), 4970-4974;
   (b) Davey, M. H.; Lee, V. Y.; Wu, L. M.; Moylan, C. R.; Volksen, W.; Knoesen, A.; Miller, R. D.; Marks, T. J., Ultrahigh-Temperature Polymers for Second-Order Nonlinear Optics. Synthesis and Properties of Robust, Processable, Chromophore-Embedded Polyimides. *CHEM MATER* **2000,** *12* (6), 1679-1693.
7. (a) Guven, O., Crosslinking & Scission in polymers. Springer: 1990; Vol. 292, p 272; (b) Ameduri, B. B., B., *Crosslinking in Materials Science*. Springer: 2005; Vol. 184.
8. Gowariker, V. R. V., N.V.; Sreedhar, J. , *Polymer Science*. New Age International (P) Ltd.: New Delhi, 2003.
9. Rudin, A., *The Elements of Polymer Science & Engineering*. Academic Press: 1998.
10. Crawford, R. J., Plastics Engineering (3rd Edition). Elsevier: 1998.
11. Ratnikova, T. V.; Zvonkov, Y. A.; Sheshina, G. M.; Gracheva, N. Y.; Ginak, A. I., A study of sulphur vulcanization of diene rubbers. Structure and properties of systems containing bis-(tetraethyldiamidophosphoryl)-disulphide, secondary accelerators and metal oxides. *POLYM SCI USSR* **1988,** *30* (3), 586-593.
12. Manas Chanda, S. R., *Plastics Technology Handbook*. 4 ed.; CRC Press: 2006.
13. Liu, Y.; Wang, R.; Chung, T.-S., Chemical cross-linking modification of polyimide membranes for gas separation. *J MEMBRANE SCI* **2001,** *189* (2), 231-239.
14. Ghosh M.K., M. K. L., *Polyimides-Fundamentals and Applications*. Marcel-Dekker, Inc.: New York, p 891.
15. Sroog, C. E., Polyimides. *PROG POLYM SCI* **1991,** *16*, 561-694.
16. Deligöz, H.; Yalcinyuva, T.; Özgümüs, S.; Yildirim, S., Preparation, characterization and dielectric properties of 4,4-diphenylmethane diisocyanate (MDI) based cross-linked polyimide films. *EUR POLYM J* **2006,** *42* (6), 1370-1377.
17. Xiao, Y.; Chung, T.-S.; Guan, H. M.; Guiver, M. D., Synthesis, cross-linking and carbonization of co-polyimides containing internal acetylene units for gas separation. *J MEMBRANE SCI* **2007,** *302* (1-2), 254-264.

18. Powell, C. E.; Duthie, X. J.; Kentish, S. E.; Qiao, G. G.; Stevens, G. W., Reversible diamine cross-linking of polyimide membranes. *J MEMBRANE SCI* **2007,** *291* (1-2), 199-209.
19. Sullivan, D. M.; Bruening, M. L., Ultrathin, cross-linked polyimide pervaporation membranes prepared from polyelectrolyte multilayers. *J MEMBRANE SCI* **2005,** *248* (1-2), 161-170.
20. Qureshi, A.; Singh, N. L.; Rakshit, A. K.; Singh, F.; Avasthi, D. K., Swift heavy ion induced modification in polyimide films. *SURF COAT TECH* **2007,** *201* (19-20), 8308-8311.
21. Dubey, M.; Nema, S. K., Alloys of polyimides with varying degree of crosslinking through antimony salts: mechanical properties characterization. *POLYMER* **1999,** *40* (21), 5947-5951.
22. Okazaki, M.; Onishi, H.; Yamashita, W.; Tamai, S., Positive-type Photosensitive Polyimide Based on Poly(amide acid), Vinyl Ether Crosslinker, and a Photoacid Generator. *J PHOTOPOLYM SCI TECH* **2008,** *21* (1), 119-123.
23. Liu, C.; Coughlin, P.; Tang, M.-W.; Serbayeva, R.; Lubo, Z. Polymer Membranes Prepared from Aromatic Polyimide Membranes by Thermal Treating and UV Crosslinking. US 2010/0133192 A1 2010.
24. Xiang-Dan Li, Z.-X. Z., Guang Jin, Seung Hee Lee, Myong-Hoon Lee, Liquid Crystal Photoalignment by Soluble Photosensitive Polyimide with Methylene Cinnamate Side Units. *MACROMOL RES* **2006,** *14* (3), 257-260.
25. Lee, W.-C., Hsu, Chain-Shu, Wu, Shin-Tson, Liquid Crystal Alignment with a Photo-Crosslinkable and Solvent-Soluble Polyimide Film. *JPN J APPL PHYS* **2000,** *39* (Part 2, No. 5B), L471-L473.
26. Sysel, P. H., R.; Sindelar, V.; Brus, J., Preparation and characterization of crosslinked polyimide-poly(dimethylsiloxane)s. *POLYMER* **2001,** *42*, 10079-10085.
27. Fukukawa, K.-i.; Ueda, M., Recent Progress of Photosensitive Polyimides. *POLYM J* **2008,** *40* (4), 281-296.
28. Tunell, H.; Selo, M.; Skarp, K.; Hilborn, J., Synthesis and Characterization of Main Chain Polyimides Containing Chalcone Derivatives for LC Alignment. *POLYM J* **2006,** *38* (7), 716-723.
29. Feng, K.; Tsushima, M.; Matsumoto, T.; Kurosaki, T., Synthesis and properties of novel photosensitive polyimides containing chalcone moiety in the main chain. *J POLYM SCI A1* **1998,** *36* (5), 685-693.
30. Allcock, H. R.; Cameron, C. G., Synthesis of Photo-Cross-Linkable Chalcone-Bearing Polyphosphazenes. *MACROMOLECULES* **1994,** *27* (12), 3131-3135.
31. (a) Wagner, S.; Dai, H.; Stapleton, R. A.; Illingsworth, M. L.; Siochi, E. J., Pendent Polyimides using Mellitic Acid Dianhydride. I. An Atomic Oxygen-resistant, Pendent 4,4′-ODA/PMDA/MADA Co-polyimide Containing Zirconium. *ADV POLYM SCI* **2006,** *18* (4), 399-419;

(b) Galperin, E. Novel Polyimides Based on APAF, 6FDA, and MADA, and their NLO Pendent Polymers. Rochester Institute of Technology, 2003.

32. Rehab, A.; Salahuddin, N., Photocrosslinked polymers based on pendant extended chalcone as photoreactive moieties. *POLYMER* **1999,** *40* (9), 2197-2207.
33. Lee, S. K.; Cho, M. J.; Jin, J.-I.; Choi, D. H., Stability control of the electrooptic effect with new maleimide copolymers containing photoreactive tricyanopyrrolidene-based chromophores. *J POLYM SCI A1* **2007,** *45* (3), 531-542.
34. Woo Lee, S.; Ree, M., Synthesis and properties of photoalignable aromatic polyesters containing phenylenediacrylate units in their backbones and n-alkyl moieties in their side groups. *J POLYM SCI A1* **2004,** *42* (6), 1322-1334.
35. Guo, W.; Li, J.; Fan, N.; Wu, W.; Zhou, P.; Xia, C., A Simple and Effective Method for Chemoselective Esterification of Phenolic Acids. *SYNTHETIC COMMUN* **2005,** *35* (1), 145 - 152.
36. Cho, M. J.; Kim, G. W.; Jun, W. G.; Lee, S. K.; Jin, J.-I.; Choi, D. H., Multifunctional photochromic spiropyran dendrimers and their relaxation behaviors of photochromism. *THIN SOLID FILMS* **2006,** *500* (1-2), 52-60.
37. Nowakowska Z, K. B., Schroeder G., Synthesis, physicochemical properties and antimicrobial evaluation of new (E)-chalcones. *EUR J MED CHEM* **2008,** *43* (4), 707-713.
38. Mitsunobu, O., The Use of Diethyl Azodicarboxylate and Triphenylphosphine in Synthesis and Transfromation of Natural Products. *SYNTHESIS* **1981**, 1-28.
39. Leng, W. N.; Zhou, Y. M.; Xu, Q. H.; Liu, J. Z., Synthesis of nonlinear optical side-chain soluble polyimides for electro-optic applications. *POLYMER* **2001,** *42* (18), 7749-7754.
40. (a) Selvam, P.; Babu, K. V.; Nanjundan, S., Synthesis, characterization and photocrosslinking properties of polyacrylamides having bromo substituted pendant cinnamoyl moieties. *EUR POLYM J* **2005,** *41* (1), 35-45;

    (b) Selvam, P.; Nanjundan, S., Synthesis and characterization of new photoresponsive acrylamide polymers having pendant chalcone moieties. *REACT FUNCT POLYM* **2005,** *62* (2), 179-193.
41. ASTM-International, ASTM Standard D882 "Standard Test Method for Tensile Properties of Thin Plastic Sheeting". www.astm.org: West Conshohocken, PA, 2009.
42. ASTM-International, ASTM D4065 "Standard Practice for Plastics: Dynamic Mechanical Properties: Determination and Report of Procedures". www.astm.com: West Conshohocken, PA, 2006.
43. Hodgkin, J. H.; Dao, B. N., Thermal conversion of hydroxy-containing polyimides to polybenzoxazoles. Does this reaction really occur? *EUR POLYM J* **2009,** *45* (11), 3081-3092.
44. Ho, B.-C.; Lin, Y.-S.; Lee, Y.-D., Synthesis and characteristics of organic soluble photoactive polyimides. *J APPL POLYM SCI* **1994,** *53* (11), 1513-1524.

45. (a) Balaji, R.; Nanjundan, S., Synthesis and characterization of photocrosslinkable functional polymer having pendant chalcone moiety. *REACT FUNCT POLYM* **2001,** *49* (1), 77-86;

(b) Nosova G.; Solovskaya, N. L. y., V.; Galaktionova, E.; Romashkova, K.; Smirnov, N.; Kudryavtsev, V., Phototransformations of chalcone moiety-containing polyimides and polyamidoimides in N, N-dimethylacetamide. *VYSOKOMOL SOEDIN SER A* **2003,** *45* (5), 723-734;

(c) Rtishchev, N. I.; Nosova, G. I.; Solovskaya, N. A.; Luk'yashina, V. A.; Galaktionova, E. F.; Kudryavtsev, V. V., Spectral Properties and Photochemical Activity of Chalcone Derivatives. *RUSS J GEN CHEM* **2001,** *71* (8), 1272-1281.

46. http://www.nmrdb.org/predictor.

47. http://www.chemistry.ccsu.edu/glagovich/teaching/316/ir/table.html.

APPENDIX A

Apparatus for UV Light Exposure

1. **Rayonet Reactor – 300 nm UV light source**

   Model Number: RPR-100

   Intensity Measurement:

   Spectro radiometer: IL 587 #205

   Photometer: IL 1500

   International Light Inc. MA.

   Measured Intensity at center: 10 $\mu W/cm^2$ nm

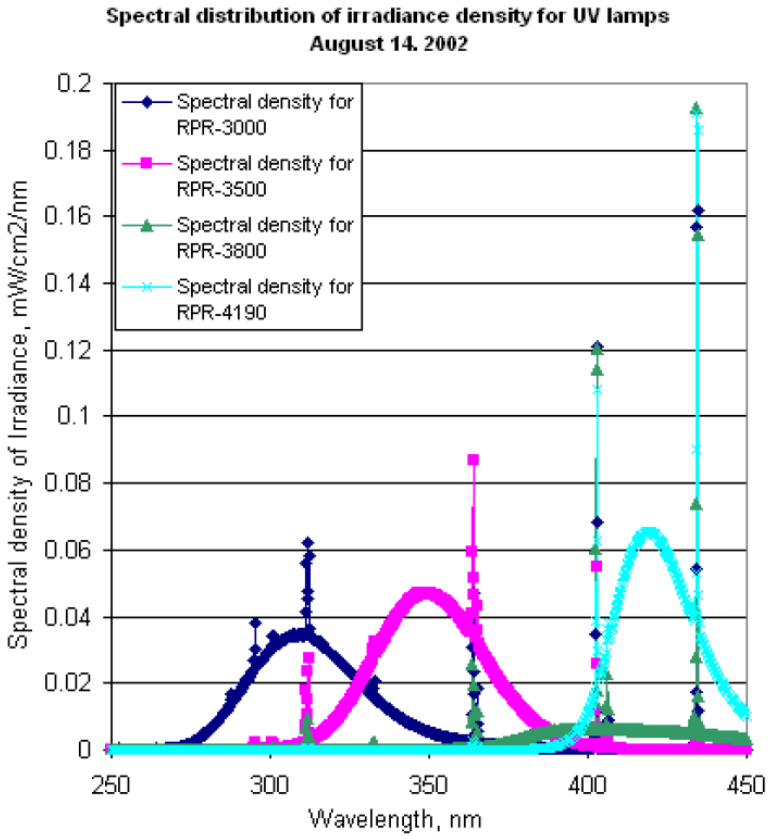

2. **UVP UV Lamp – 366 nm UV light source**

   Model Number: UVGL-25

APPENDIX B

Elucidation of Peak Assignments Using 2-D NMR

2-D NMR for UV cross-linkable pendent group and Model Compound was performed not only to establish the accurate assignments for aromatic and olefin protons, but also to confirm the presence of cis-trans isomers of each compound by studying the coupling constants (J) for protons in cis- and trans-structures separately. For this purpose two solvents, deuterated chloroform (d^1-$CDCl_3$) and deuterated dimethylsulfoxide (d^6-DMSO) were used. Different chemical shifts for same compound in two solvents can be explained on the basis of difference in internal hydrogen bonding, more prominently seen in d^1-$CDCl_3$ as against d^6-DMSO.

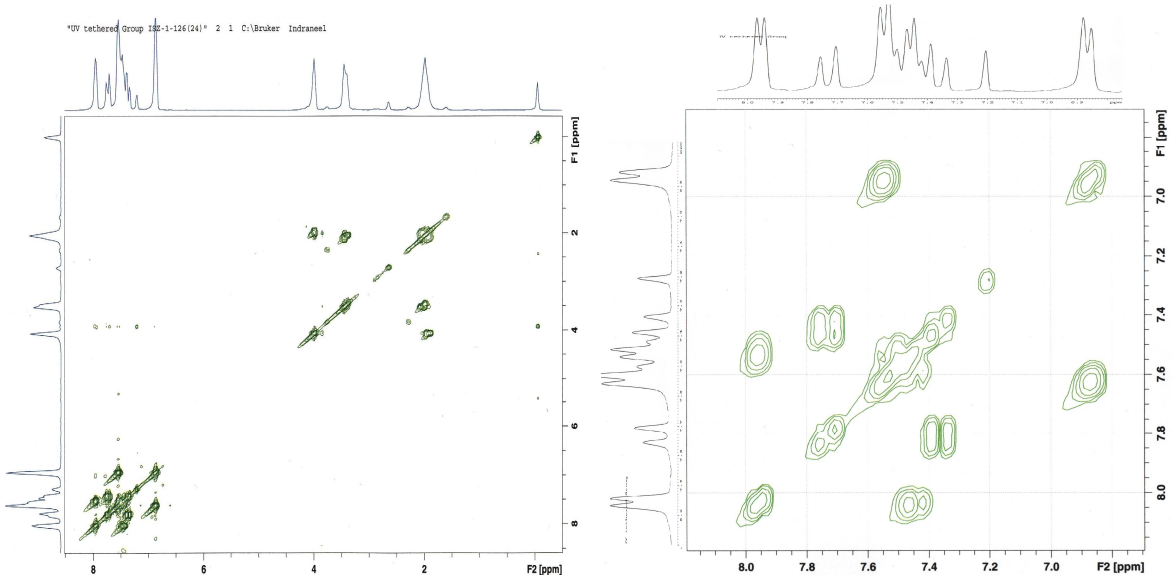

2-D NMR of UV cross-linkable pendent group in d^1-$CDCl_3$

For UV cross-linkable pendent group in d^1-$CDCl_3$, olefinic protons associated with photo-reactive unsaturation in chalcone were observed at 7.75 ppm and 7.35 ppm with large coupling constant. Such strong nuclear interaction is characteristic feature of protons in trans- structure, which confirmed presence of trans-isomer of UV cross-linkable pendent group.

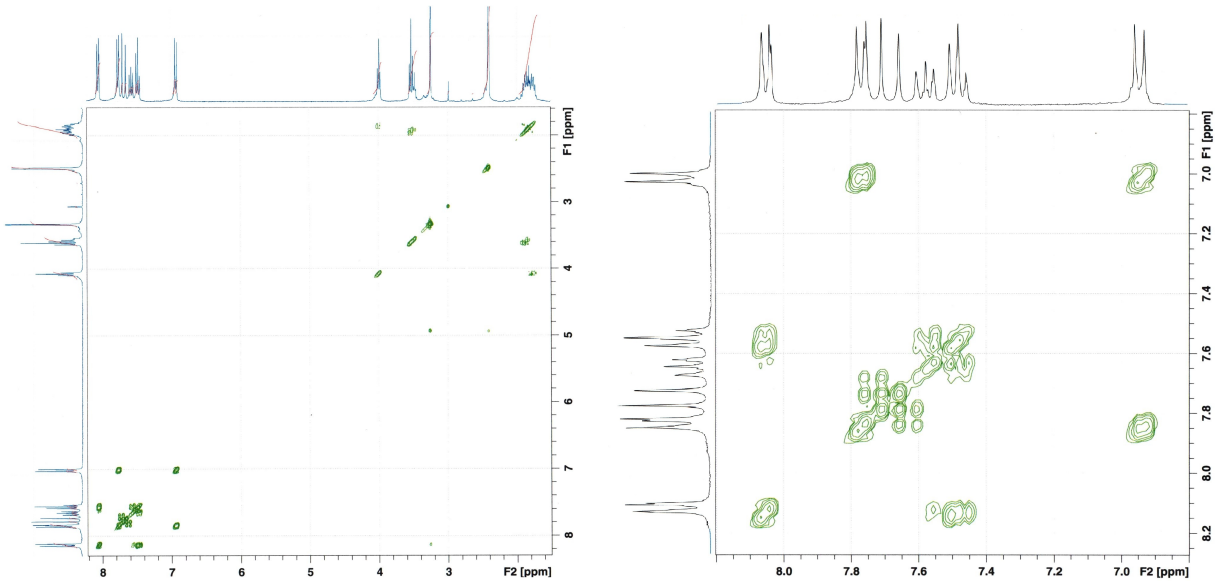

2-D NMR of UV cross-linkable pendent group in d^6-DMSO

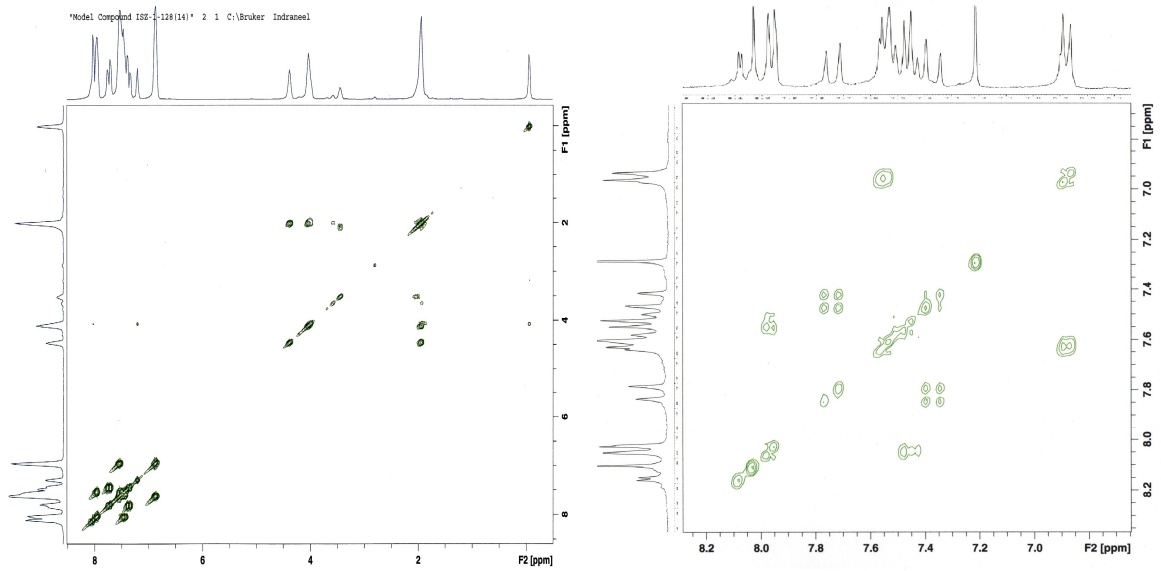

2-D NMR of Model Compound in d^1-$CDCl_3$

Apart from congruent proton peaks for Model Compound and UV cross-linkable pendent group in d^1-$CDCl_3$, small peaks at 8.1 ppm, 7.55 ppm and 6.9 ppm indicated presence of cis- isomer along with trans- isomer.

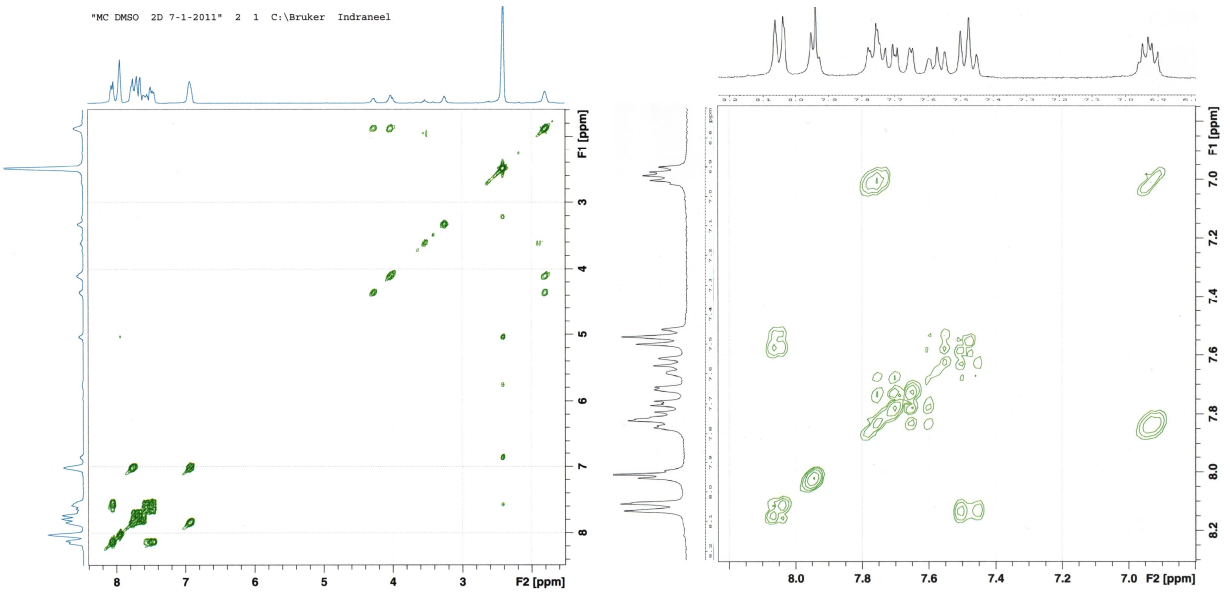

2-D NMR of Model Compound in d^6-DMSO

For Model Compound in d^6-DMSO, the peaks for olefin protons were observed at 7.70 ppm and 7.65 ppm. In polar d^6-DMSO, the adjacent carbonyl group is more involved in hydrogen bonding with DMSO, leading to similar chemical shifts and locating olefinic protons farther apart. This smaller coupling interaction is consistent with a cis- arrangement around olefin bond, confirming presence of a cis- isomer.

APPENDIX C

Tensile Test Results for Each Specimen and for Each Exposure Time

I) UV Exposure Time : 15 min

Sample No.	Load (kgf)	Load F (N)	Tensile Strength S (Mpa)	Elongation ε	Young's Modulus E (Gpa)	Failure
1	11.2890	110.7112	14.1937	0.0181	0.7854	Normal Break
2	9.2890	91.0972	11.3544	0.0138	0.8217	Near Bottom Grip
3	8.5640	83.9871	10.7272	0.0147	0.7315	Near Bottom Grip
4	8.2820	81.2216	10.2965	0.0138	0.7440	Normal Break

II) UV Exposure Time : 30 min

Sample No.	Load (kgf)	Load F (N)	Tensile Strength S (Mpa)	Elongation ε	Young's Modulus E (Gpa)	Failure
1	12.6980	124.5293	14.8564	0.0226	0.6563	Normal Break
2	9.1950	90.1754	11.9280	0.0154	0.7739	Near Top Grip
3	14.4430	141.6425	17.5753	0.0179	0.9800	Normal Break
4	12.5370	122.9504	15.1047	0.0154	0.9787	Near Both Grips

III) UV Exposure Time : 45 min

Sample No.	Load (kgf)	Load F (N)	Tensile Strength S (Mpa)	Elongation ε	Young's Modulus E (Gpa)	Failure
1	11.7320	115.0557	21.5872	0.0169	1.2752	Normal Break
2	12.0670	118.3411	21.1702	0.0253	0.8369	Normal Break
3	6.6850	65.5598	15.7218	0.0122	1.2882	Near Top Grip
4	16.5230	162.0411	26.0717	0.0204	1.2772	Normal Break
5	6.1740	60.5484	11.1425	0.0097	1.1458	Near Top Grip

IV) UV Exposure Time : 90 min

Sample No.	Load (kgf)	Load F (N)	Tensile Strength S (Mpa)	Elongation ε	Young's Modulus E (Gpa)	Failure
1	9.1140	89.3810	15.9294	0.0130	1.2242	At Bottom Grip
2	8.4160	82.5357	15.3216	0.0097	1.5788	At Bottom Grip
3	14.8590	145.7222	24.9867	0.0171	1.4624	Normal Break
4	16.2010	158.8832	25.1477	0.0179	1.4054	Near Both Grips
5	9.5840	93.9903	16.2321	0.0122	1.3300	Near Bottom Grip

V) UV Exposure Time : 180 min

Sample No.	Load (kgf)	Load F (N)	Tensile Strength S (Mpa)	Elongation ε	Young's Modulus E (Gpa)	Failure
1	2.3890	23.4289	13.2742	0.0146	0.9076	At Top Grip
2	8.8990	87.2725	32.6692	0.0110	2.2336	Near Top Grip
3	2.4830	24.3508	13.6419	0.0219	0.9327	At Top Grip
4	4.4430	43.5725	24.6172	0.0181	1.6831	At Bottom Grip

VI) UV Exposure Time : 300 min

Sample No.	Load (kgf)	Load F (N)	Tensile Strength S (Mpa)	Elongation ε	Young's Modulus E (Gpa)	Failure
1	17.2890	169.5532	28.0759	0.0171	1.6432	Normal Break
2	17.3690	170.3378	26.2098	0.0179	1.4615	Normal Break
3	8.6580	84.9090	13.4971	0.0122	1.1095	Near Top Grip
4	20.2280	198.3760	31.4174	0.0237	1.3267	At Both Grips

APPENDIX D

DMA Results for Each Specimen, Each Frequency and Each Exposure Time

E` (GPa)							
Frequency	**UV Exposure Time**	**Sample 1**		**Sample 2**		**Mean**	**Standard Deviation**
0.1	15	4.67	4.66	4.65	4.68	4.66	0.0129
	30	5.02	5.03	5.03	5.06	5.03	0.0164
	45	6.08	6.07	6.02	6.03	6.05	0.0294
	90	6.20	6.18	6.17	6.14	6.17	0.0250
	180	5.81	5.81	5.82	5.80	5.81	0.0082
	300	6.22	6.25	6.22	6.22	6.23	0.0150
1	15	4.78	4.75	4.78	4.76	4.77	0.0144
	30	5.15	5.12	5.15	5.14	5.14	0.0133
	45	6.21	6.18	6.20	6.19	6.19	0.0108
	90	6.36	6.34	6.32	6.31	6.33	0.0222
	180	5.97	5.96	5.97	5.94	5.96	0.0141
	300	6.38	6.37	6.38	6.37	6.37	0.0048
10	15	4.92	4.90	4.91	4.89	4.90	0.0115
	30	5.27	5.25	5.25	5.25	5.26	0.0105
	45	6.36	6.35	6.38	6.35	6.36	0.0118
	90	6.54	6.48	6.43	6.39	6.46	0.0648
	180	6.14	6.12	6.12	6.09	6.12	0.0206
	300	6.62	6.59	6.53	6.51	6.56	0.0512
20	15	4.96	4.92	4.98	4.95	4.95	0.0250
	30	5.30	5.28	5.31	5.31	5.30	0.0141
	45	6.40	6.38	6.38	6.45	6.40	0.0343
	90	6.59	6.59	6.61	6.44	6.56	0.0814
	180	6.25	6.20	6.14	6.20	6.20	0.0450
	300	6.64	6.66	6.57	6.58	6.61	0.0443

E" (GPa)							
Frequency	**UV Exposure Time**	**Sample 1**		**Sample 2**		**Mean**	**Standard Deviation**
0.1	15	0.1228	0.1237	0.1181	0.1217	0.1216	0.00246
	30	0.1697	0.1735	0.1660	0.1705	0.1699	0.0031
	45	0.1678	0.1748	0.1643	0.1700	0.1693	0.00439
	90	0.1705	0.1749	0.1580	0.1646	0.1670	0.00736
	180	0.1569	0.1540	0.1484	0.1520	0.1528	0.00355
	300	0.1611	0.1656	0.1617	0.1679	0.1641	0.00325
1	15	0.1339	0.1359	0.1305	0.1333	0.1334	0.00223
	30	0.1791	0.1823	0.1736	0.1784	0.1783	0.0036
	45	0.1799	0.1811	0.1798	0.1840	0.1812	0.00194
	90	0.1819	0.1864	0.1725	0.1735	0.1786	0.00669
	180	0.1648	0.1678	0.1630	0.1556	0.1628	0.00517
	300	0.1734	0.1752	0.1786	0.1752	0.1756	0.00219
10	15	0.1711	0.1657	0.1635	0.1682	0.1671	0.00328
	30	0.2140	0.2196	0.2074	0.2151	0.2140	0.00505
	45	0.2269	0.2362	0.2346	0.2388	0.2341	0.00509
	90	0.2394	0.2417	0.2302	0.2352	0.2366	0.00506
	180	0.2192	0.2203	0.2188	0.2162	0.2186	0.00174
	300	0.2400	0.2389	0.2305	0.2324	0.2354	0.00469
20	15	0.1939	0.1948	0.1785	0.1906	0.1895	0.00752
	30	0.2268	0.2355	0.2257	0.2390	0.2317	0.0065
	45	0.2784	0.2833	0.2550	0.2709	0.2719	0.01236
	90	0.2751	0.2768	0.2849	0.2773	0.2785	0.00434
	180	0.2625	0.2666	0.2579	0.2740	0.2653	0.00685
	300	0.2915	0.2924	0.2746	0.2829	0.2854	0.00833

tan δ							
Frequency	**UV Exposure Time**	**Sample 1**		**Sample 2**		**Mean**	**Standard Deviation**
0.1	15	0.0263	0.0266	0.0254	0.0260	0.0261	0.0005
	30	0.0338	0.0345	0.0330	0.0337	0.0338	0.0006
	45	0.0276	0.0288	0.0273	0.0282	0.0280	0.0007
	90	0.0275	0.0283	0.0256	0.0268	0.0271	0.0011
	180	0.0270	0.0265	0.0255	0.0262	0.0263	0.0006
	300	0.0259	0.0265	0.0260	0.0270	0.0264	0.0005
1	15	0.0280	0.0286	0.0273	0.0280	0.0280	0.0005
	30	0.0348	0.0356	0.0337	0.0347	0.0347	0.0008
	45	0.0290	0.0293	0.0290	0.0297	0.0293	0.0003
	90	0.0286	0.0294	0.0273	0.0275	0.0282	0.0010
	180	0.0276	0.0282	0.0273	0.0262	0.0273	0.0008
	300	0.0272	0.0275	0.0280	0.0275	0.0276	0.0003
10	15	0.0348	0.0338	0.0333	0.0344	0.0341	0.0007
	30	0.0406	0.0418	0.0395	0.0410	0.0407	0.0010
	45	0.0357	0.0372	0.0368	0.0376	0.0368	0.0008
	90	0.0366	0.0373	0.0358	0.0368	0.0366	0.0006
	180	0.0357	0.0360	0.0358	0.0355	0.0357	0.0002
	300	0.0363	0.0363	0.0353	0.0357	0.0359	0.0005
20	15	0.0391	0.0396	0.0359	0.0385	0.0383	0.0017
	30	0.0428	0.0446	0.0425	0.0450	0.0437	0.0013
	45	0.0435	0.0444	0.0400	0.0420	0.0425	0.0019
	90	0.0418	0.0420	0.0431	0.0431	0.0425	0.0007
	180	0.0420	0.0430	0.0420	0.0442	0.0428	0.0011
	300	0.0439	0.0439	0.0418	0.0430	0.0432	0.0010

APPENDIX E

Viscosity Data for Each Exposure Time

Number of Reading	Control	Unexposed	Exposure Times					
	8NMP-4THF		15 min	30 min	45 min	90 min	180 min	300 min
	sec	sec	sec	sec	sec	sec	sec	sec
1	35.1	193.5	201.9	218.0	231.4	232.1	235.3	237.4
2	34.8	194.6	200.4	217.6	228.5	231.8	233.6	235.3
3	34.8	195.3	200.6	217.4	227.9	233.0	238.5	232.4
4	34.7	194.7	200.1	216.4	228.6	233.1	234.5	235.6
5	34.8	195.6	201.4	216.3	230.7	233.6	235.1	235.7
6	-	195.4	201.8	216.5	230.1	232.1	230.8	237.0
7	-	193.0	201.6	217.6	228.2	233.8	235.8	233.7
Mean	34.82	194.59	201.11	217.11	229.34	232.77	234.80	235.30

Normalized Viscosity Data w.r.t. Control (mean)							
Number of Reading	Unexposed	Exposure Times					
		15 min	30 min	45 min	90 min	180 min	300 min
1	5.56	5.80	6.26	6.65	6.67	6.76	6.82
2	5.59	5.76	6.25	6.56	6.66	6.71	6.76
3	5.61	5.76	6.24	6.55	6.69	6.85	6.67
4	5.59	5.75	6.21	6.57	6.69	6.73	6.77
5	5.62	5.78	6.21	6.63	6.71	6.75	6.77
6	5.61	5.80	6.22	6.61	6.66	6.63	6.81
7	5.54	5.79	6.25	6.55	6.71	6.77	6.71
Mean	5.59	5.78	6.24	6.59	6.68	6.74	6.76